FUZZY BASED DETECTION AND CLASSIFICATION OF SINGLE PHASING CONDITION IN POWER DISTRIBUTION SYSTEMS IN PRESENCE OF DISTRIBUTED GENERATION

A THESIS Submitted

In the partial fulfillment of the requirements for the award of the degree of

MASTER OF ELECTRICAL ENGINEERING

By

SANJOY PONDIT

Examination Roll No: M4ELE19012

Registration No: 140655 of 2017-18

Under The Guidance and Supervision of

Dr. Sudipta Debnath

Electrical Engineering Department

Faculty of Engineering and Technology

JADAVPUR UNIVERSITY

KOLKATA- 700032, W.B. INDIA

2017-2019

Dedicated to

My parents and family

Electrical Engineering Department

Faculty of Engineering and Technology

JADAVPUR UNIVERSITY

KOLKATA- 700032, W.B. INDIA

CERTIFICATE

This is to certify that this thesis entitled "**FUZZY BASED DETECTION AND CLASSIFICATION OF SINGLE PHASING CONDITION IN POWER DISTRIBUTION SYSTEMS IN PRESENCE OF DISTRIBUTED GENERATION"** is being submitted by **MR. SANJOY PONDIT,** with **Examination Roll No. M4ELE19012** in partial fulfillment of the requirements for the award of the degree of **Master of Electrical Engineering** from JADAVPUR UBIVERSITY, KOLKATA, WEST BENGAL has been carried out by him under our guidance and supervision. The project, in our opinion, is worthy of its acceptance.

SUPERVISOR

_____

Dr. Sudipta Debnath
Professor
Electrical Engineering Department
Jadavpur University

COUNTERSIGNED

_____

Prof. (Dr.) Kesab Bhattacharyya
Head of the Department
Electrical Engineering Department
Jadavapur University

_____

Prof. Chiranjib Bhattacharjee
Dean of the Faculty of Engineering
and Technology
Jadavpur University

Electrical Engineering Department

Faculty of Engineering and Technology

JADAVPUR UNIVERSITY

KOLKATA- 700032, W.B. INDIA

*CERTIFICATE OF APPROVAL**

The foregoing thesis is hereby approved as a creditable study of ***Master of Electrical Engineering*** *and presented in a manner satisfactory to warrant its acceptance as a prerequisite to the degree for which it has been submitted. It is understood that by this approval the undersigned do not necessarily endorse or approve any statement made, opinion expressed or conclusion therein but approve this thesis only for the purpose for which it is submitted.*

Committee on Final
Examination for
Evaluation of the Thesis

……

……

……

……

Only in case the thesis is approved *(Signature of the Examiners)*

Electrical Engineering Department

Faculty of Engineering and Technology

JADAVPUR UNIVERSITY

KOLKATA- 700032, W.B. INDIA

DECLARATION

I certify that except where due acknowledgement has been made, the work is that of the candidate alone. This thesis is a presentation of my original research work and has not been submitted previously, in whole or in part, to quality for any other academic award. Furthermore, the content of the thesis is the result of work which has been carried out since the official commencement date of the approved research program.

The work was done under the guidance of Professor Dr. Sudipta Debnath, Electrical Engineering Department of Jadavpur University, Kolkata.

The information and data given in the report is authentic to the best of my knowledge.

Name (Block Letters)	:	SANJOY PONDIT
Exam Roll no.	:	M4ELE19012
Thesis Name	:	FUZZY BASED DETECTION AND CLASSIFICATION OF SINGLE PHASING CONDITION IN POWER DISTRIBUTION SYSTEMS IN PRESENCE OF DISTRIBUTED GENERATION
Signature with date	:	

ACKNOWLEDGEMENT

First of all, I would like to express my sincere gratitude to my project supervisor, ***Dr. Sudipta Debnath****, Department of Electrical Engineering, Jadavpur University, Kolkata, for her invaluable guidance, suggestions and encouragement throughout the project, which helped me a lot to improve this project work. It has been very nice to be under her guidance.*

I am also indebted to ***Prof. (Dr.) Kesab Bhattacharyya****, Head, Department of Electrical Engineering, Jadavpur University, for his kind help and co-operation during this thesis work. I am also thankful to* ***Prof. Chiranjib Bhattacharjee****, Dean of Faculty of Engineering and Technology for his kind help and co-operation during this thesis work.*

I would also like to convey my gratitude to Prof. (Dr.) Subrata Pal, Prof. (Dr.) Swapan Kumar Goswami, Dr. Sunita Halder nee Day, Prof. Ayan Kumar Tudu and Prof. Madhumita Mandal, of Electrical Engineering, Jadavpur University for their guidance, encouragement and valuable suggestions in the course of thesis work.

Special thank also to my friends, especially Arup kumar Das, Payel Banerjee and all PhD scholars of power system simulation lab, especially Subhra De, for their useful idea, information and moral support during the course of study and for all the fun we have had in the last years.

I would like to express my heartiest appreciation to my parents, bother and my family for their love and active support throughout the endeavor.

Last but not the least, I wish to thank all my well-wishers for their constant source of encouragement and moral support during the course of my work.

Date:

Sanjoy Pondit
Electrical Engineering Department
Jadavpur University
Kolkata - 700032

ABSTRACT

This thesis aims at classifying and detecting the single phasing in power distribution systems in presence of distributed generation. In this study, accurate electrical modal on a power system network is developed and simulated using MATLAB/Simulink tools. The test system considered in this research is a three phase 60 Hz, 6 bus power system having wind farm of rating 690 V/9 MVA in distribution system.

Single phasing phenomenon is difficult to detect in presence of distributed generation (DG) as the current in the lost phase is compensated by the DG unit. It causes mal operation of power system equipment which are designed to operate under balanced condition. This work presents a transient based algorithm for single phasing detection in distribution system. Discrete wavelet transform (DWT) has been applied to capture three bands of frequencies in the transient modal current signal. The spectral energies of these three bands are extracted and fed to fuzzy inference system to detect and classify single phasing. Solid faults, load switching and capacitor bank switching which cause similar transient phenomenon are also simulated to discriminate single phasing from these transients. Simulated results under various dynamic situations show that this fuzzy based algorithm can reliably distinguish single phasing event from other disturbances.

Keywords: Distribution system, Distributed Generation, Wavelet Transform, Fuzzy Inference System, Single phasing Detection, Single phasing Classification

LIST OF ABBREVIATIONS

DG …….Distributed Generation

RRMF …….Reverse Rotating Magnetic Field

ASDs …….Adjustable Speed Drives

ANN …….Artificial Neural Network

DWT …….Discrete Wavelet Transform

WT …….Wavelet Transform

ANFIS ……Adaptive Neuro-Fuzzy Inference system

DSE ……Detail-Spectrum-Energy

MRA …… Multi Resolution Analysis

HVB ……. High Voltage Class-B

WSE ……. Wavelet Singular Entropy

FIA ……. Fault Inception Angle

DFT ……. Discrete Fourier Transforms

UPFC ……..Unified Power Flow Controller

MATLAB ……..Matrix Laboratory

FACTS ……...Flexible Alternating Current Transmission System

SSSC ……...Static Synchronous Series Compensator

PQ ……Power Quality

WE ……Wavelet Entropy

WPT ……Wavelet Packet Transform

SVM ……Support Vector Machines

EMTP ……Electro-Magnetic Transient Programs

CWT ……Continuous Wavelet Transform

HIF ……....High Impedance Fault

FFT ……Fast Fourier Transform

MF ……Membership Function

FIS ……Fuzzy Inference System

NSP ……Non-Single Phasing

SPA ……Single Phasing at phase A

SPB ……Single Phasing at phase B

SPC ……Single Phasing at phase C

RMS ……Root Mean Square

STFT ……Short Time Fourier Transform

SLG ……Single Line to Ground

LL ……Line to Line

LLG ……Double Line to Ground

LLL ……..Three Phase

HPF ……..High Pass Filter

LPF ……..Low Pass Filter

NOMENCLATURE

ψ	……..Mother wavelet
ω	……..Angular frequency (rad/sec)
cA	…….. Approximation components
cD	……...Detail components
E_4	……Spectral energy at 4 level composition
E_5	……Spectral energy at 5 level composition
E_6	……Spectral energy at 6 level composition
R_f	……Fault Resistance (ohm)
Hp	……...Horsepower
T_s	……...Sampling Time
Ω	……Ohm
I_a	……Current at phase A
I_b	……Current at phase B
I_c	……Current at phase C
I_m	……Modal Signal

LIST OF FIGURES

LIST OF TABLES

TABLE OF CONTENTS

CHAPTER 1

INTRODUCTION

Modern power system is spreading over large geographical areas and becoming more complex. All electrical power systems are equipped with generators, transformer, transmission lines and loads. The transmission line is an important component of power system network. Transmission lines in power system network are vulnerable to environmental and other external interferences. In radial distribution system, power supply to the consumers is affected when faults occur at any point in the network. There are mainly two types of fault in power system, one is short circuit fault and another one is open circuit fault. If one of the live conductors of a three phase system is open and other two phases remain in live condition, then it is open circuit fault and introduces unbalance in the power system, also known as single phasing. Short circuit faults can be easily detected and cleared by overcurrent relays, whereas open circuit faults are detected upon the receipt of information of power supply interruption from the customers. Again, open circuit fault in any one phase results in zero current in the faulty phase and normal current in the other two phases which causes significant current unbalance in three phase system. This may actuate current unbalance relays and open circuit fault can be detected.

Increasing penetration of distributed generation imposes serious challenges in power system. If an open circuit fault occurs in presence of wind farm or distributed generation, current unbalance relays are not actuated as the current from the wind farm continues to supply the lost phase and open circuit fault is not detected. Thus single phasing condition is developed. The power supply to the consumers is considerably affected as the distribution network suffers from abnormal phase voltages. Hence detection of single phasing condition in presence of distributed generation is a challenging task.

Single phasing in an electrical power system cannot be avoided. With the rapid development of micro grid, it is more important to detect single phasing and single phasing detection and classification are the focus of research efforts in the area of distribution system.

1.1 GENERAL OVERVIEW

The main objective of all the power system networks is to maintain continuity in service and to minimize the outage times whenever abnormal conditions arise i.e. to assure reliable operation. The open circuit fault in any one phase of three phase system (single phasing) in presence of DG units causes significant unbalance in the system i.e. abnormal condition. Some of the causes of single phasing are as follows:

- One of the most common causes of single phasing is the opening of only one phase conductor of three or four wire transmission system, when a branch of a tree falls on that conductor.
- Most common short circuit fault is single line to ground fault, after occurrence of which the faulty phase may be disconnected from the system causing single phasing with other two healthy phases.
- Power system equipment like power transformer, distribution transformer bank etc. can cause single phasing due to the opening of transformer winding of one phase of three phase transformer.
- Another most frequent cause of single phasing is the malfunctioning of protection equipment like circuit breaker, isolator, fuses etc. At the time of energizing a circuit, any two poles of the breaker may close and the third pole may be stuck and remain open. The utilization of single-phase protective devices is another common cause for single-phasing. Most electrical utilities use single-phase fuses to protect three-phase distribution networks. The blowing of fuse of one phase develops single phasing.

As single phasing results in unbalanced operation, it has many negative impacts on power system equipment. Unbalanced currents due to single phasing generate negative sequence components and it produces a reverse rotating magnetic field (RRMF) in the air gap between the rotor and stator of the machines. This RRMF rotates at synchronous speeds in opposite direction to the rotor of the machine. It induces double frequency currents into the rotor body in the cylindrical rotating machines and induces double frequency currents in the pole faces of salient pole machines. This induced current in the rotor provides high resistance path to the normal induced currents (due to synchronous rotating magnetic field) resulting in rapid heating. This heating may cause insulation failure and loss of mechanical integrity in the machine in a few seconds.

Three phase power electronic loads like adjustable-speed drives (ASDs) draw unequal current in each phase due to unbalance voltage caused by single phasing. This kind of effect is more dominant in smaller drives (less than 10 hp) where the percentage current unbalance may be 20 times the percentage voltage unbalance. High magnitudes of phase currents may result in overcurrent or excessive high dc bus ripple. High ripple causes reduction of the life of the dc bus capacitor of the ASD.

Ferroresonance is a special form of resonance that involves the system capacitance and the magnetizing reactance of a transformer. A common form of ferroresonance occurs during single phasing of three phase distribution transformers. Ferroresonance most commonly occurs on cable-fed transformers because of the high capacitance of the cables. During single-phasing, a ferroresonant circuit may be set up between the cable capacitance and the transformer reactance. If these impedances are in the range of magnitudes where ferroresonance can occur, then high voltages up to 5 times the rated voltage can occur on the open legs of the transformer. The most common problem that can occur is overheating of metal-oxide surge arresters. Also overvoltage due ferroresonance may lead to insulation failure of transformer.

Single phasing causes de-rating of power cables which may increase ohmic losses in the cable. It also causes overheating in transformers connected to the transmission lines.

Hence, the sensitive load present in the system need to be protected from this kind of abnormal condition. The abnormal condition in power system affect the overall power quality of the system. Hence it is necessary to detect the single phasing event and the phase which causes the single phasing and clear the single phasing event as soon as possible in order not to cause any damages.

The single phasing condition can be detected by wavelet transform as wavelet transform is a powerful tool for analyzing transient signals and is extensively used by researchers to detect abnormal situations in power system. Wavelet theory deals with building a model for non-stationary signals, using a set of components that look like small waves, called wavelets. The wavelet based techniques have several power system application and open circuit fault or single phase detection is one of them. In this thesis, some important information of signal under single

phasing condition is extracted by wavelet transform. The wavelet transform based approaches have been quite successful in fault detection and classification due to its ability to express faulted signal in both time and frequency domain.

Fuzzy logic is a form of multi-valued logic in which the truth values of variables may be any real number between certain range. In other words, it is the concept of partial truth, where the true value may range between completely true and completely false. In this thesis, fuzzy logic based detection and classification of single phasing scheme is proposed.

1.2 LITERATURE SURVEY

Single phasing in power system distribution lines needs to be found out as quickly as possible, otherwise power supply may collapse. Researchers have suggested techniques for detection and classification of single phasing, which mainly depends upon studying the pattern of the voltage and current associated with single phasing.

ElNozahy et al. [1] presented a robust wavelet-ANN based algorithm for single-phasing detection and single-phasing classification in distribution systems with a high penetration of distributed generation (DG). DWT has been applied for feature extraction and the extracted features were fed to artificial neural network (ANN) to detect single phasing condition and classify the lost phase. This proposed algorithm have accuracy of 99.3 percent in detection of single phasing event and accuracy of 93 percent in classification of single phasing.

Also there are several approaches proposed by researchers for detection of fault and fault classification in power system network. Wavelet Transform (WT) based methods, Artificial Neural Network (ANN), Adaptive Neuro-Fuzzy Inference system (ANFIS) based methods are adopted for detection of faults and their classification in power system.

Gafoor et al. [2] used WT multi resolution approach for detection, classification and localization of fault in the transmission line. It was accomplished within half cycle using detail coefficient of current at both ends. Fault location was estimated with a fair degree of accuracy from the approximate decomposition of phase voltages and current of local end using ANN.

Othman et al. [3] proposed an algorithm for fault detection, classification and locating it in the transmission line using Multi resolution Analysis (MRA) wavelet transform which decomposes

the signal into different resolutions allowing a detail analysis of its energy content and characteristics.

Zarbita et al. [4] used the detail-spectrum-energy (DSE) analysis for fault detections and classifications in High Voltage Class-B (HVB) transmission lines. The DSE is computed at scale-1 and applied on the phases and ground currents using db4 mother wavelet. The performance of the method was tested and evaluated on real data records and could accurately detect the fault within one half cycle from the instant of fault occurrence. Discrete Wavelet Transform (DWT) approach for detection, classification and localization of faults in the transmission line was accomplished within one cycle of the fundamental power frequency.

Allipilli et al. [5] proposed Wavelet Transform (WT), Multi- resolution analysis (MRA), Wavelet Singular Entropy (WSE) for detection, classification and location of fault in overhead transmission line with accurate and quick calculation including the effect of factors such as fault impedance, fault inception angle (FIA) and fault distance.

Reddy et al. [6] proposed an algorithm for fault classification employing wavelet Multi resolution Analysis (MRA) to overcome the shortcomings of conventional voltage and current based measurements due to effect of factors such as fault inception angle, fault impedance and distance of occurrence of fault. A new real time wavelet-fuzzy combined approach was presented to identify location of transmission line faults within one cycle.

Das et al. [7] et al. described a novel technique using Discrete Fourier Transforms (DFT) and Discrete Wavelet Transforms (DWT) techniques for fault detection, classification and location in high voltage transmission line.

Goli et al. [8] discussed a fuzzy-wavelet multi resolution for detection, classification and localization of faults in the double line transmission line. The approach is accurate and successful even in the presence of UPFC one of the line.

Li et al. [9] integrated WT-based MRA technique with ANN for fault detection and classification with high accuracy. It was proved to be robust to various faults and inception of changes in electrical parameters like fault resistance and loads. The mother wavelet is chosen as wavelet db10 and scale 9. ANN was then adopted to classify the extracted features to identify the

fault types automatically. Finally, the proposed algorithm was implemented in LabVIEW for the purpose of online practical use.

Gayathri et al. [10] proposed a method for fault identification and classification on extra high voltage transmission line using DWT. The multi resolution analysis wavelet transform was implemented and proved to be accurate and efficient for the classification of fault. The proposed method is also applicable to a double-circuit un-transposed line.

Shaaban and **Hiyama** [11] used information from Discrete Wavelet Transform (DWT) analysis of transient disturbances due to fault occurrence for power system fault identification and detection. Three phase current signals at normal condition were recorded and decomposed using DWT (db4 level 1) to get their maximum detail coefficient and energy. The ratio of energy change from the normal condition has been used for fault detection because fault inception has great effect on detail coefficients as it generates a high frequency component to signal.

Karekar et al. [12] proposed a model using MATLAB software Wavelet Transform along with the Sim-Power System toolbox in Simulink for analysis and detection of faults on three phase 100 km/ 33 kV overhead transmission line.

Saravanababu et al. [13] used DWT to extract information from three phase current signals and to process the high frequency details to derive information about the fault signal by performing decomposition at different levels. The logic provided by them is fully deterministic, easy to understand and also the classifier operation is fast and reliable and simulation results are verified under various fault cases using MATLAB/ Simulink.

Rana et al. [14] also proposed a wavelet Transform based technique to detect and classify the faults using Sim-Power System MATLAB toolbox for different operating conditions on transmission line.

Uyar et al. [15] proposed an automatic power quality (PQ) disturbance classification method with a norm entropy-based effective feature extraction employing wavelet and neural network. The classification performance of different wavelet family for proposed algorithm was tested. The most important advantage of the proposed method is the reduction of data size as well indication and recognition of the main characteristic of signal without losing its distinguishing characteristics. It

has great potential to improve the performance of the automatic PQ monitoring equipment with on-line classification abilities.

Zonkoly and Desouki [16] proposed a new algorithm to detect and classify fault and identify the fault position in a transmission line in presence of two important FACTS device, SSSC and UPFC placed in the midpoint of the transmission line. The Discrete Wavelet Transform (DWT) and Wavelet Entropy (WE) calculations were used to analyze the fault current and voltage signals of the compensated transmission line. The effectiveness of the proposed algorithm under various types and any position of faults were also tested.

Ekici et al. [17] utilized Wavelet Packet Transform (WPT) which provides more features about the signal than classical wavelet as a data technique for estimate of fault location on transmission lines rapidly and accurately. After wavelet packet decomposition, the energy and entropy of the wavelet packet coefficients are calculated for each faulty current and voltage waveforms. The wavelet packet transform (WPT) extracted features are applied to ANN for the estimation fault location.

Jung et al. [18] proposed the fault detection technique using wavelet transform and the fault location estimation technique using least square error method for accurate and rapid fault detection and fault location estimation regardless of mutual coupling between parallel transmission lines. The fault was detected rapidly within 1 cycle by using D_1 component and fault location was accurately estimated within 1.5 cycles after fault using least square error method.

Safty and Zonkoly [19] proposed wavelet analysis with wavelet entropy principle to detect and classify faults using PSCAD/EMTDC simulation for different types of fault.

Madhavi et al. [20] presented an accurate and efficient technique to detect and classify the different types of fault in transmission lines using wavelet transform in conjunction with Support Vector Machines (SVM) and feed-forward neural network under variable fault resistances and variable loading conditions. The proposed scheme used both voltage and current signals from one end of the line.

Rao and Hasabe [21] presented discrete wavelet transform and ANN based approach for accurate fault detection and classification using the detail coefficients of energy of currents in transmission line which may be extended for finding fault location.

Silva et al. [22] proposed a novel method for transmission line fault detection and classification from real oscillographic data of a Brazilian utility company with excellent results. An Artificial Neural Network (ANN) classified the fault from the voltage and current waveform pattern in the time domain.

Bhowmik et al. [23] proposed a neural network based approach for accurate identification of fault and its location. A lumped parameters model of a real transmission system was developed that used electromagnetic transient programs (EMTP). The main purpose of this paper is to identify the fault types.

Etemadi and Pasand [24] proposed a fuzzy based detection of High Impedance Fault. A wavelet multi resolution signal decomposition method is used for feature extraction. Extracted feature are fed to an adaptive neural fuzzy inference system for fault identification and classification.

Yadav and Thoke [25] presented an accurate fault detection, classification and direction estimation of double end fed transmission lines based on application of artificial neural networks. This method is adaptive to the variation of fault inception angle, fault location and high fault resistance. The algorithm detects the type of fault, identifies the faulted phase and the direction of fault whether it is forward or reverse fault.

Koley et al. [26] proposed an ANN based six phase to ground fault detection and classification on transmission line. This algorithm employed the fundamental components of voltage and current signals for analysis.

Yadav et al. [27] presented an accurate fault classification and distance location algorithm for teed transmission circuit based on artificial neural networks (ANN). This adaptive protection scheme based on application of ANN has been tested for shunt faults, varying fault location, fault resistance and fault inception angle.

Nam et al. [28] proposed a modeling method for high impedance fault in a distribution system using two series time varying resistances. Two series time-varying resistances are controlled by transient analysis of control system in EMTP.

Emanuel et al. [29] presented an analysis of the measured values of current harmonics at a staged high impedance ground fault on sandy soil. The measured low frequency spectrum has been compared with current harmonics recorded continuously for one week at the substation.

Youssef [30] described an approach to fault classification on transmission lines for high speed protective relaying. This scheme is based on the use of wavelet transform and implementation of digital signal processing concep**ts.**

Borghetti et al. [31] proposed a method based on CWT for analysis of voltage transients due to line faults in distribution power system accurately represented by an EMTP model. The various types of fault and network characteristics were examined.

Zhihua [32] developed a novel fault diagnostic method based on node voltage vector ambiguity sets for analog circuits. The proposed method is found to be useful in improving fault coverage of analog circuits with several capacitors. It is also proposed to apply the method to nonlinear analog circuits and to monitor node voltage vector locus to detect and diagnose faults as future work. Finally, a programming strategy to extend the proposed method to large scale analogue circuit designs has also been described.

Martin and Aguado [33] proposed a new approach of digital relays for transmission line protection. The proposed technique consists of a preprocessing module based on discrete wavelet transforms (DWTs) in combination with an artificial neural network (ANN) for detecting and classifying fault events.

Megahed et al. [34] presents a new method for the boundary protection of series-compensated transmission lines, as well as fault classification. This boundary protection is based on detecting distinct frequency bands contained in the transient fault current wave.

[35] is a Wavelet Toolbox user's guide. It provides knowledge of wavelet programming language in MATLAB.

1.3 CONTRIBUTIONS OF THIS THESIS

The focus of the present work is to develop a technique to identify single phasing by using fuzzy inference system and classify it in presence of distributed generation. Researchers in [1] proposed ANN based detection and classification of single phasing in distribution systems with high penetration of distributed generation. Fault detection and classification [25, 26, 27] have also

been developed using ANN scheme. However, the disadvantage of these ANN based methods is that it requires tedious training process which requires large training data set to learn the relationship between no-fault and fault patterns with varying fault parameters. Also, the selection of the transfer functions, number of hidden layers, number of neurons, mean square error goal, training algorithms and epochs to achieve a good performance in training is not an easy task. Hence, a method without training and without complex computation will be better, such as proposed fuzzy based scheme.

1.4 TEST SYSTEM MODELING

A normal distribution system has time graded, current graded or combination of both time and current graded protection scheme against any type of short circuit fault. Again if current of any one phase becomes zero i.e. open circuit fault occurs, it can be easily detected by sensing current using current unbalance relay. Now, renewable resources like wind farm, solar farm, tidal energy etc. are connected to the system for the development of micro-grid. In this scenario, if an open circuit fault occurs in the system, the lost phase will continuously get supply from the renewable sources and it can't be detected by current unbalance relay. In this thesis a radial distribution system is taken for experiment and study the single phasing event in presence of wind farm.

The test system of [1] has been considered here, the schematic diagram of which is shown in Fig. 1. The test system is a 25 kV radial distribution system which is feeding three loads (Load 1, Load 2 and Load 3). It is connected with a grid of 120kV, 500 MVA through a line of 12.5 km using a star delta step down transformer of 120/25 kV, 600 MVA. The system is also fed with a wind farm of 690 V, 9MVA through a line of 12.5 km using star delta step up transformer of 690 V/ 25 kV, 10.5 MVA. The rating of Load 1 and Load 2 are 500 kW and 375kVAR and that of Load 3 is 1 MW, 750 MVA. All the loads are connected to the distributor through lines of 6 km each. A star connected capacitor bank of 8.5 MVAR is connected to the grid to consider the effect of transient due to capacitive switching. Load 3 is considered as the sensitive load, the current signals of which are analyzed to detect single phasing condition.

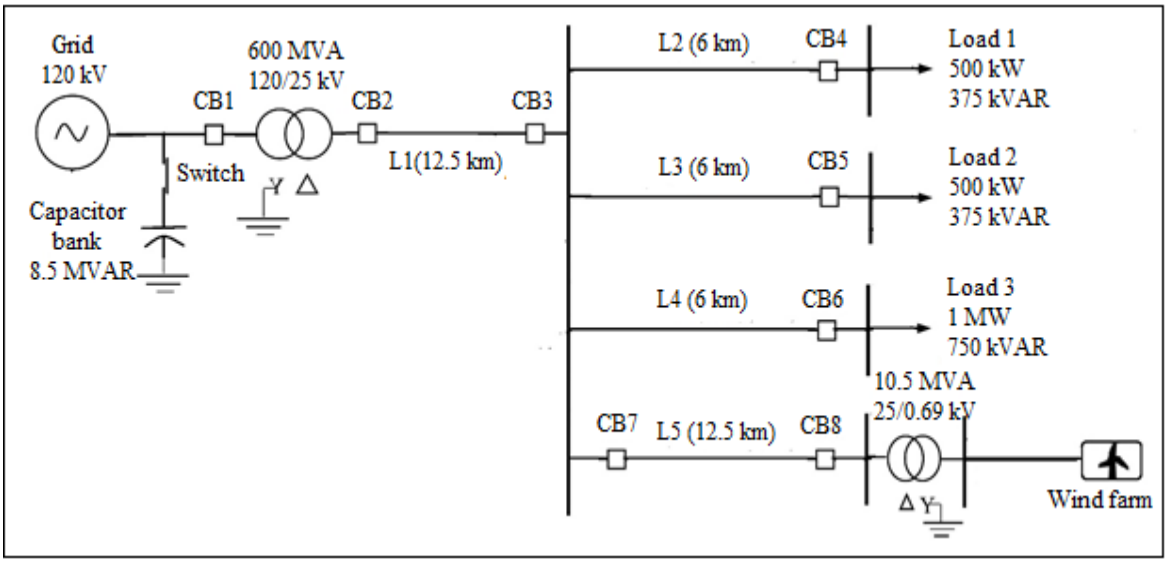

Fig.1.1 Single line diagram of test model

The windfarm used in test model has three wind turbine. The mechanical output of each turbine is 1.5 MW with inertia constant of 4.32 MJ/ MVA. The normal operation wind speed range of wind turbine must be between 6 m/s and 30 m/s. Each turbine is connected with a 6 pole doubly-fed induction generator. The rating of each induction generator is 690 V, 3 MVA. All the lines present in system is modeled as nominal pi model with resistance of 0.012 ohms/ km, inductance of 0.93 mH/ km and capacitance of 12.74 nF/ km.

In the absence of DG, if there is single phasing then the current in the lost phase becomes zero Fig 2. But in presence of DG this is not the case. Fig. 3 shows the rms current in the three phases in load 3 under single phasing condition. It is seen that the rms currents in the three phases changes from 1 p.u. when single phasing occurs at 6.25 km from CB2 in line L1 at t=18 second, but none of the phase currents are zero.

A high impedance fault (HIF) has been modeled to evaluate the proposed method of this work. Some models of HIF have been proposed in the past. Two varying time series resistors were used in [28]. A simplified two-diode model of HIF, shown in Fig. 1.4, has been used in the simulation to model arcing fault involving sandy soil [29].

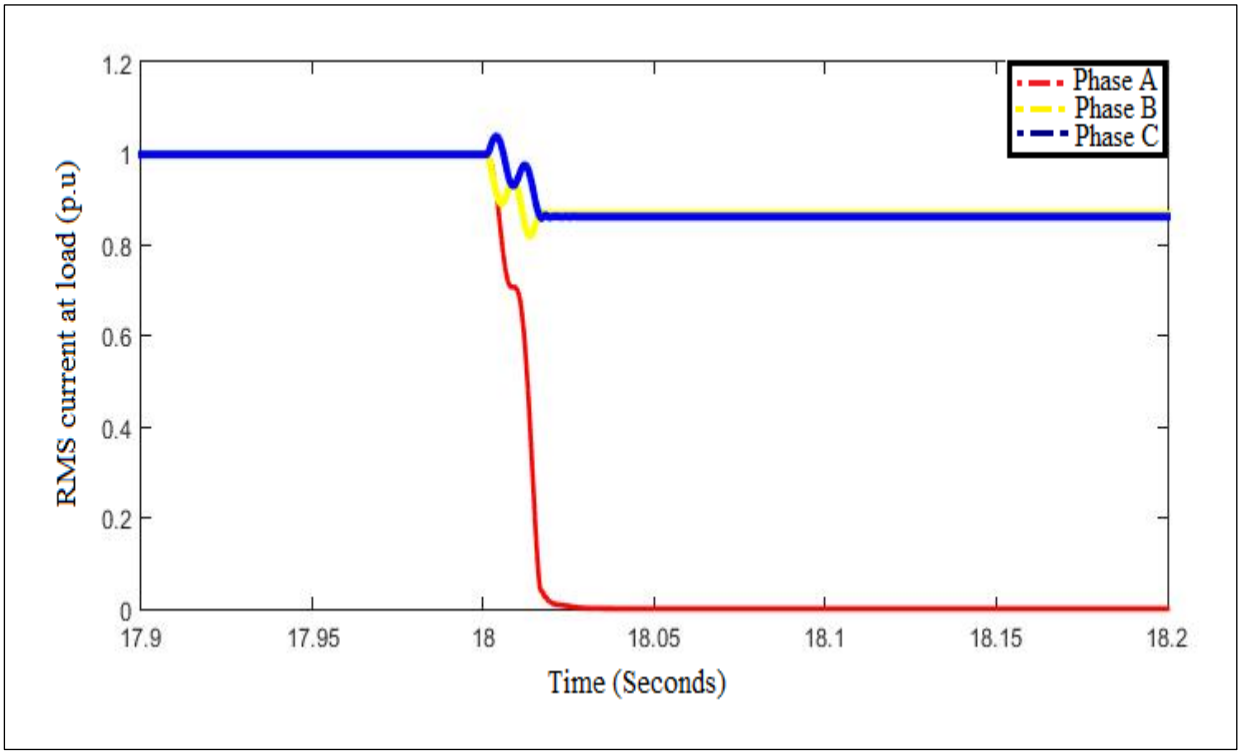

Fig. 1.2 RMS Current at sensitive load without presence of DG unit

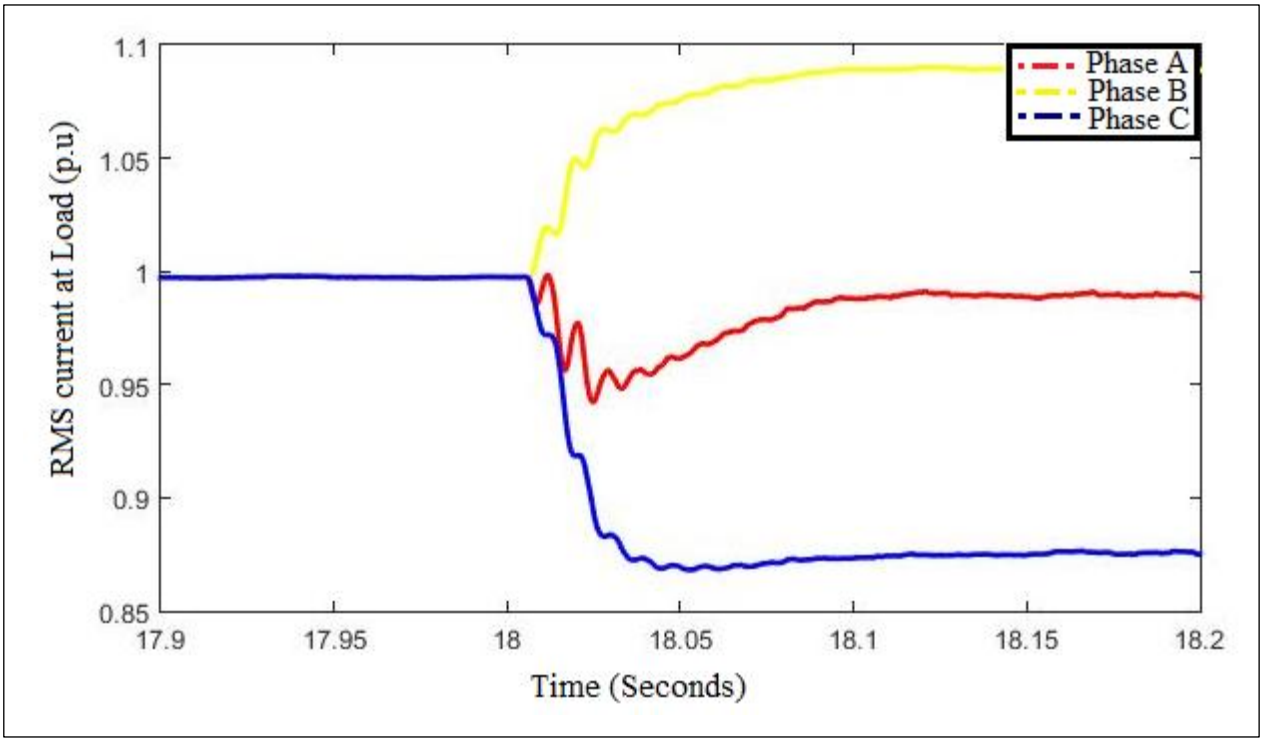

Fig. 1.3 RMS current at sensitive load in presence of DG units

The model comprises of two DC sources, V_p and V_n, which represent the inception voltage of air in soil and the distribution line. The two variable resistances, R_p and R_n, represent the fault resistances. Different values of resistors allow asymmetric fault current modelling. If $V_{phase}>V_p$, the fault current flows towards the ground. The fault current reverses when $V_{phase}<Vn$. For $V_n \leq V_{phase} \leq V_p$, no fault current flows.

Also, a nonlinear load is added to evaluate the proposed method of this work. A DC load is used here as nonlinear load. The DC load is connected in parallel to the load 2 with the help of a transformer and converter. The rating of the load is 4.8 kV dc, 75 kW. The converter is a three phase thyristor bridge type rectifier. The rating of transformer is 25 kV/ 3.6 kV, 200 kVA star delta type.

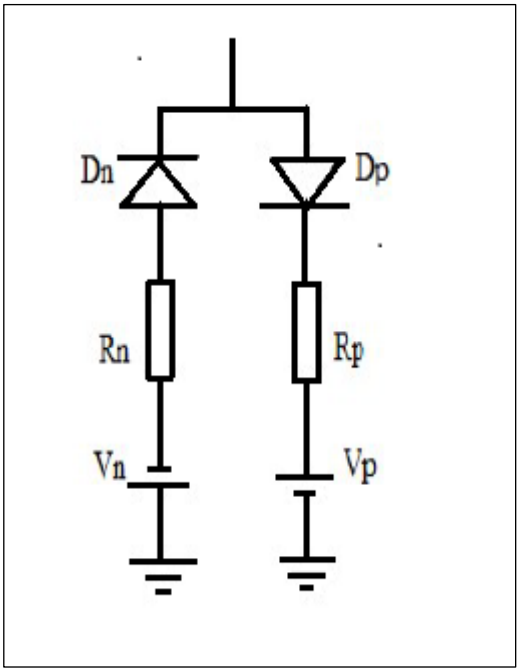

Fig. 1.4 HIF model

1.5 OBJECTIVES OF THE PRESENT WORK

The main objectives of the present work are summarized as follows:

- To review the algorithm available in the literature for detection and classification of single phasing in presence of DG units in power distribution system.
- To develop the MATLAB/SIMULINK model of power distribution system with DG units.
- To analyze modal signal formed using three phase current at sensitive load.

- To calculate the spectral energies of the low frequency component of modal signal using db4 discrete wavelet transform.
- To detect and classify the single phasing event with the help of fuzzy inference system using the spectral energies.

1.6 ORGANIZTION OF THE THESIS

This dissertation consists of six chapters. The chapters are organized as follows:

Chapter-1 gives a brief introduction on single phasing in distribution system in presence of DG units and it includes literature survey on detection and classification of single phasing. The objective, contribution, test model and organization of this dissertation are also presented.

Chapter-2 provides the concept of wavelet transform. Brief discussions on discrete wavelet transform and implementation of wavelet transform are presented.

Chapter-3 provides the concept of fuzzy inference system. Brief discussions on fuzzy inference system and implementation of fuzzy inference system are presented.

Chapter-4 presents the proposed methodology to detect and classify of single phasing in presence of DG units and software implementation in MATLAB/Simulink of this dissertation.

Chapter-5 discusses the simulation results.

Chapter-6 presents the conclusions and future scope of this dissertation.

CHAPTER 2

WAVELET TRANSFORM

Most of the signal are in their raw format in time domain. It means signal is a function of time. But, it is observed in several cases that, the significant information is hidden in the frequency domain of the signal. Frequency is nothing but the rate of change of the variable, which is measured in periodic cycle per second. The analysis of frequency domain is mainly done by gathering information of frequency spectrum of the signal. Frequency spectrum is the existing frequencies in the signal. Fourier transform is oldest technique to analyze a signal in frequency domain. In late nineteenth century, Wavelet transform became popular in the field of frequency analysis of a signal. Wavelet transform is capable to extract those information, which are not directly available from the original signal.

Wavelet analysis has attracted much attention recently in signal processing. It has been successfully applied in many applications such as transient signal analysis, image analysis, communication systems, and other signal processing applications. It is not a new theory in the sense that many of the ideas and techniques involved in wavelets were developed independently in various signal processing applications and have been known for some time. The new development of recent results on the mathematical foundations of wavelet provides a unified framework for the subject.

Within this framework a common link is established between diversified problems that are of interest to different fields, including electrical engineering (signal processing, data compression), mathematical analysis (harmonic analysis, operator theory), etc. Wavelet theory has become an active area of research in these fields. There are opportunities for further development of both the mathematical understanding of wavelets and a wide range of applications in science and engineering.

Like Fourier analysis, wavelet analysis deals with expansion of functions in terms of a set of basic functions. Unlike Fourier analysis, wavelet analysis expands functions not in terms of trigonometric polynomials but in terms of wavelets, which are generated in the form of translations

and dilations of a fixed function called mother wavelet. The wavelet obtained in this way has special scaling properties. They are localized in time and frequency, permitting a closer connection between the function being represented and their coefficients. Greater numerical stability in the reconstruction and manipulation is ensured. The objective of wavelet analysis is to define these powerful wavelet basis functions and find efficient method for their computations. It can be shown that every application using the fast Fourier transform (FFT) can be formulated using wavelets to provide more localized temporal and frequency information.

In this research work wavelet transform has been used to extract useful information from the modal signal. A wavelet is a waveform effectively of limited duration with zero average value, whereas, Fourier analysis is splitting up of a signal into sine waves of various frequencies. Similarly, wavelet analysis is the breaking up of a signal into shifting and scaling version of the signal. A function which is called wavelet, is multiplied with the signal like the window function in short time Fourier transform. Hence a brief overview on Fourier transform and short time Fourier transform has been presented in the next section before discussing wavelet transform.

2.1 FOURIER TRANSFORM

Fourier transform is most popular and oldest analysis in frequency domain of signals. Fourier transform is a reversible transform, i.e. Fourier transform converts time domain signal into frequency domain signal and also vice-versa. The problem with the time domain signal is that it does not have any information about frequency. Again frequency domain signal does not have any information about time. So, either time or frequency is only available at a time.

Stationary signals are the signals whose frequency content does not change with time. In such cases, all frequency components are present at all time. Hence, Fourier transform is suitable for stationary signals. Non-stationary signals are the signals whose frequency content does change with time. Fourier transform of the non-stationary signal provides the frequency content of the signal, but it does not provide any information about time corresponding to the respective frequency component. In such cases, it is important to know the time with respect to the frequency spectrum. Hence, Fourier transform is not suitable for non-stationary signals.

Fourier transform of a time domain signal, $x(t)$ can be obtained as given below:

$$X(f) = \int_{-\infty}^{\infty} x(t).\, e^{-2j\pi ft}\, dt \qquad \ldots 2.1$$

Inverse Fourier transform of a frequency domain signal $X(f)$ can be obtained as given below:

$$x(t) = \int_{-\infty}^{\infty} X(f).\, e^{2j\pi ft}\, df \qquad \ldots 2.2$$

Fourier transform can be applied effectively for analyzing the frequency content of any signal, if the entire time of the signal is taken for analysis. Short time Fourier transform (STFT) which uses a sliding window, can also be used to find information of both frequency and time. The basic formula for Short time Fourier transform is:

$$STFT_x^{(w)}(t,f) = \int [x(t).\, w^*(t-t')].\, e^{-2j\pi ft}\, dt \qquad \ldots 2.3$$

However, the window length limits the resolution of frequency. The wavelet transform is the ultimate solution of these problems. Small wavelets having limited duration are considered in wavelet transform.

2.2 WAVELET TRANSFORM

Wavelet Transform (WT) is capable to extract the time and frequency domain information simultaneously and hence providing a time-frequency representation of the signal. Wavelet transform gives the information about which frequency band occurs at what time interval. The wavelet analysis is easier to implement and much more compact. The signals can be represented compactly and in several levels of resolution, using the powerful multi resolution analysis, which is the major strength of wavelet analysis.

Consider a complex valued function ψ satisfying the following Conditions:

$$\int_{-\infty}^{\infty} |\psi(t)|^2 dt \; < \; \infty \qquad \ldots 2.4$$

$$C_\varphi = \int_{-\infty}^{\infty} \frac{|\Psi(\omega)|^2}{|\omega|} d\omega \; < \; \infty \qquad \ldots 2.5$$

where, Ψ is the Fourier transform of ψ.

The first condition implies finite energy of the function ψ, and the second condition, the admissibility condition, implies that if $\Psi(\omega)$ is smooth then $\Psi(0) = 0$. If ψ satisfies above two conditions, then the function ψ is called the mother wavelet. So, mother wavelet is a wavelet that

integrates to zero and is square integral i.e., has finite energy and satisfy the admissibility condition. It is a prototype for generating other window functions. Scale represents the frequency parameter and translation represents the location of the window.

Continuous Wavelet Transform (CWT) is computed by changing the scale of the analysis window, shifting the window in time, multiplying by the signal and integrating over all time. If ψ satisfies the conditions described above, then the wavelet transform of a real signal s(t) with respect to the wavelet function $\psi(t)$is defined as:

$$S(b,a) = \frac{1}{\sqrt{a}} \int_{-\infty}^{\infty} \psi' \left(\frac{t-b}{a}\right) s(t) dt \quad \ldots 2.6$$

where ψ' denotes the complex conjugate of ψ, and this is defined on the open (b, a) half plane ($b \in R, a > 0$). The parameter b corresponds to the time shift and the parameter a corresponds to the scale of the analyzing wavelet.

The mother wavelet function $\psi_{a,b}(t)$ is defined as

$$\psi_{a,b}(t) = a^{-1/2} \psi \left(\frac{t-b}{a}\right) \quad \ldots 2.7$$

which means rescaling by a and shifting by b, equation 2.6 can be written as scaler or inner product of the real signal s(t) with the mother wavelet function $\psi_{a,b}(t)$.

$$S(b,a) = \int_{-\infty}^{\infty} \psi'(\mathrm{t}) \mathrm{s}(\mathrm{t}) \mathrm{dt} \quad \ldots 2.8$$

When function $\psi(t)$ satisfies the admissibility condition, equation 2.5, the original signal s(t) can be obtained from the wavelet transform S(b,a) by the following inverse formula:

$$s(t) = \frac{1}{C_\psi} \int_{-\infty}^{\infty} \int_{-\infty}^{\infty} S(b,a) \psi_{a,b}(t) \frac{dadb}{a^2} \quad \ldots 2.9$$

In Discrete Wavelet Transform (DWT), filters of different cutoff frequencies are used to analyze the signal at different scales. The signal is passed through a series of high pass filters to analyze the high frequency components and it is passed through a series of low pass filters to analyze the low frequency components. In the discrete domain, if the scale and shift parameters are discretized as $a = a_0^m$ and $b = nb_0$, then the analyzing wavelets are discretized as follows:

$$\psi_{m,n}(t) = a_0^{-\frac{m}{2}} \psi(\frac{t - nb_0}{a_0^m}) \quad \text{...2.10}$$

where, m and n have integer values. The discrete wavelet transform and its inverse transform are defined as follows:

$$S_{m,n} = \int_{-\infty}^{\infty} \psi'_{m,n}(t) s(t) dt \quad \text{...2.11}$$

$$s(t) = k_\psi \sum_m \sum_n S_{m,n} \psi_{m,n}(t) \quad \text{...2.12}$$

where k_ψ is a constant value for normalization. The function $\psi_{m,n}(t)$provides sampling points on the scale time plane: linear sampling in the time direction but logarithmic in the scale direction. The most common situation is that when a_0 is chosen as:

$$a_0 = 2^{1/V} \quad \text{…2.13}$$

where *V* is an integer, and that *V* pieces of $\psi_{m,n}(t)$ are processed as one group, which is called a voice. The integer V is the number of voice per octave. This is analogous to use of a set of narrowband filters in conventional Fourier analysis. Wavelet analysis is not limited to dyadic scale analysis. By using an appropriate number of voices per octave, wavelet analysis can effectively perform the 1/3-octave, 1/6-octave, or 1/12- octave analyses that are used in acoustics.

Wavelet transform is an efficient mean of analyzing transient currents and voltages. A wavelet-based signal processing technique is an effective tool for power system transient analysis and feature extraction [30]. The time domain signal passes through numerous low pass and high pass filters, which filter either the low or high frequency part of the signal [31]. This process is repeated, and each time a certain part of the signal equivalent to some frequencies is removed from the signal. A set of basic function called wavelets, are used to decompose the signal in various frequency bands, which are obtained from mother wavelet by dilation and translation. Hence the amplitude and incidence of each frequency can be found precisely. Unlike Discrete Fourier Transform (DFT), WT not only analyzes the signal in frequency bands but also provides non-uniform division of frequency domain, i.e., WT uses short window at high frequencies and long window for low frequencies [32]. This helps to analyze the signal in both frequency and time domains effectively. WT is able to provide the frequency and time information simultaneously, thus provides the time-frequency representation of the given signal. WT can detect the low

frequency and high frequency precisely. One of the main properties of the WT is that it has the great ability to locate the signal's short-time high frequency features and determine the low frequency performance.

There are various types of mother wavelets i.e., Haar, Symlets, Meyer, Discrete Mayer and Daubechies. WT can extracted information from a portion of an unknown signal using correlation with the mother wavelet ψ under a determined position and scale. Basically, wavelet transform is used to evaluate the non-stationary signals, those frequency response changes with time.

Wavelet Transform is a technique in which the decomposition of the signal will form not one, but many wavelet bases out of which one may choose the appropriate one to analyze the signal in a better way. For many signals, the low-frequency content is the most important part. It provides identity of a signal. One the other hand, the high frequency content imparts nuance. The approximations are the high scale, low frequency components of the signal. The details are the low scale, high frequency components. The most basic level of the filtering process is as shown in Fig 2.1.

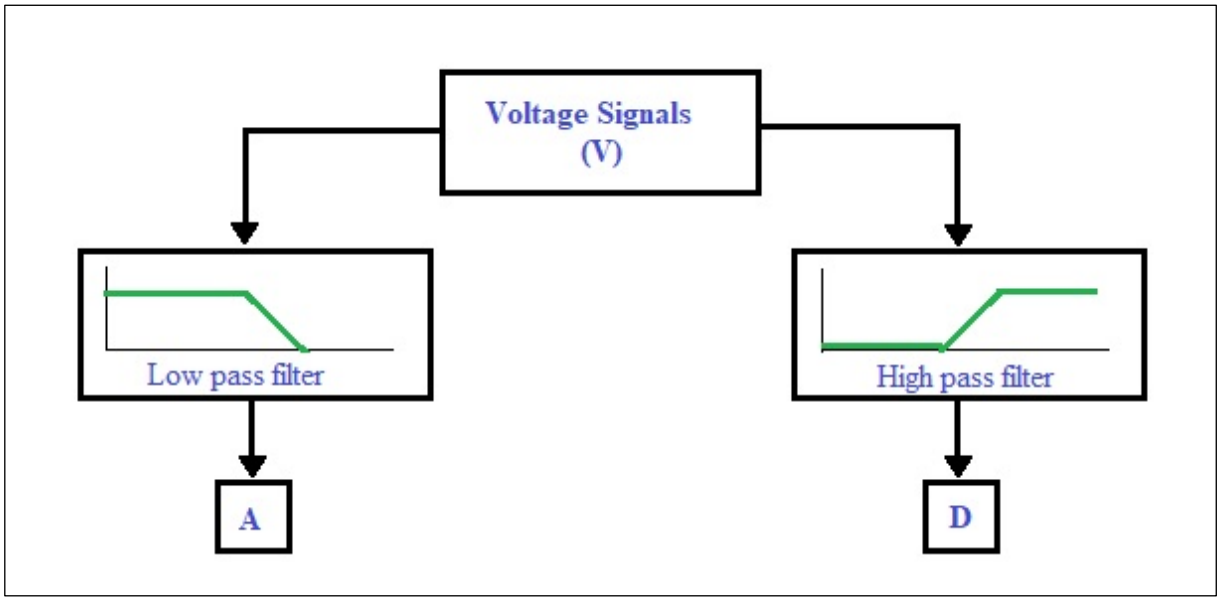

Fig 2.1 Extraction of Approximation (A) and Details (D) from of a voltage signal.

The original signal is filtered and then sampling is done in DWT. This process reduces the data, but necessary information is kept unaltered [33]. Signal can be analyzed at different frequency bands in DWT process. Two data sequences cA and cD are obtained after the process as shown in

Fig. 2.2. Approximation (cA) part of the signal consists of low frequency and high scale components of the signal while detail (cD) consists of high frequency and low scale components of the signal [34].

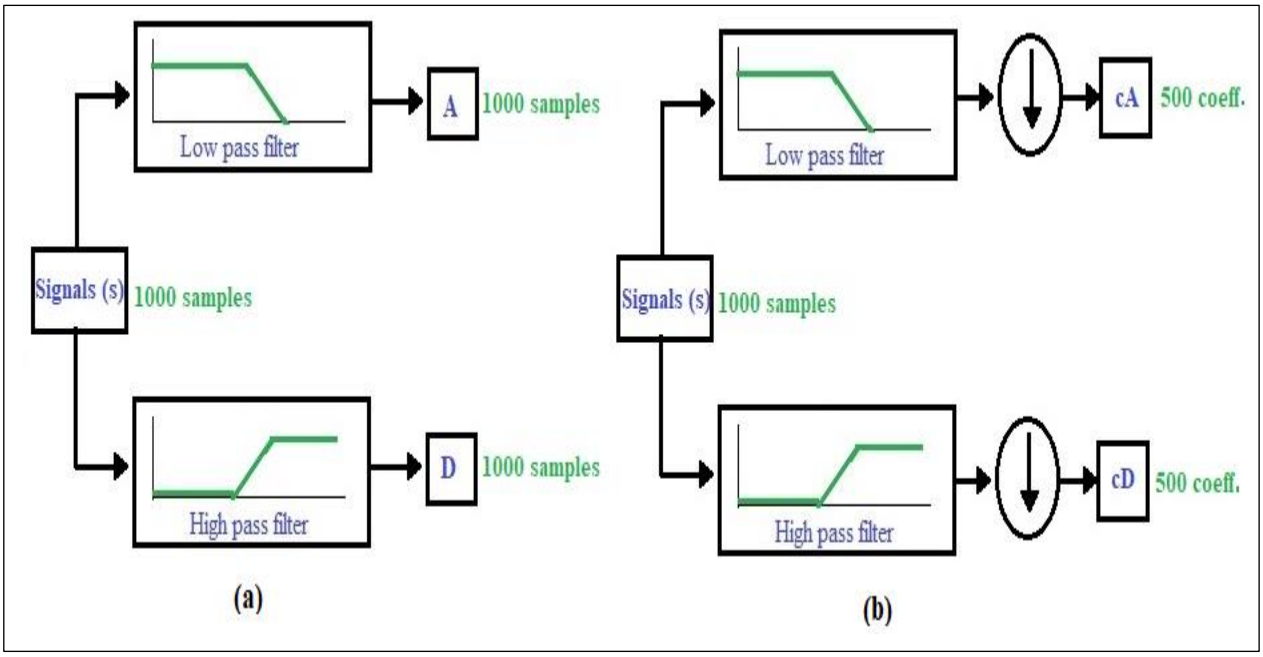

Fig. 2.2 Signal without and with down sampling
(a) Without down sampling (b) With down sampling

The resolution of the signal which is the measure of the amount of detail information in the signal is changed by the filtering operations and the scale is changed by up sampling and down sampling operations. Down sampling a signal corresponds to reducing the sampling rate or removing some of the samples of the signal. Down sampling by a factor *n* reduces the number of samples in the signal by *n* times. Up sampling a signal corresponds to increasing the sampling rate or adding new samples to the signal.

The sequence of the signal in discrete time function is denoted by *x[n]*, where *n* is an integer. The procedure starts with passing this signal i.e., sequence *x[n]* through a half band digital low pass filter with impulse response *h[n]*. A half band low pass filter removes all frequencies that are above half of the highest frequency in the signal. For example, if a signal has a maximum of 1000 Hz component, then half band low pass filtering removes all the frequencies above 500 Hz.

2.2.1 WAVELET FILTER BANK

The DWT analyzes the signal at different frequency bands with different resolutions and decomposes the signal into a coarse approximation and detail information. DWT employs two sets of functions called wavelet function and scaling functions which are associated with high pass and low pass filter respectively. The decomposition of the signal into different frequency bands is obtained by successive high pass and low pass filtering of the time domain signal.

The original signal *x[n]* is first passed through a half band high pass filter *g[n]* and a low pass filter *h[n]*. In discrete signals, frequency is expressed in terms of radians. The sampling frequency of the signal is equal to 2π radian in terms of radial frequency. Therefore, the highest frequency that exists in a signal will be π radian, if the signal is sampled at the twice of the maximum frequency present in the signal i.e. at Nyquist's rate. After passing the signal *x[n]* through a half band low pass filter, half of the samples will be eliminated. According to Nyquist's rule, the signal has a highest frequency of π/2 radian instead of π radian.

The decomposition halves the time resolution since only half the number of samples characterizes the entire signal. However, this operation doubles the frequency resolution. So the frequency band of the signal spans in time domain only half the previous frequency band, thus effectively reducing the uncertainty in the frequency to half. The above procedure can be repeated for further decomposition. At every level, the filtering and down sampling will result in half the number of samples i.e. the time resolution and half the frequency band spanned i.e. double frequency resolution. Fig 2.3 illustrates this procedure, where *x[n]* is the original to be decomposed, *h[n]* and *g[n]* is low pass and high pass filter respectively. For example, assume that the original signal *x[n]* has 1024 sample points, spanning a frequency band of zero to π rad/s. At the first decomposition level, the signal is passed through the high pass and low pass filters, followed by down sampling by 2. The outputs of the high pass filters have 512 sample, hence half the time resolution, but it only spans the frequency from π/2 to π rad/s. These 512 samples constitute the first level of DWT coefficients and also called detail coefficients at level 1 i.e., d1. The output of the low pass filter also has 512 samples, but it spans the other half of the frequency band, frequencies from 0 to π/2 rad/s and

called as approximation coefficients at level i.e., a1. This signal is then passed through the same low pass and high pass filters for further decomposition. The output of the second low pass filter i.e. a2 followed by down sampling has 256 samples, spanning a frequency band from 0 to π/4 rad/s and the output of the second high pass filter followed by down sampling has 256 samples spanning a frequency band from π/4 to π/2 rad/s. The signal has half the time resolution, but twice the frequency resolution of the first level signal. The low pass filter output is then filtered once again for further decomposition.

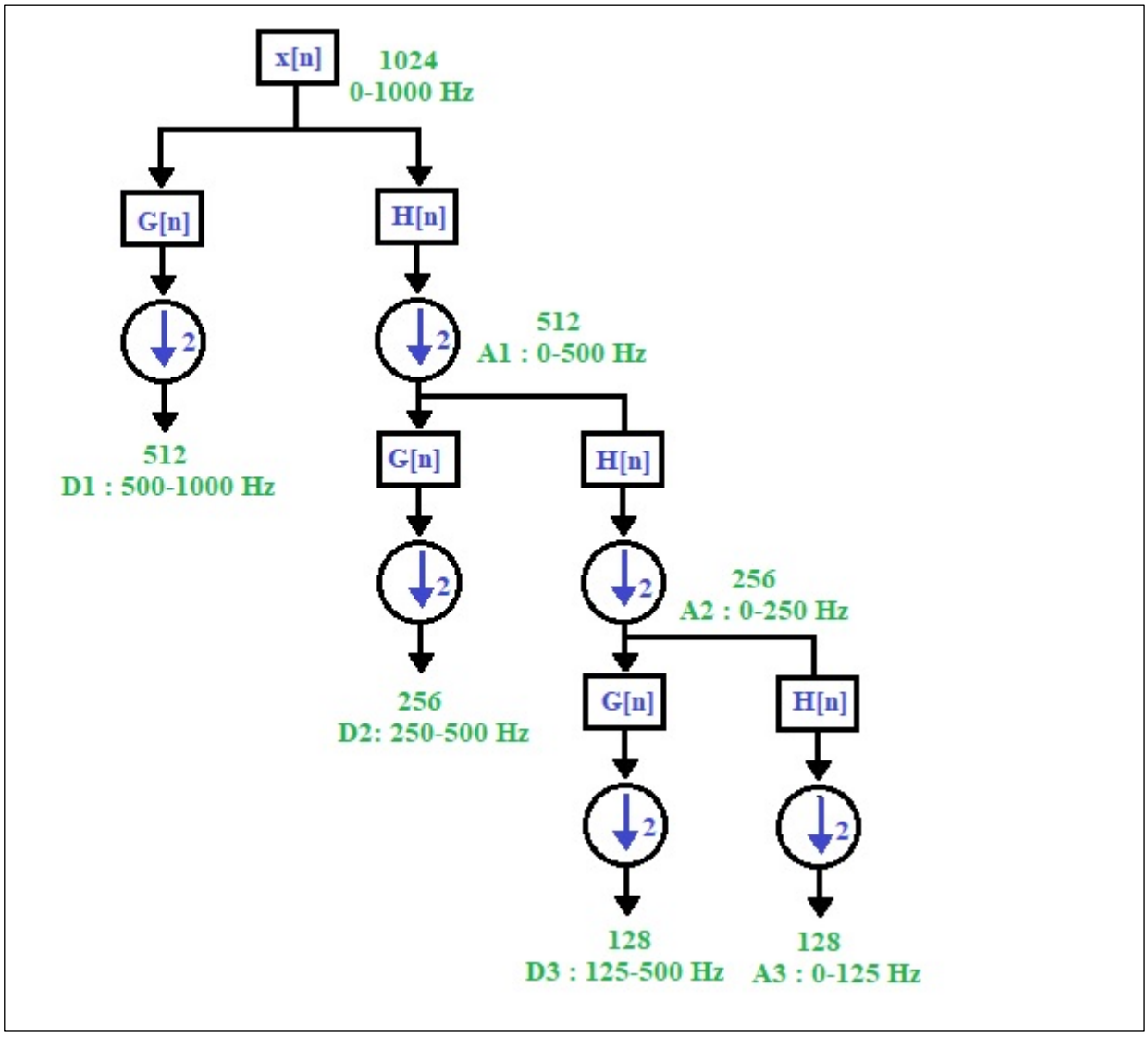

Fig. 2.3 Three level filter bank

This process may continue upto desired level of decomposition each having half the number of samples of the previous level. The DWT of the original signal is then obtained by concatenating all coefficients starting from the last level of decomposition. Then, DWT will have the same number of samples of coefficient as the number of samples of the original signal. Let us assume that the original signal is one cycle of a distorted sinusoidal signal, as shown in Fig. 2.4 (a). We used db4 wavelet for single level decomposition. The reconstructed versions of each detail and the approximation are shown in Fig. 2.4 (b). The information of original signal is clearly represented at each frequency band. The original signal can be reconstructed by adding up those wavelet signals at the same sample point. The wavelet toolbox in MATLAB provides a lot of useful techniques for wavelet analysis [35].

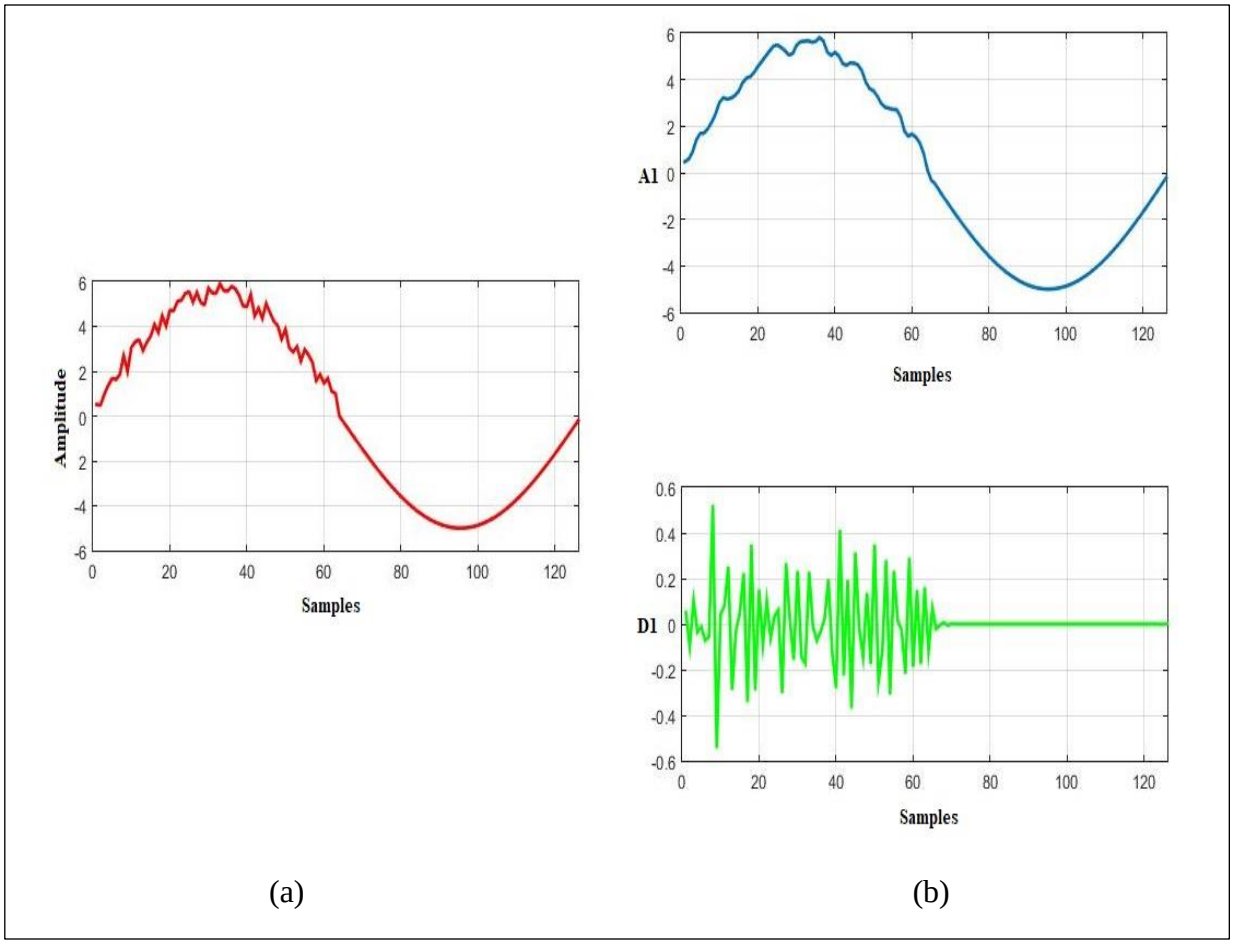

Fig. 2.4 Wavelet multi-resolution analysis

(a) Original signal (b) Decomposed Signal

The reconstructed detail and approximations are true constituents of the original signal. Thus the original signal is obtained as: $S = A_1 + D_1$.

2.2.2 SELECTION OF MOTHER WAVELET

Selecting an appropriate wavelet function is important. Choosing an improper wavelet function will make the wavelet transform complex and difficult. There are many types of mother wavelets such as Haar, Daubechies, Coiflet and Symmlet wavelets. One of the most popular and widely known orthonormal wavelet is Daubechies wavelet. In this research, Daubechies family wavelet is selected as mother wavelet. This is because the decomposition solution using Daubechies wavelet is orthogonal, compactly supported and no marginal overlaps will happen during the signal reconstruction. The Daubechies wavelet is further categorized into db1, db2 etc. for the purpose of frequency range discretion. Different kinds of Daubechies wavelets are derived. The db4 is chosen in this thesis because it gives a more accurate solution, minimum reconstruction error and is widely used. Daubechies wavelet transform is fundamentally same as Haar wavelet transform, the only difference is in the contents of wavelet and scale function. DWT using db4 will often produce less fluctuations than those produced by the other Daubechies transforms.

CHAPTER 3

FUZZY INFERENCE SYSTEM

A fuzzy logic calculus is a kind of logic in which the truth values are fuzzy subsets of the set truth values of a non-fuzzy many valued logic. Thus, a simple many-valued logic has a fix number of truth values, while a fuzzy logic has a free number of truth values; it will be the user who will choose each time, how many truth values he or she wants to employ. The user will find the truth-values of the fuzzy system inside the evaluation set of the many valued calculus, which is the basis of the fuzzy system. This freedom in choice, of how many truth values are to be employed, makes Fuzzy logic a dynamic device to treat the complex phenomena.

Fuzzy Logic is a logic built over a polyvalent logic. The Fuzzy Logic system was proposed by Zadeh in 1975. The basic of Fuzzy Logic system is many valued logic in which the set of truth values contains all the real numbers of the interval [0, 1]. Fuzzy logic can take "linguistic" truth values which belong to a set *T* of infinite cardinality: *T = {True = {Very True, Not very True, More or less True, Not True,…}, False = {Very False, Not very False, More or less False, Not False,…},…}*. Each linguistic truth value of Fuzzy Logic is a fuzzy subset of the set *T* of the infinite numeric truth values. The employment of linguistic truth values permits to formulate vague answer to vague questions.

In a wide sense, Fuzzy Logic is a form of soft computing method which accommodates the imprecision of the real world. Fuzzy Logic is an extension of multivalued logic whose objective is approximate reasoning rather than exact solution. Unlike traditional crisp logic, such as binary logic, where variables may only take truth values i.e. true and false represented by 1 and 0 respectively, but the variables in fuzzy logic may have a truth value that ranges in degree between 0 and 1. Instead of describing absolute yes or no, the truth value, or membership in Fuzzy Logic explains a matter of degree. 0 shows completely false, while 1 expresses completely true, and any value within the range indicates the degree of truth. Furthermore, the concept of membership in Fuzzy Logic is close to human words and intuition, so the number and variety of applications of Fuzzy Logic have increased significantly.

A concrete example permits to understand what is fuzzy truth. To the question “Is Arup YOUNG?” I can answer “It is Very True that Arup is YOUNG”. As we see in this example, Fuzzy Logic works with vague sentences, i.e. with sentences which contain fuzzy predicates. As in this case of truth values, the fuzzy predicates are fuzzy subsets of universe of discourse which is the “age”. Let, a set A contains finite numeric values [0, 100]. Inside the classical set A it is possible to define the linguistic variables (YOUNG, OLD,…) as fuzzy subsets. A = {YOUNG = {Very YOUNG, Not very YOUNG, More or less YOUNG, Not YOUNG,…}, OLD = {Very OLD, Not very OLD, More or less OLD, Not OLD,…},…}. Given that inside the set A = {0, 100}, a subset of values which can be considered internal to the vague concept of “YOUNG ” is e.g. {0, 30}, the employment of modifiers (Very …, Not Very …, More or less …, etc.) makes fuzzy the subset YOUNG.

3.1 BASIC CONCEPTION OF FUZZY LOGIC

The fuzzy inference system is a primary application of fuzzy logic. The main approach of fuzzy inference is taking input variables through a mechanism which is comprised of “If-Then” rules and fuzzy logical operations. “If-Then” rules are expressed directly by human words, and each of the word is regarded as a fuzzy set. All of these fuzzy sets are required to be defined by membership functions before they are used to build “If-Then” rules.

3.1.1 FUZZY SET AND LINGUISTIC VARIABLES

A fuzzy set is an extension of a crisp set. Crisp sets permit only full membership or no membership at all, whereas fuzzy sets permit partial membership. In a crisp set, membership or non-membership of element x in set A is expressed by a characteristic function $\mu(x)$, where $\mu(x)=1$ if $x \in A$ and $\mu(x) = 0$ if $x \notin A$. Fuzzy set theory enlarges this concept by defining partial membership, where $\mu(x)=1$ if $x \in A$; $\mu(x) = 0$ if $x \notin A$ and $\mu(x)= p$ $(0 < p < 1)$if x partially belongs to A. Mathematically, a fuzzy set A on a universe of discourse U is characterized by a membership function $\mu(x)$ that takes values in the interval [0 1] that can be defined as: $U \rightarrow [0,1]$. Fuzzy set represents commonsense linguistic labels viz., very fast, fast, very slow, slow, suitable, moderate, unsuitable etc. A given element can be a member of more than one fuzzy set at a time. A fuzzy set A in U may be represented as a set

of ordered pairs. Each pair consists of a generic element x and its grade of membership function; that is, A = $\{(x, \mu(x)/ x \in U\}$, x is called a support value if $\mu(x)>0$. The concept of a linguistic variable plays important role particularly in fuzzy logic. A linguistic variable is a variable whose values are expressed in words or sentences in natural language. For each input and output variables, fuzzy sets are generated by dividing its universe of discourse into a number of sub-regions and are called linguistic variable.

3.1.2 MEMBERSHIP FUNCTIONS

A membership function (MF) is a curve that defines the feature of fuzzy set by assigning to each element the corresponding membership value, or degree of membership. It maps each point in the input space to a membership value in a closed unit interval [0, 1]. Fig 3.1 shows a general membership function curve. The horizontal axis represents an input variable x, and the vertical axis defines the corresponding membership value $\mu(x)$ of the input variable x. The support of membership function curve explains the range where the input variable will have non-zero membership value. In this figure, $\mu(x) \neq 0$ when x is any point located between point a and point d. While the core of membership function curve interprets the range where the input variable x will have full degree of membership ($\mu(x) = 1$), in other words any arbitrary point within the interval [b, c] completely belongs to fuzzy set.

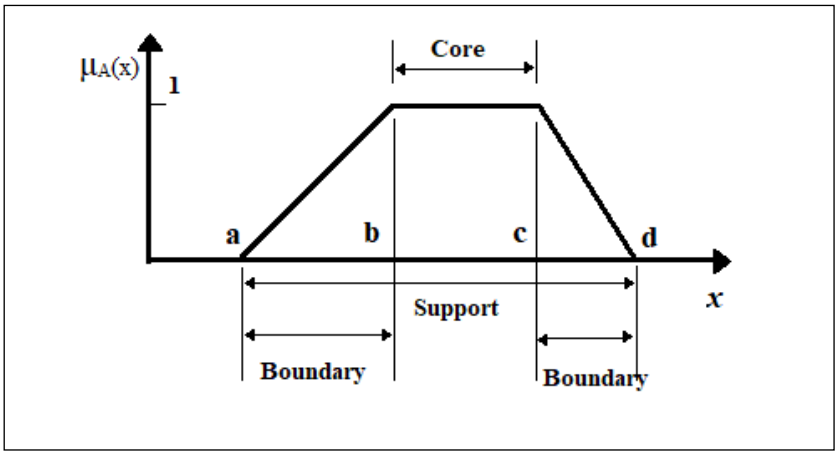

Fig 3.1 Membership function in fuzzy set

Generally, there are five common shapes of membership function: Triangle MF, Trapezoidal MF, Gaussian MF, Generalized Bell MF and Sigmoidal MF. A single MF may

only define one set fuzzy set despite the shape of MF. Usually, more than one MF are used to define a single input variable. The membership functions can be defined by different parameters. For example, triangular curves depend upon parameters a, b, c and expressed as,

$$f(x,a,b,c) = \begin{cases} 0 & (x \le a) \\ \frac{x-a}{b-a} & (a \le x \le b) \\ \frac{c-x}{c-b} & (b \le x \le c) \\ 0 & (c \le x) \end{cases} \quad \ldots 3.1$$

Trapezoidal curves depend upon four parameters a, b, c, d and expressed as

$$f(x,a,b,c) = \begin{cases} 0 & (x \le a) \\ \frac{x-a}{b-a} & (a \le x \le b) \\ 1 & (b \le x \le c) \\ \frac{d-x}{d-c} & (c \le x \le d) \\ 0 & (d \le x) \end{cases} \quad \ldots 3.2$$

Gaussian curves depend upon two parameters σ, m and expressed as

$$f(x,\sigma,m) = e^{-\frac{1}{2}(\frac{x-m}{\sigma})^2} \quad \ldots 3.3$$

3.1.3 LOGICAL OPERATORS

Fuzzy set is related to crisp set operations. Union, intersection and complement are the most crisp elementary set operations like logic gate operation, which relate to OR, AND and NOT operators respectively. Let *P* and *Q* are the two subsets of set *U*. The union operation of *P* and *Q* is denoted as $P \cup Q$ i.e. this operation includes all points from either P or Q, $\mu_{P\cup Q}(x) = 1$ for all $x \in P$ or $x \in Q$. The compliment operation of *P* denoted as P' i.e. it includes all points excluding the points in P, $\mu_{P'}(x)=1$ if $x \notin P$and $\mu_{P'}(x)=0$ if $x \in P$. Also the intersection operation of *P* and *Q* is denoted as $P \cap Q$. It includes all common points from *P* and *Q* and mathematically expressed as $\mu_{P\cap Q}(x) = 1$ for all $x \in P$ and $x \in Q$.

In fuzzy logic, OR, AND and NOT operators are represented as max, min and complement respectively and they are expressed as

$$\mu_{P\cup Q}(x) = \max[\mu_P(x), \mu_Q(x)]$$

$$\mu_{P\cap Q}(x) = \min[\mu_P(x), \mu_Q(x)]$$

$$\mu_{P'}(x) = 1 - \mu_P(x) \qquad \ldots 3.4$$

The union operation of two fuzzy sets P and Q are defined by a binary mapping S that aggregates two MFs as

$$\mu_{P\cup Q}(x) = S[\mu_P(x), \mu_Q(x)] \qquad \ldots 3.5$$

These fuzzy union operators are known as S-norm operators and they fulfill the following binary mapping T:

Boundary:	$S(1,1) = 1,\ S(a,0) = S(0,a) = a$
Monotonicity:	$S(a,b) \leq S(c,d)$ if $a \leq c$ and $b \leq d$
Commutatively:	$S(a,b) = S(b,a)$
Associatively:	$S(a,S(b,c)) = S(S(a,b),c)$ …3.6

The fuzzy intersection operator is expressed by the binary mapping T:

$$\mu_{P\cap Q}(x) = T[\mu_P(x), \mu_Q(x)] \qquad \ldots 3.7$$

These fuzzy intersection operations are specified as Triangular norm (T-norm) operators and they fulfill the below basic conditions:

Boundary:	$T(1,1) = 1, T(a,0) = T(0,a) = a$	
Monotonicity:	$T(a,b) \leq T(c,d)$ if $a \leq c$ and $b \leq d$	
Commutatively:	$T(a,b) = T(b,a)$	
Associatively:	$T(a,T(b,c)) = T(T(a,b),c)$	…3.8

3.1.4 IF-THEN RULES

A fuzzy system is a combination of if-then rules that associate with a string input of linguistic variable to an output variable. In the process of fuzzy inference, If-Then rules create a parallel deducing mechanism that indicates how to input variable onto output space. A single fuzzy If-Then rule is expressed as

If x is P, Then y is Q …3.9

The first If-section is known as the antecedent, where x is the input variable. The second Then-section is known as the consequent, where y is output variable. The reason behind the universal acceptance of If-Then conditional statements is that both P and Q are linguistic values, or adjectives in most cases, and this expression of conditional statement works in concordance with human judgment. For example, an appropriate If-Then rule might be “If material hardness is soft, Then cutting speed is high”. *P* can be regarded as fuzzy set and defined by specific MF, and *Q* can be either a fuzzy set or a polynomial with respect to input *x* depending upon specific FIS method. The If-section in the antecedent is aimed at working out the MF value of input variable *x* corresponding fuzzy set *P*. The Then-section in the consequent which assigns a crisp value back to the output variable *y*.

3.2 FUZZY INFERENCE SYSTEM

A basic fuzzy inference system has four basic blocks and they are Fuzzifier, Knowledge base, Fuzzy inference engine and Defuzzifer. The Fuzzifier converts the crisp input variables into fuzzy input with the help of membership functions that represent fuzzy sets of input vectors. The knowledge base that converts the information given by the expert in the form of linguistic fuzzy rules. An inference engine uses them together with the knowledge base for inference by the method of implication and aggregation. A defuzzifier converts the fuzzy results of the inference into crisp output value using defuzzification method.

The knowledge base comprises of two components: a database which defines the membership functions of the fuzzy sets used in the fuzzy rules, and a rule base comprising a collection of linguistic rules that are joined by a specific operator. Based on the consequent type of fuzzy rules, there are two common types of FIS, which vary according to differences between the specifications of the consequent part given equations 3.8 and 3.9. The first fuzzy system uses the inference method proposed by Mamdani, in which the rule consequence is defined by fuzzy sets and has the following structure.

IF x is P and y is Q THEN z is R …3.10

The second fuzzy system proposed by Takagi, Sugeno and Kang, contains an inference engine in which the conclusion of a fuzzy rule comprises a constant according to equation 3.11a, or a weighted linear combination of the crisp inputs according to equation 3.11b. A fuzzy rule for the zero-order Sugeno method is of the form

IF x is P and y is Q THEN $z = R$ …3.11a

where P and Q are fuzzy sets in the antecedent and R is a constant. The first-order Sugeno model has rules of the form

IF x is A and y is B THEN $z = ax+by+c$ …3.11b

where P and Q are fuzzy sets in the antecedent and a, b, and c are constants.

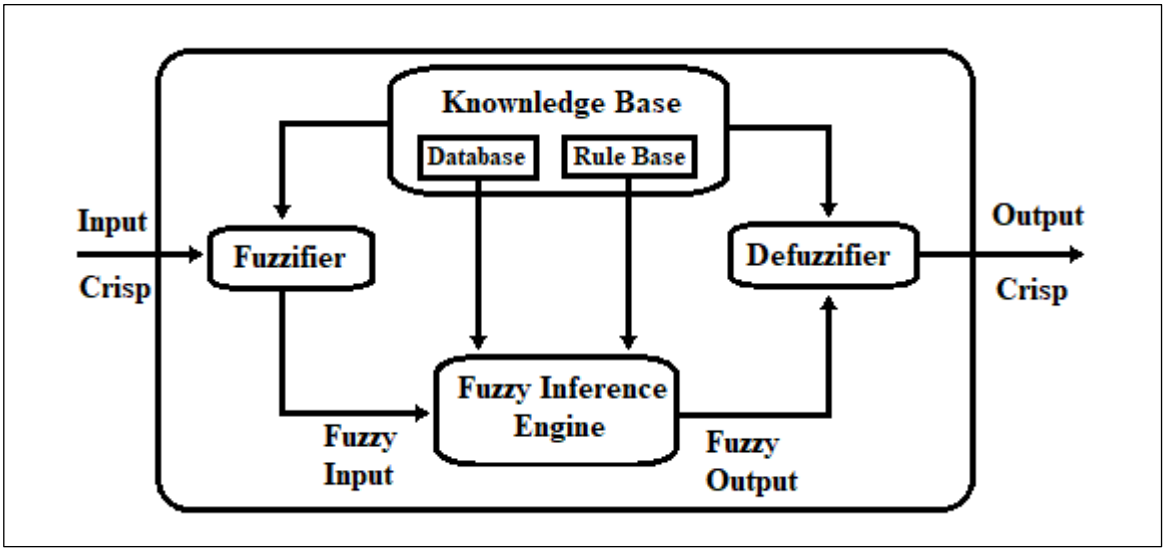

Fig 3.2 Fuzzy Inference System

3.3 FUZZY INFERENCE PROCESS

The fuzzy inference process has five steps. Each step is explained briefly below.

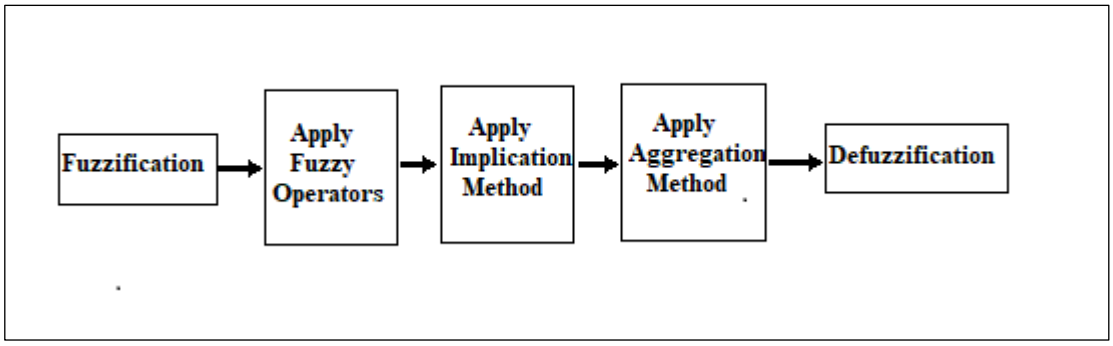

Fig. 3.3 Fuzzy Inference Process

3.3.1 FUZZIFICATION

The first step in evaluating the output of a FIS is to apply the inputs and determine the degree to which they belong via membership function. This is required in order to activate rules that are in terms of linguistic variables. Once membership functions are defined, fuzzification takes a real time input value and compares it with the stored membership function to produce fuzzy input values. In order to perform this mapping, we can use fuzzy sets of any shape, such as triangular, Gaussian, π-shaped, etc.

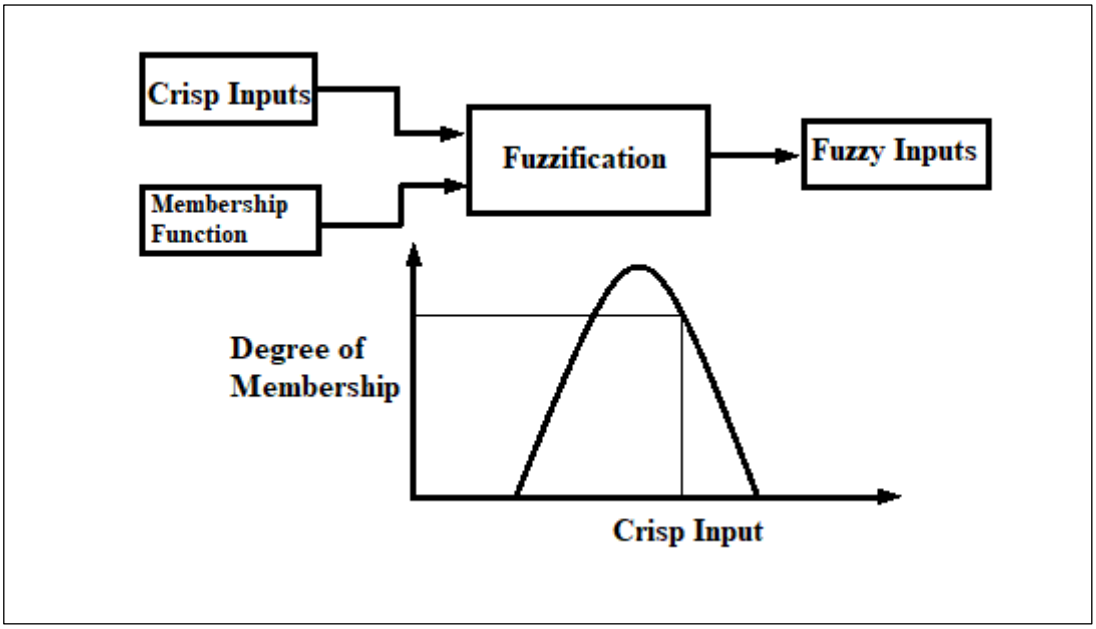

Fig. 3.4 Fuzzification

3.3.2 APPLYING FUZZY OPERATORS

A fuzzy rule base contains a set of fuzzy rule R. A multi-input, single-output system is represented by

$$R = (R_1, R_2, \ldots, R_n) \quad \ldots 3.12$$

where R_i can be expressed as

$$R_i : \text{If } (x_1 \text{ is } T_{x1}, \text{ and } \ldots, x_m \text{ is } T_{xm}) \text{ Then } (y_1 \text{ is } T_{y1}) \quad \ldots 3.13$$

In this rule, m preconditions of R_i form a fuzzy set ($T_{x1} \times T_{x2} \times \ldots \times T_{xm}$), and the consequent is single output. Generally, if-then rule can be interpreted by the following three steps:

- Resolve all fuzzy statements in the antecedent to a degree of membership between 0 and 1.
- If the rule has more than one antecedent, the fuzzy operator is applied to obtain one number that expresses the result of applying that rule. This is known as firing strength or weight factor of that rule. For example, consider that an i^{th} rule has two parts in the antecedent.

$$R_i : \text{If}(x_1 \text{ is } T_{x1}^i, \text{ and } \ldots, x_m \text{ is } T_{x2}^i) \text{ Then } (y \text{ is } T_y^i) \quad \ldots 3.14$$

The weight factor can be defined using either intersection operators equation 3.15 or product operator equation 3.16.

$$\alpha_i = \min\left[\mu_{x1}^i(x_1), \mu_{x2}^i(x_2)\right] \quad \ldots 3.15$$

$$\alpha_i = \mu_{x1}^i(x_1) \times \mu_{x2}^i(x_2) \quad \ldots 3.16$$

- The weight factor is used to shape the output fuzzy set that expresses the consequent part of the rule.

3.3.3 APPLYING IMPLICATION METHOD

The implication method is defined as the shaping of the consequent, which is the output fuzzy set, based on the antecedent. The input for the implication process is a single number given by the antecedent, and the output is a fuzzy set. Minimum or product are two commonly used methods, which are represented by equations 3.17and 3.18, respectively.

$$\mu_y^i(o) = \min\left(\alpha_i, \mu_y^i(o)\right) \quad \ldots 3.17$$

$$\mu_y^i(o) = \alpha_i \times \mu_y^i(o) \quad \ldots 3.18$$

where o is the variable that represents the support value of the membership function.

3.3.4 APPLYING AGGREGATION METHOD

Aggregation takes all truncated or modified output fuzzy sets obtained as the output of the implication process and combines them into a single fuzzy set. The output of the aggregation process is a single fuzzy set that represents the output variable. The aggregated output is used as the input to the defuzzification process. Aggregation occurs only once for each output variable. Since the aggregation method is commutative, the order in which the rules are executed is not important. The commonly used aggregation method is the max method which can be defined as follows:

$$\mu_y(o) = \max\left(\mu_y^i(o), \mu_y^i(o)\right) \quad \ldots 3.19$$

To illustrate the process in Mamdani system, let us consider the following rules having two input variables (X_1 and X_2) in the premise part and one variable (y) in the consequence part.:

Rule 1: If (x_1 is T_{x1}^1 and x_2 is T_{x2}^1) Then (y is T_y^1)

Rule 2: If (x_1 is T_{x1}^2 and x_2 is T_{x2}^2) Then (y is T_y^2)

Suppose that x_1 and x_2 are inputs for the X_1 and X_2 variables respectively. The calculations of weight factor, implication and aggregation methods for these inputs using rules (1 &2) are illustrated in Figure 3.5 and explained as follows:

- The weight factor α_i of each rule is calculated by using the MIN (AND) operator as follows:

Weight factor of Rule 1: $\alpha_1 = \min\left(\mu_{x1}^1(x_1), \mu_{x2}^1(x_2)\right)$ …3.20

Weight factor of Rule 2: $\alpha_2 = \min\left(\mu_{x1}^2(x_1), \mu_{x2}^2(x_2)\right)$ …3.21

- The output fuzzy sets of each rule are obtained by applying weight factor of each rule to the fuzzy sets in the consequence part as follows:

Implication of Rule 1: $\mu_y^1(o) = \min\left(\alpha_1, \mu_y^1(o)\right)$ …3.22

Implication of Rule 2: $\mu_y^2(o) = \min\left(\alpha_2, \mu_y^2(o)\right)$ …3.23

- An overall fuzzy set is obtained by aggregating the individual output fuzzy sets of each rule using max (OR) operation as follows:

Aggregation of Rule 1 and Rule 2: $\mu_y(o) = \max\left(\mu_y^1(o), \mu_y^2(o)\right)$ …3.24

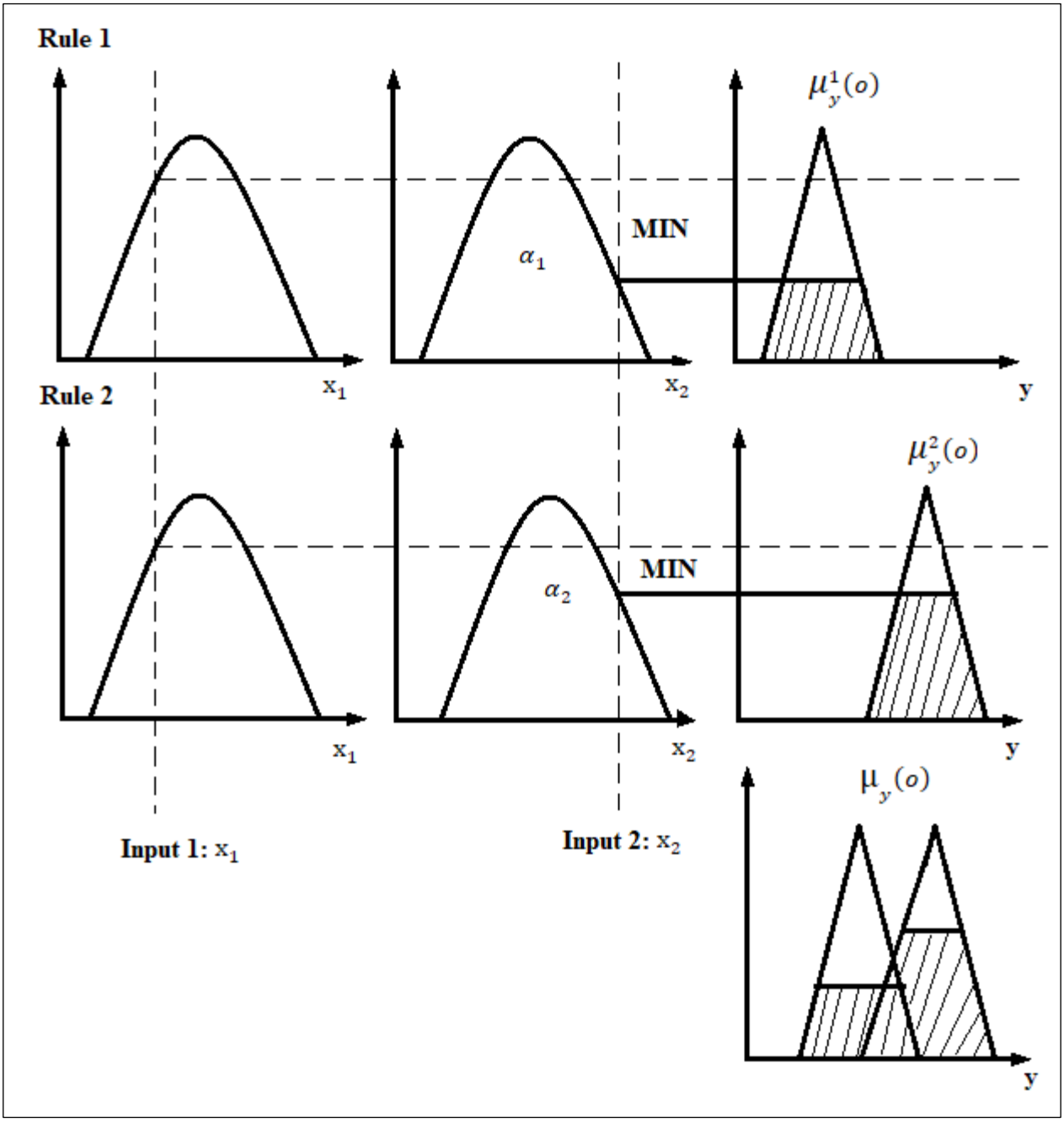

Fig. 3.5 Weight Factor, Implication and aggregation methods in Mamdani System

3.3.5 DEFUZZIFICATION

The defuzzifier maps output fuzzy sets into a crisp number. Defuzzification can be performed by several methods such as: center of gravity, center of sums, center of the largest area, first of the maxima, middle of the maxima, maximum criterion and height defuzzification. Of these, center of gravity (centroid method) and height defuzzification are the methods commonly used. The centroid defuzzification method finds the center point of the solution fuzzy region by calculating the weighted mean of the output fuzzy region. It is the most widely used technique because the defuzzified values tend to move smoothly around the output fuzzy region.

3.4 SELECTION FUZZY INFERENCE METHOD

Generally, there are three types of fuzzy inference method: Mamdani fuzzy inference, Sugeno fuzzy inference and Tsukamoto fuzzy inference. All of these three methods can be divided into two processes. The first process is fuzzifying the crisp values of input variables into membership values according to appropriate fuzzy sets, and these three methods are exactly the same in this process. While the differences occur in the second process when the results of all rules are integrated into a single precise value for output. In Mamdani inference, the consequent of If-Then rule is defined by fuzzy set. The output fuzzy set of each rule will be shaped by a matching number, and defuzzification is required after aggregating all of these reshaped fuzzy sets. But in Sugeno inference, the consequent of IF-Then rule is expressed by a polynomial with respect to input variables, thus the output of each rule is a single number. Then a weighting mechanism is implemented to work out the final crisp output. Although Sugeno inference avoids the complex defuzzification, the work of determining the parameters of polynomials is inefficient and less straightforward than defining the output fuzzy sets for Mamdani inference. Thus Mamdani inference is more popular and this thesis work only focuses on Mamdani inference method. Tsukamoto inference seems like a combination of Mamdani and Sugeno method, but it is even less transparent than these two methods.

CHAPTER 4

PROPOSED METHOD OF DETECTION AND CLASSIFICATION OF SINGLE PHASING IS PRESENCE OF DG UNITS

This chapter presents the application of wavelet transform and fuzzy inference system for analysis of single phasing in presence of distributed generation in distribution system. The simulated power system network using MATLAB is described here. The technique for feature extraction using wavelet from the simulated network and fuzzy inference system for detection and classification has been explained.

4.1 PROPOSED METHOD

The proposed method to detect single phasing condition as well as the lost phase comprises of three stages. In the first stage the three phase instantaneous current signals are combined to form a common signal known as modal signal. In the second stage, discrete wavelet transform is applied to this modal signal to extract useful information at different frequency spectrum band. Finally in the third stage, this information is used to detect single phasing condition and determine the lost phase using fuzzy logic. The three different stages of proposed method are explained in the subsequent subsections. The flowchart of the proposed method is shown in Fig. 4.1.

The rms value of the current is continuously monitored and when the per unit rms current of any one phase becomes less than 0.95 p.u. or more than 1.05 p.u. for ten successive samples, then disturbance is detected. The modal signal for hundred consecutive samples after the occurrence of disturbance is decomposed into six levels by DWT. The spectral energies of 4^{th}, 5^{th} and 6^{th} level detail coefficients are fed to the fuzzy inference system to detect single phasing and also the lost phase simultaneously. The proposed technique can detect and classify single phasing in presence of distributed generation within one cycle after the occurrence of single phasing. Each stage of proposed method is explained briefly below.

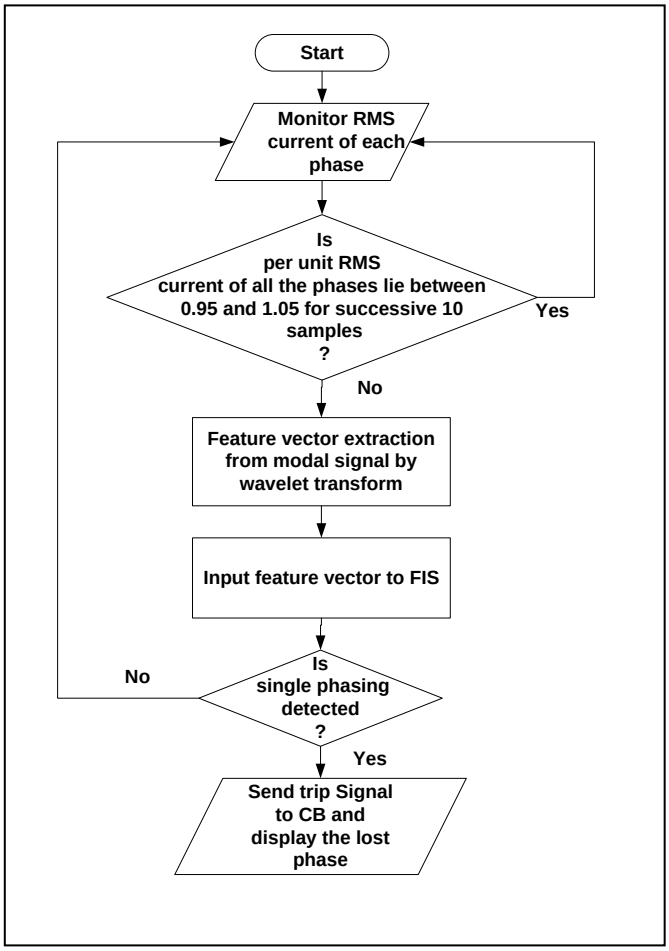

Fig. 4.1 Flowchart of proposed method

4.1.1 MODAL SIGNAL

The three phase currents are observed at the sensitive load to detect disturbances and form the mixed signal. Instead of analyzing three individual line currents, all three phase instantaneous currents I_a, I_b and I_c are linearly combined to form a mixed signal, known as modal signal. The modal signal should preserve all the transient information contained in the three signals. To form a modal signal from three phase signals, each phase current is multiplied by different constants. As there is no direct addition or subtraction of any two phase currents, the cancellation of transients of same magnitudes contained in any two phase currents can be avoided. The modal signal considered in this paper is given by

$$I_m = I_a + 2I_b - 3I_c \quad \ldots 4.1$$

The use of modal signal reduces the computational time and complexity, as instead of three signals, only one signal needs to be analyzed. This single modal signal effectively accomplishes the objective of single phasing detection, instead of two modal signals used in paper [36] to meet the goal. The other advantage of the modal signal is that it eliminates the common-mode signal due to mutual coupling with adjacent lines and also ensures immunity against other disturbances for which equipment is not installed. In the modal signal each current is multiplied with different coefficients, which provides the amplification of mismatch among different phase currents.

4.1.2 FEATURE EXTRACTION

For feature extraction, discrete wavelet transform is used in this work. DWT is an efficient and powerful tool to analyze transient signal because it has the ability to extract frequency domain information from the transient signal. In DWT a signal is decomposed into low frequency components which are known as approximation (*a*) and high frequency components known as detail (*d*). These are obtained by passing the signal through low pass and high pass filter respectively. The coefficients of filters depend on the mother wavelet. In this paper Daubechies mother wavelet is considered. Fig. 4.2 illustrates the different frequency bands captured by detail coefficients at different levels of decomposition for an input signal with sampling frequency of 5 kHz.

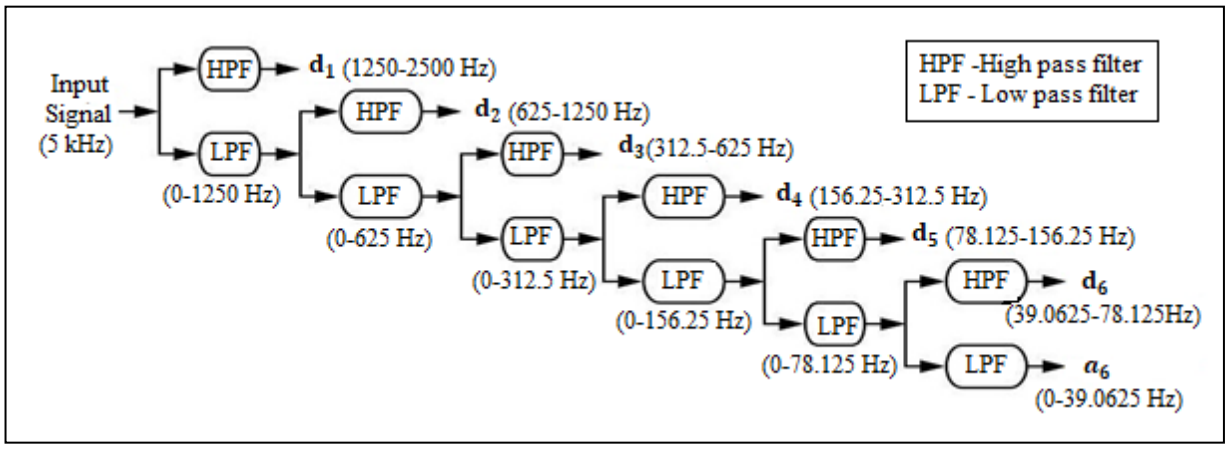

Fig 4.2 Wavelet decomposition upto level 6 for sampling frequency of 5 kHz

The synthesized modal signal observed at the sensitive load is applied to DWT to determine the feature vector which assists in the detection of single phasing condition and determination of the lost phase. Choice of mother wavelet plays an important role in extracting useful features for transient event detection. Daubechies mother wavelet, which is very commonly used, has been considered in this paper. Db4 and db6 mother wavelets give better results for short and fast transient disturbances, whereas for slow transient disturbances db8 and db10 are useful. Therefore mother wavelet db4 (db6 is a good candidate as well) has been chosen for this work.

The fault current comprises of transient signals of different frequency ranges. In order to capture the useful frequency band, the sample frequency is taken as 5 kHz and wavelet decomposition upto level 6 is considered. The spectral energy of detail level 4, detail level 5 and detail level 6, which covers frequency ranges from 156.25 Hz to 312.5 Hz, 78.125 Hz to 156.25 Hz and 39.0625 Hz to 78.125 Hz respectively, have been considered. These three different frequency band spectral energies form the necessary feature vector for single phasing detection. The spectral energies of the modal signal are as follows:

$$E_4(r) = \sum_{k=n}^{r} I_{d4}^2(k\Delta T)\Delta T \quad \ldots 4.2$$

$$E_5(r) = \sum_{k=n}^{r} I_{d5}^2(k\Delta T)\Delta T \quad \ldots 4.3$$

$$E_6(r) = \sum_{k=n}^{r} I_{d6}^2(k\Delta T)\Delta T \quad \ldots 4.4$$

where $E_4(r)$, $E_5(r)$ and $E_6(r)$ are the spectral energy of the 4th, 5th and 6th level detail coefficients of the modal signal; I_{d4}, I_{d5} and I_{d6} are the 4th, 5th and 6th level detail coefficients of the modal signal; ΔT is the sampling time step; n is the fault inception sample number; r is the current sample where $r > n$.

Fig. 4.3 shows the three phase currents when single phasing occurs in line L_1, at 6.25 km from CB2 at 0° inception angle at 18 second, along with the modal signal and detail coefficients of 4th, 5th and 6th level decomposition.

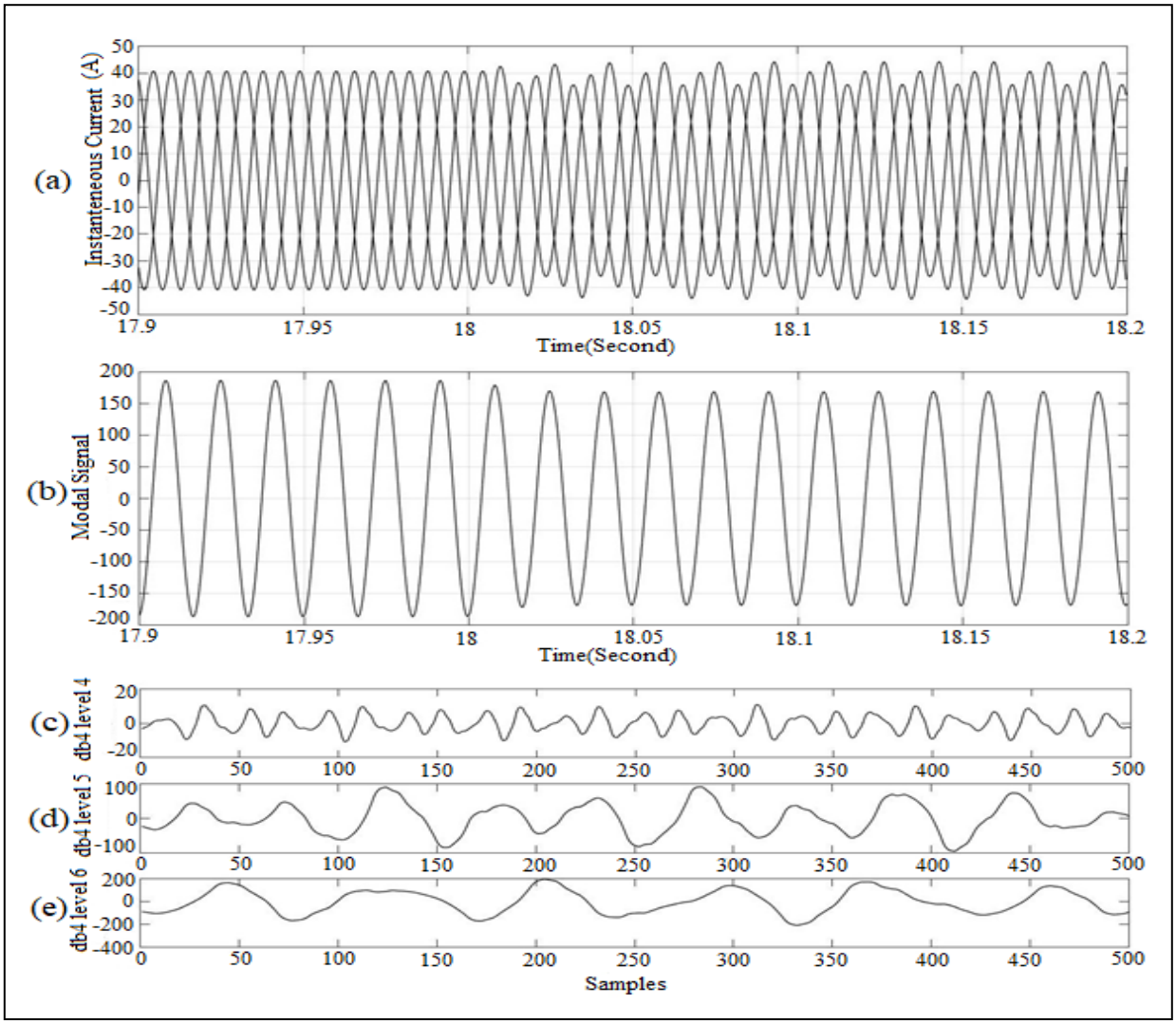

Fig.4.3 Currents observed from load 3 under single phasing condition.

(a) Three phase currents (b) modal signal (c) detail coefficients of level 4 (d) detail coefficients of level 5 (e) detail coefficients of level 6.

4.1.3 DETECTION AND CLASSIFICATION

In order to detect and classify the single phasing event in presence of DG unit, a fuzzy inference system (FIS) is used in this thesis work. The feature vector extracted from the modal signal by DWT is fed to the FIS. FIS has human capacity in taking decisions in situations where imprecision and uncertainties exist, by mapping crisp input real values to crisp output real values. IF-THEN rules decide the degree of membership function and their decisions on inputs in the form of linguistic variable, derived from membership functions.

Fuzzification, fuzzy inference, IF-THEN rules and defuzzification are four basic elements of FIS, which are described in chapter 3. Mamdani type FIS has been designed and implemented in this paper to detect single phasing and the lost phase with three input variables and one output variable. The FIS uses Min-Max composition and centroid of area method for defuzzification. There are 343 IF-THEN rules used in this FIS.

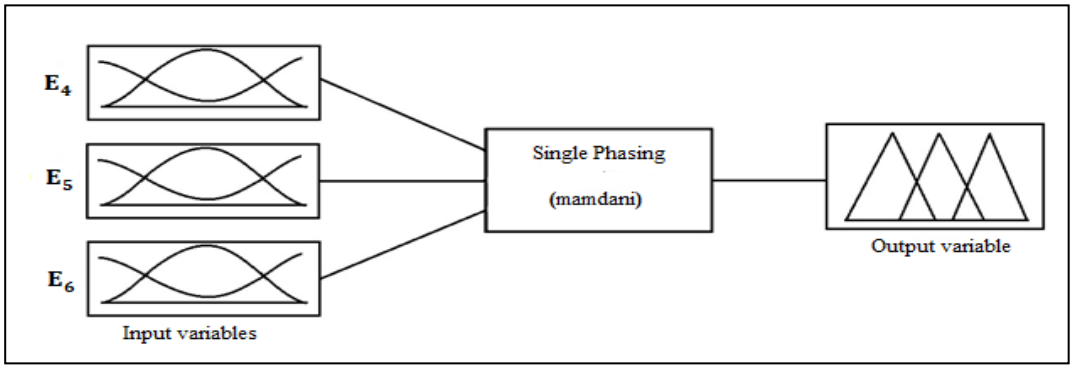

Fig 4.4 Fuzzy inference system for single phasing detection.

The input variables to the FIS are E_4, E_5 and E_6 which are extracted from modal signal using DWT as shown in Fig. 4.4, and the output is a discrete number indicating the phase due to which single phasing has occurred or non-occurrence of single phasing. The range of input variables E_4, E_5 and E_6 are 0-0.5, 0-20 and 0-100 respectively. The membership functions of input variables and output variable are shown Fig. 4.5. The input variables E_4, E_5 and E_6 each have seven triangular membership functions and the output has four discrete numbers 1, 2, 3 and 4 indicating *NSP* (no single phasing), *SPA* (single phasing with A phase disconnected), *SPB* (single phasing with B phase disconnected), and *SPC* (single phasing with C phase disconnected), respectively. The input and output membership functions as shown in Fig. 4.5.

The seven triangular membership function of input variable E_4 are named as E_{41}, E_{42}, E_{43}, E_{44}, E_{45}, E_{46} and E_{47} and they range from [0-0.0575], [0.055-0.068], [0.067-0.0895], [0.089-0.113], [0.11-0.315], [0.31-0.375] and [0.368-0.5] respectively.

Similarly the seven triangular membership function of input variable E_5 are named as E_{51}, E_{52}, E_{53}, E_{54}, E_{55}, E_{56} and E_{57} and they range from [0-0.396], [0.395-0.55], [0.53-3.2], [3.15-4.3], [4.18-13.3], [13.15-14.55] and [14.4-20] respectively.

Again the seven triangular membership functions of input variable E_6 are named as E_{61}, E_{62}, E_{63}, E_{64}, E_{65}, E_{66} and E_{67} and Params ranges are [0-17.3], [17.2-17.75], [17.75-34.88], [34.85-38.8], [38.45-67.52], [67-74.2] and [73.9-100] respectively.

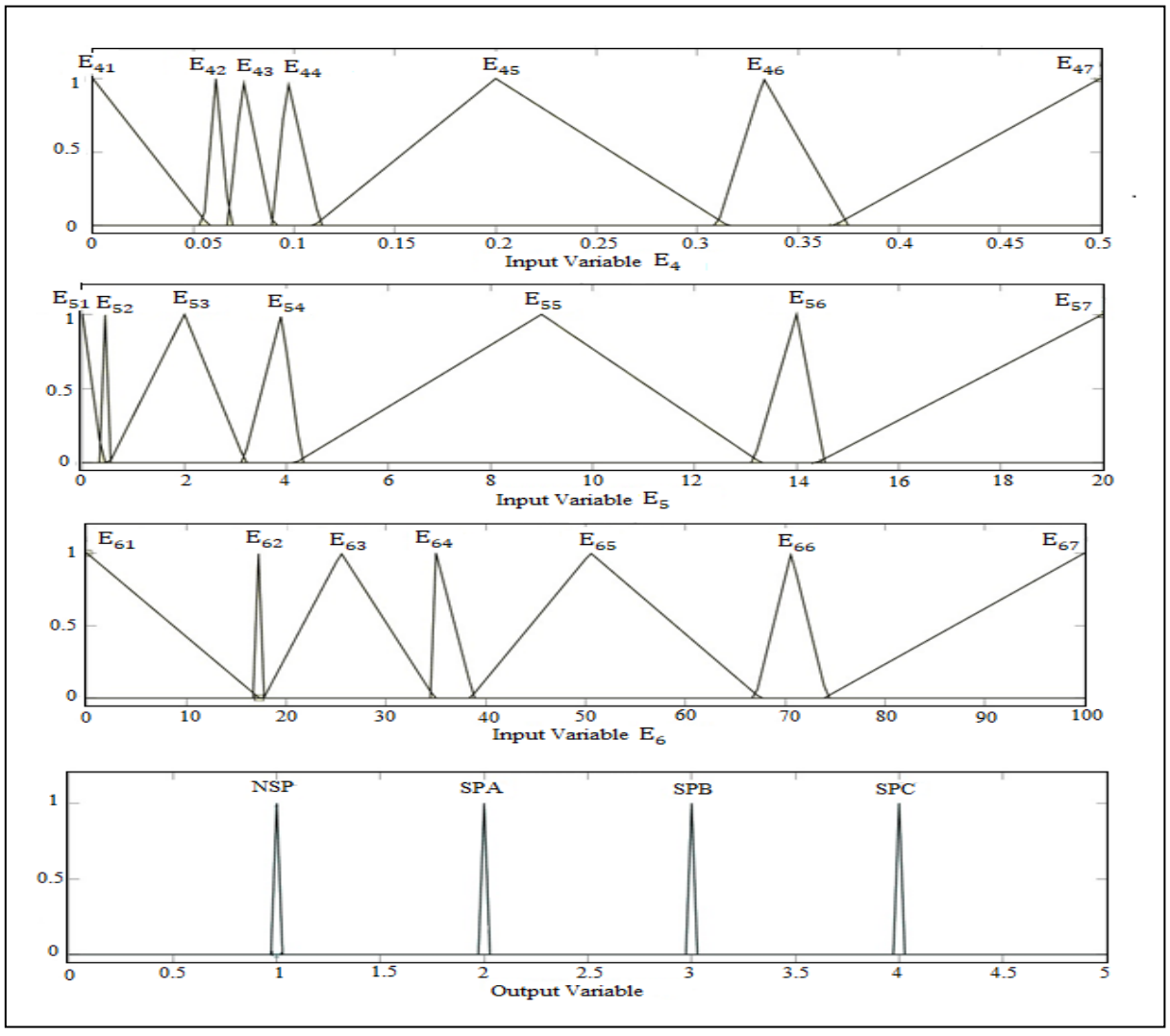

Fig 4.5 Input and output membership functions of FIS

So, when single phasing event occurrs in phase A, the values of E_4, E_5, E_6 must be in the range of E_{42}, E_{52}, E_{62}. Similarly, when single phasing event occurrs in phase B, the values of E_4,

E_5, E_6 must be with in the range of E_{44}, E_{54}, E_{64}. Again, if single phasing event occurrs in phase C, the values of E_4, E_5, E_6 must be with in the range of E_{46}, E_{56}, E_{66}.

4.2 SIMULATED POWER SYSTEM NETWORK

There are six steps to modeling any system:

i. Defining the system
ii. Identifying the system components
iii. Modeling the system with equation
iv. Building the simulation block diagram
v. Running the simulation
vi. Validating the simulation results

A three phase, six bus power system network as shown in Fig. 4.6 is considered. This power system distribution model is developed and simulated using MATLAB/Simulink. The rating of all components of this model are set according to the test system which has been discussed in chapter 1, subsection 1.4. All the components in this power system are modeled at 60 Hz.

The inception angles for every single phasing event, fault and switching events are tested at 0^0, 45^0 and 90^0. The simulation run time is 20 seconds. The sampling frequency of the model is 200 kHz. The power system is discretized so as to expedite the simulation. In powergui block, the sample time is 5 μs. The sampling frequency for monitoring of disturbance is 5 kHz.

The range of fault resistance (R_f) considered for all types of faults is 0.0001 – 1000 Ω. The positive, negative and zero sequence parameters of the transmission line are shown in Table 4.1.

Table 4.1

Transmission Line Parameters

Line Inductance (mH/ km)	Positive and negative sequence	0.9337
	Zero sequence	4.1264
Line Capacitance (nF/ km)	Positive and negative sequence	12.74
	Zero sequence	7.751
Line Resistance (Ω/ km)	Positive and, negative sequence	0.01273
	Zero sequence	0.3864

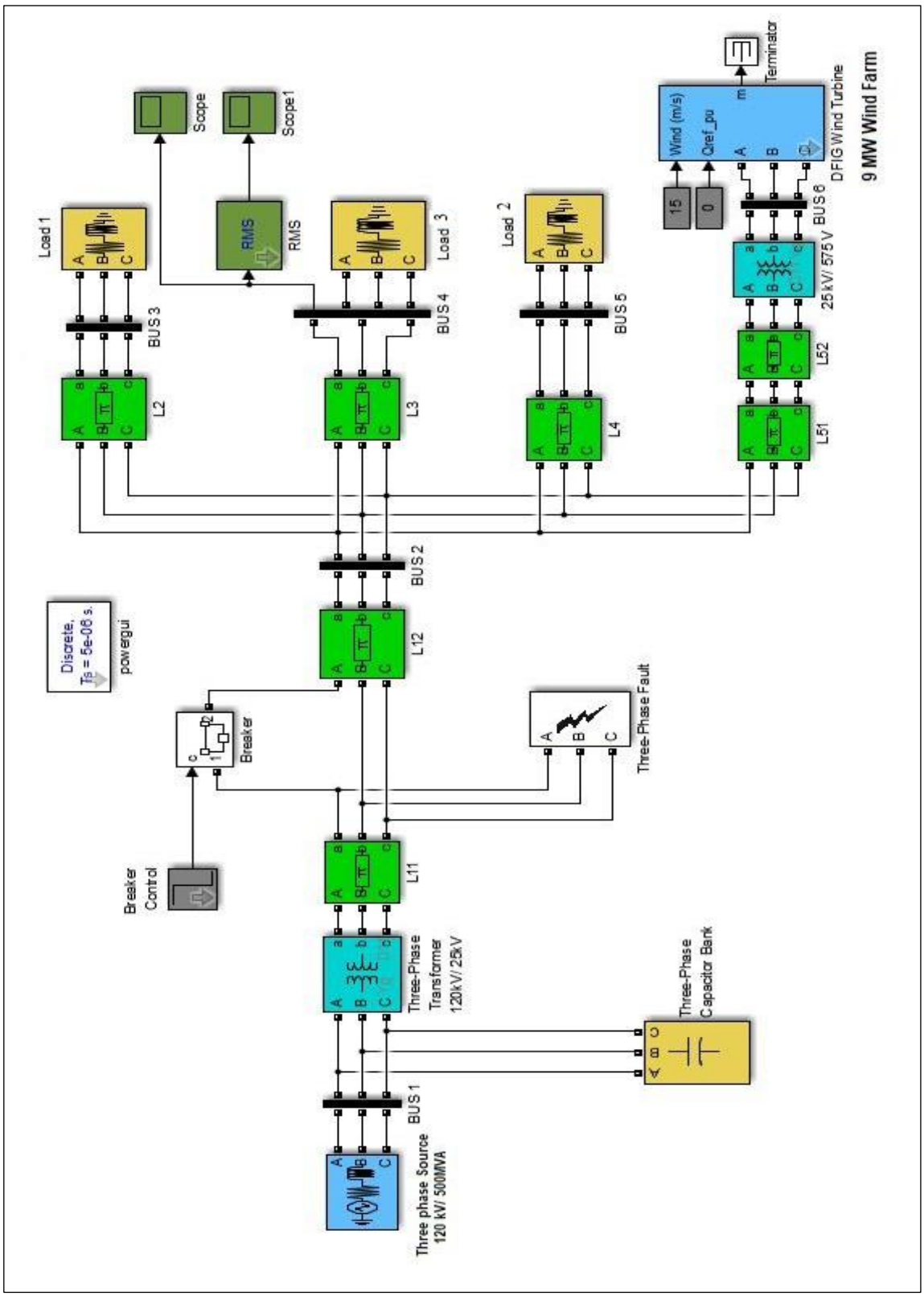

Fig 4.6 Simulated Test Power System Distribution Model in Simulink

CHAPTER 5

SIMULATION RESULTS

Single Phasing event under different conditions, different types of faults and different types of switching event are simulated using MATLAB/ Simulink toolbox and after recording transient signals in the MATLAB workspace, these recorded signals are decomposed using wavelet toolbox with Daubechies discrete wavelet transform for extraction of the important features. Then these features are used to detect and classify the single phasing event with the help of fuzzy inference system. In this dissertation, all kinds of events have been simulated under the inception angle of 0^o, 45^o and 90^o. Different types of events are simulated considering one cycle post fault data at different locations of a 12.5 km long line L_1 at an interval 1.5 km. Db4 mother wavelet is used to calculate spectral energy of modal signal which is formed using all three phase instantaneous currents at sensitive load 3.

5.1 NORMAL CONDITION

The three phase instantaneous current at sensitive load 3 under normal operating condition, modal signal and its detail coefficients of 4^{th}, 5^{th} and 6^{th} level decomposition are shown in Fig. 5.1(a), 5.1(b) and 5.1(c), respectively.

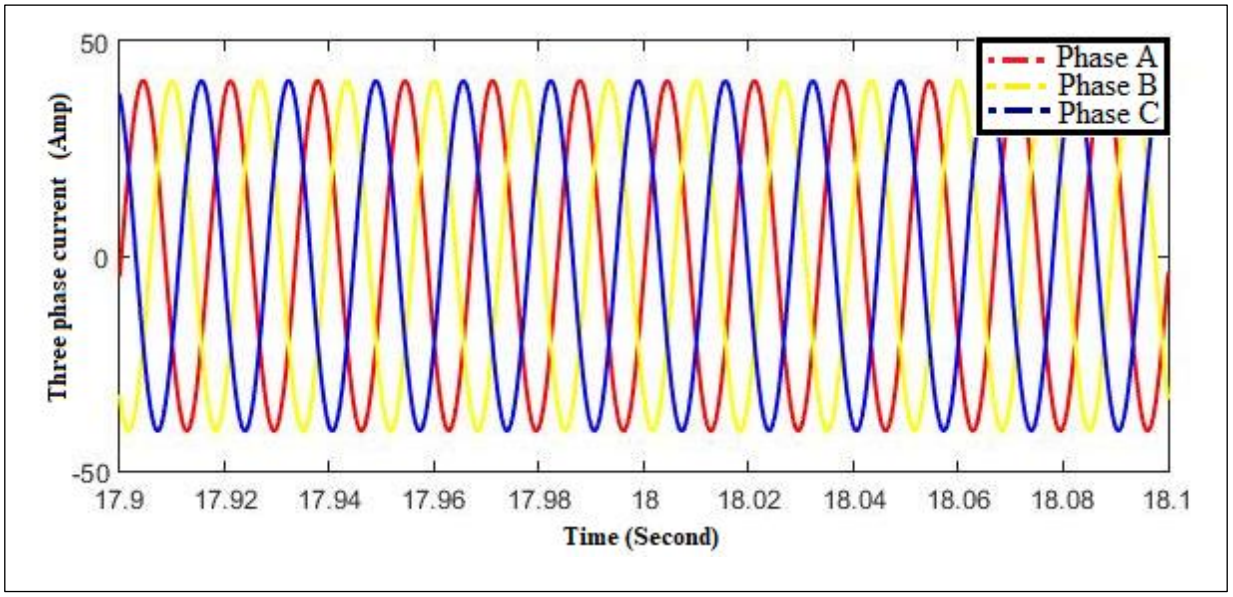

Fig. 5.1(a) Three phase currents observed from load 3 under normal condition

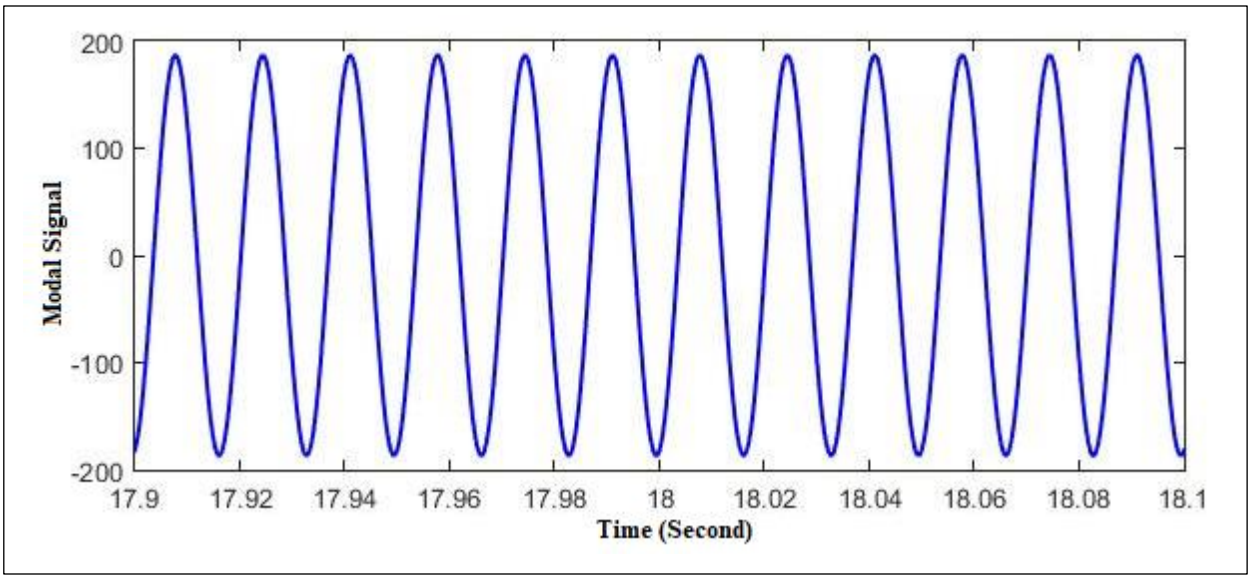

Fig. 5.1 (b) Modal signal under normal condition

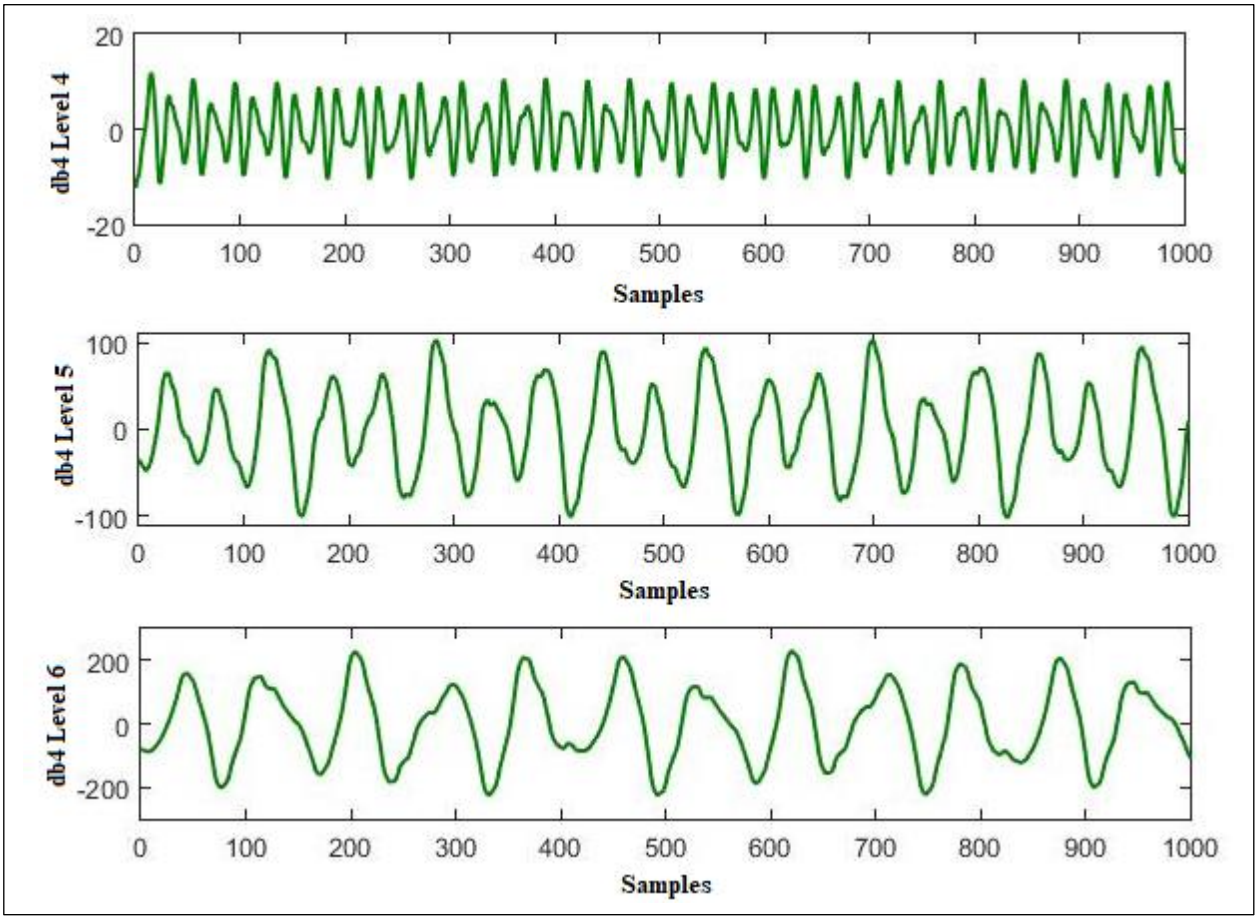

Fig 5.1 (c) Detail coefficients of modal current of Level 4, Level 5 and Level 6 under normal condition

The feature vector under normal condition (one cycle) [E_4 E_5 E_6] = [0.128 1.18 18.27].

5.2 SINGLE PHASING EVENT

Single phasing event is created by opening any one conductor of three phase line L_1 i.e. single phase open circuit fault. Three phase instantaneous current at sensitive load 3 with single phasing event in phase A at line L_1 is shown in Fig. 5.2(a). In Fig. 5.2(a) the single phasing event occurred at an inception angle 0^o in phase A and distance of 6.25 km in line L_1 from Bus 1. Modal signal corresponding to Fig 5.2(a) is shown in 5.2(b). When single phasing event occurs on transmission line, then current at sensitive load 3 becomes unbalanced. Db4 detail coefficients of 4^{th}, 5^{th} and 6^{th} level decomposition of modal signal which is formed using this unbalance current is depicted in Fig.5.2(c).

Similarly in Fig. 5.3(a) the single phasing event occurred at an inception angle 45^o in phase B and distance of 6.25 km in line L_1 from Bus 1. Modal signal and detail coefficients of 4^{th}, 5^{th} and 6^{th} level decomposition corresponding to Fig 5.3(a) are shown in 5.3(b) and 5.3(c) respectively. Again, In Fig. 5.4(a) the single phasing event occurred at an inception angle 90^o in phase C and distance of 6.25 km in line L_1 from Bus 1. Modal signal and detail coefficients of 4^{th}, 5^{th} and 6^{th} level decomposition corresponding to Fig 5.4(a) are shown in 5.4(b) and 5.4(c) respectively.

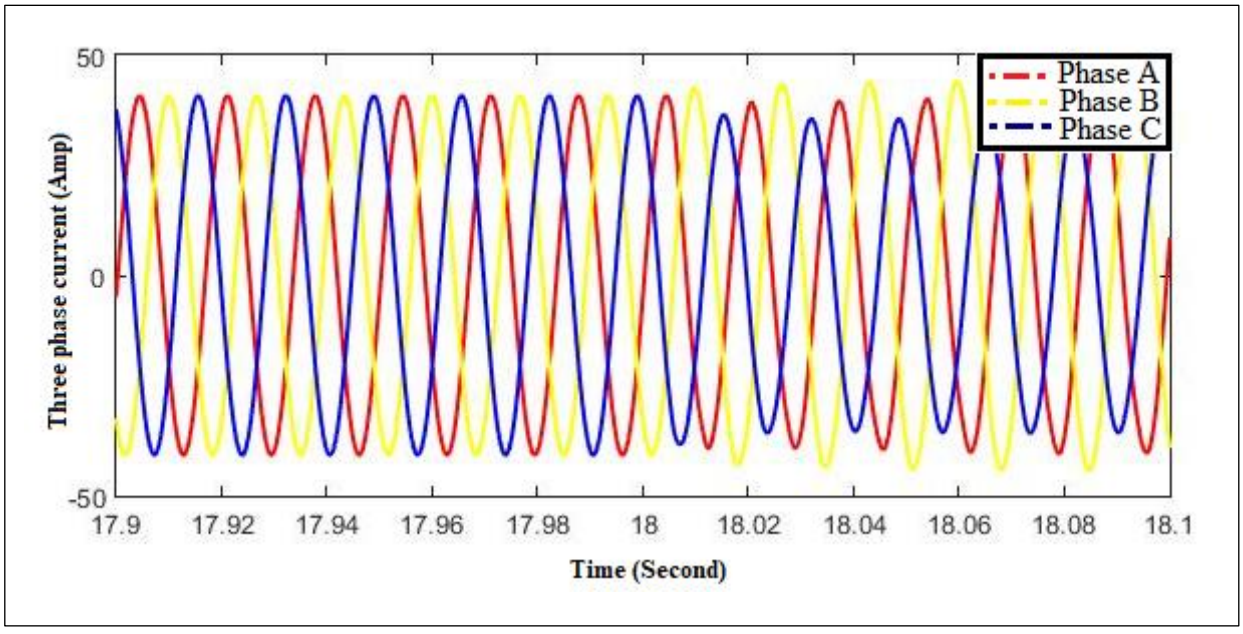

Fig. 5.2(a) Three phase currents observed from load 3 under single phasing at A phase

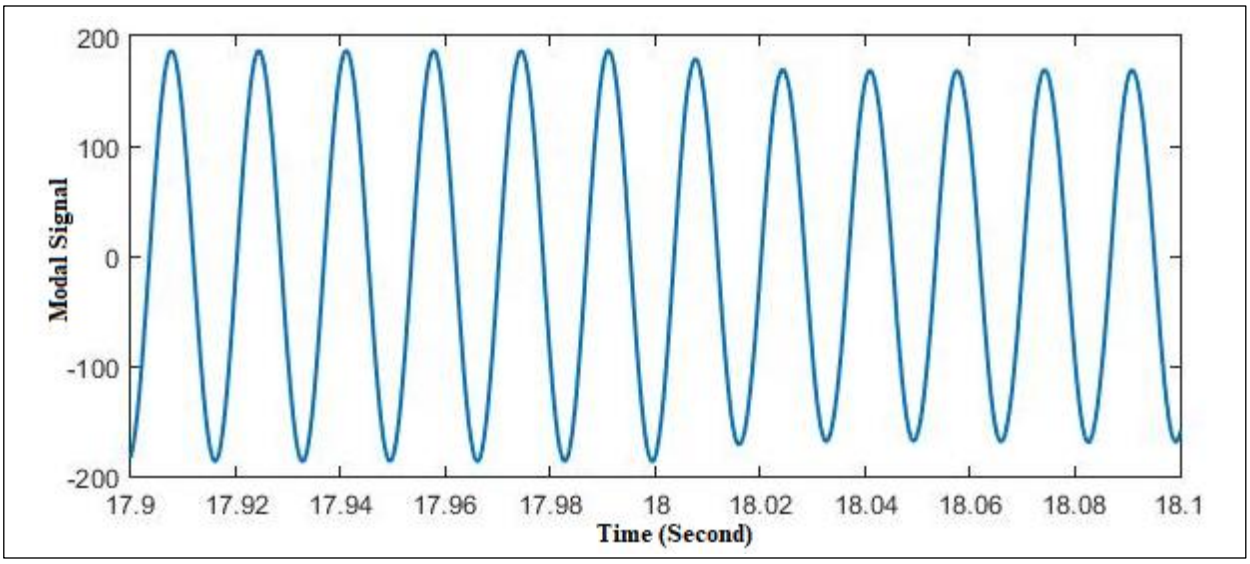

Fig. 5.2 (b) Modal Signal under single phasing at phase A

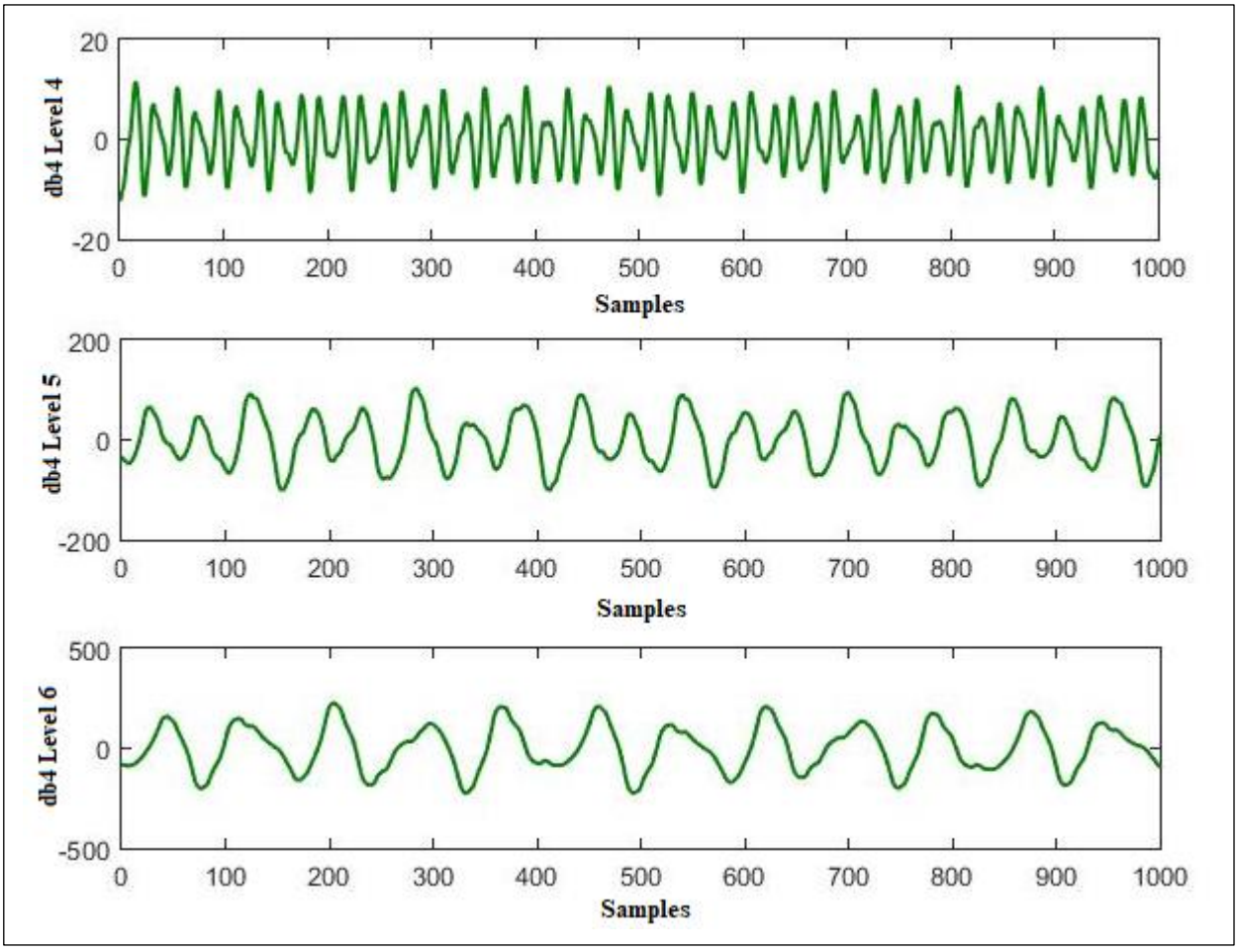

Fig 5.2 (c) Detail coefficients of modal current of Level 4, Level 5 and Level 6 under single phasing at phase A

The feature vector under single phasing event at phase A and distance of 6.25 km in line L1 from Bus 1 (one cycle) is [E_4 E_5 E_6] = [0.06343 0.51442 17.5826]. If this feature vector feed to FIS, then FIS will detect and classify it as single phasing with lost phase A.

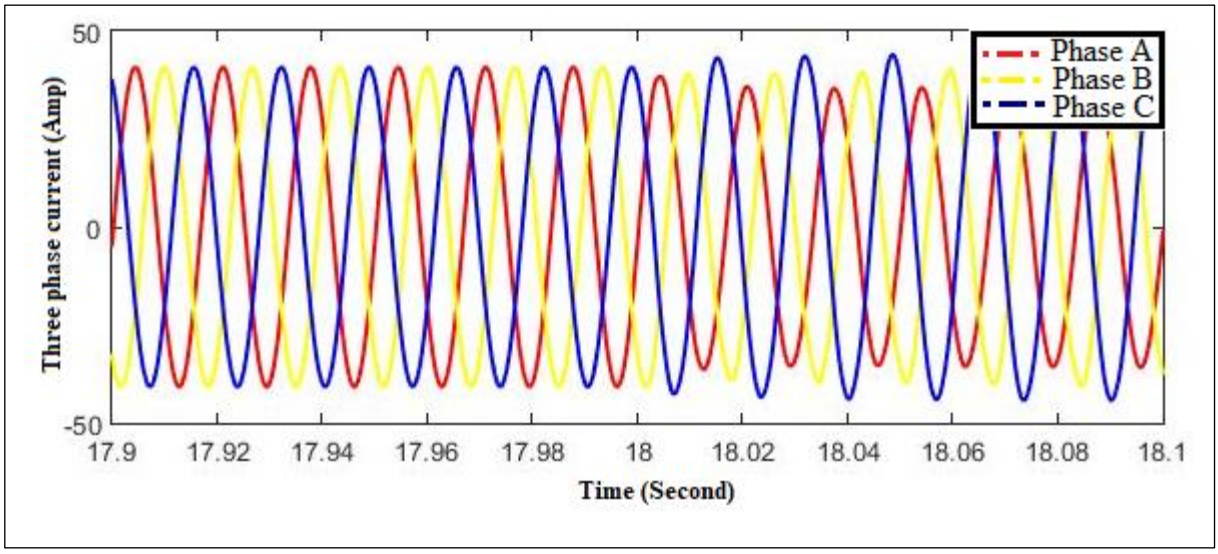

Fig. 5.3(a) Three phase currents observed from load 3 under single phasing at B phase

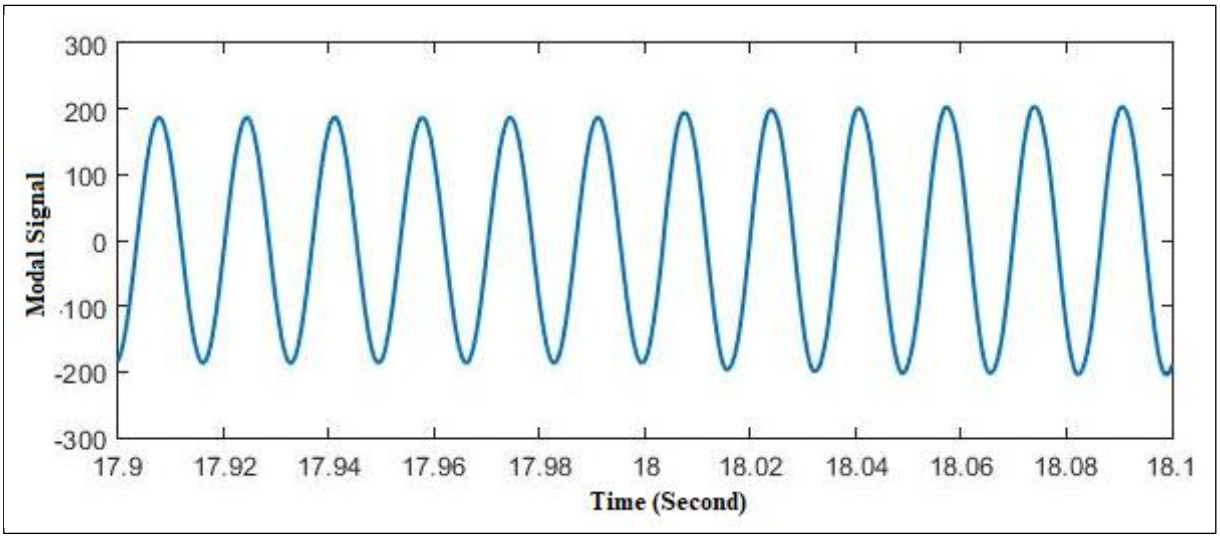

Fig. 5.3 (b) Modal Signal under single phasing at phase B

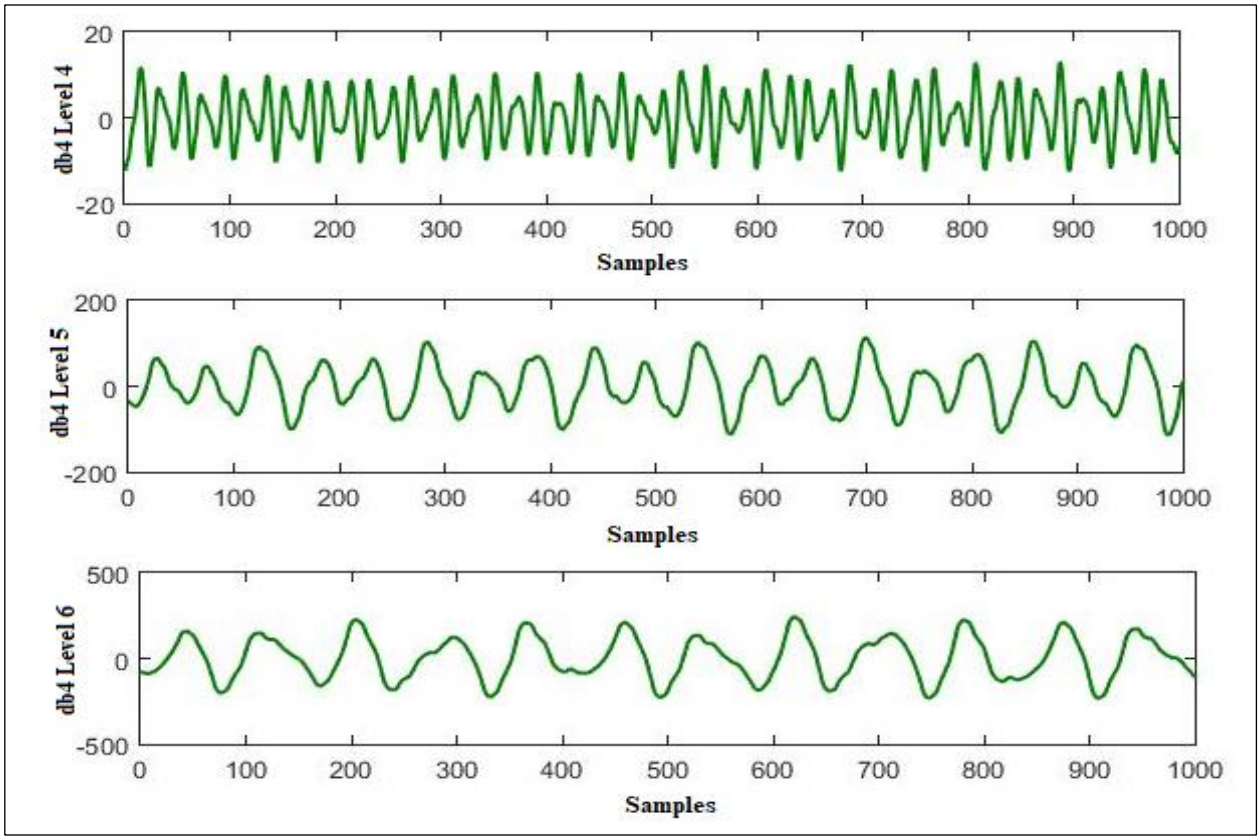

Fig 5.3 (c) Detail coefficients of modal current of Level 4, Level 5 and Level 6 under single phasing at phase B

The feature vector under single phasing event at phase B and distance of 6.25 km in line L1 from Bus 1 (one cycle) is [E_4 E_5 E_6] = [0.100702 4.028296 38.33058]. If this feature vector feed to FIS, then FIS will detect and classify it as single phasing with B as lost phase.

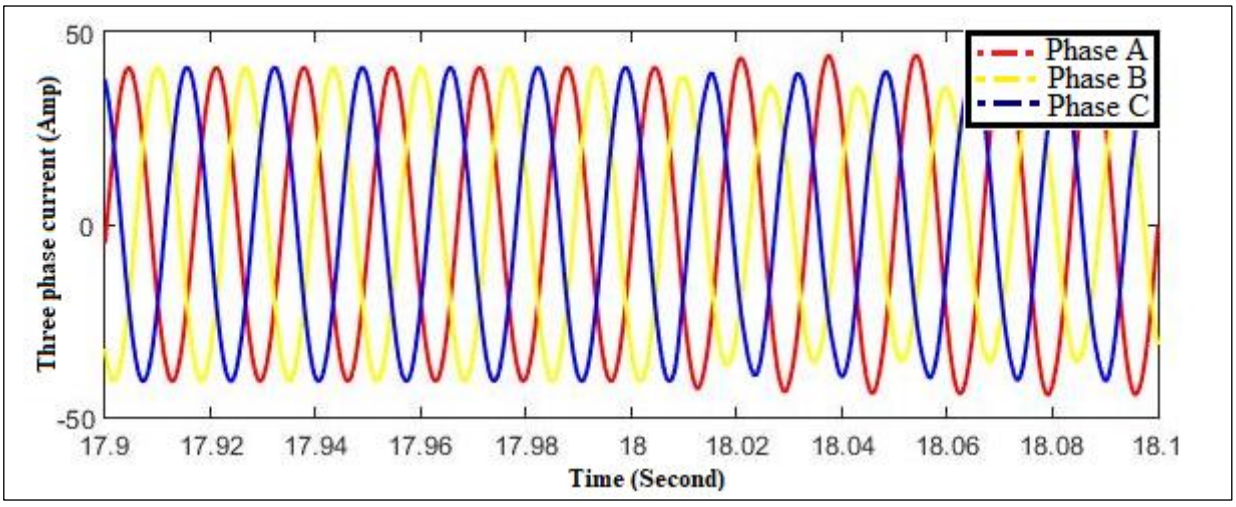

Fig. 5.4(a) Three phase currents observed from load 3 under single phasing at C phase

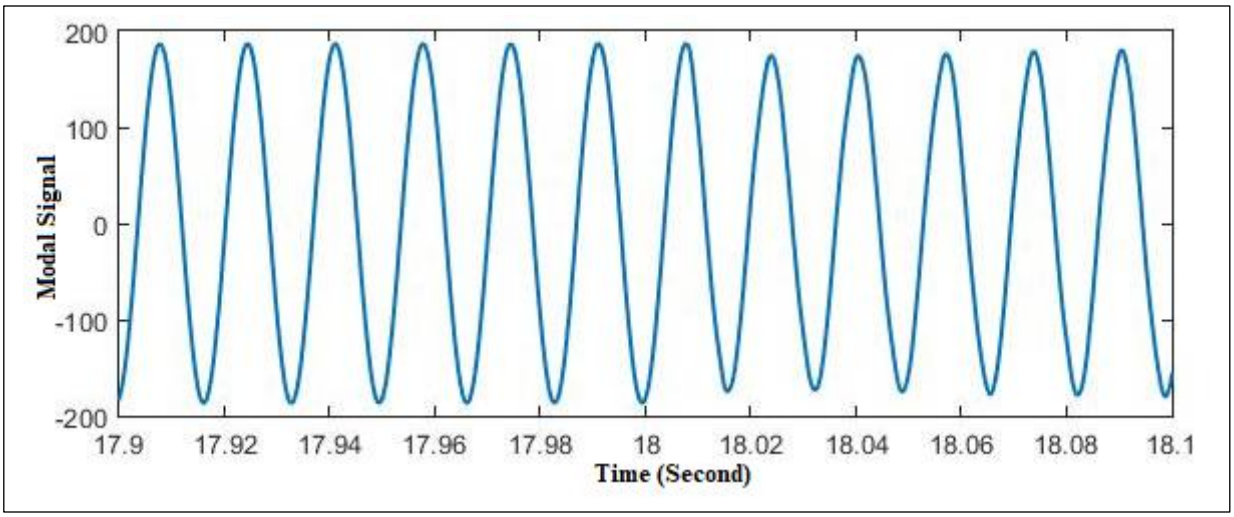

Fig. 5.4 (b) Modal Signal under single phasing at phase C

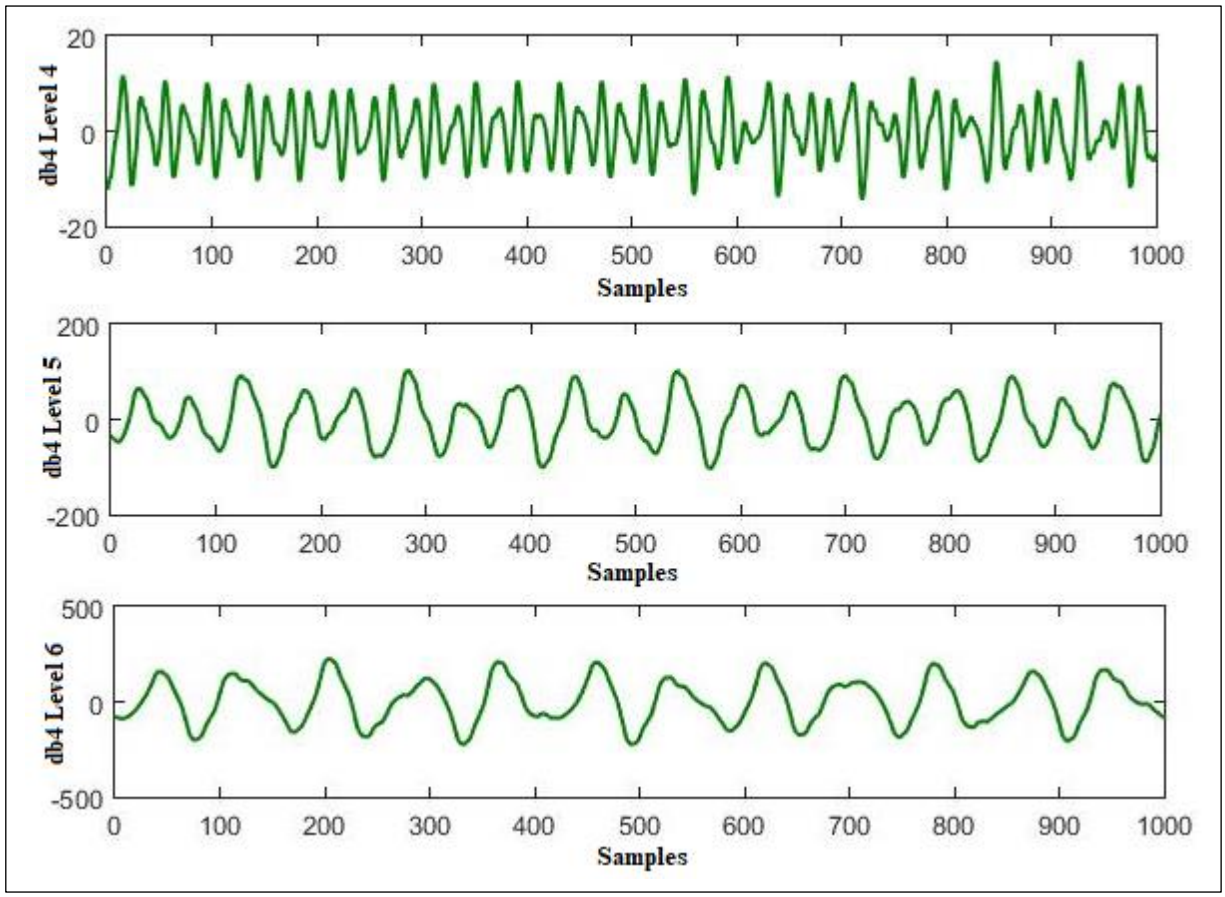

Fig 5.4 (c) Detail coefficients of modal current of Level 4, Level 5 and Level 6 under single phasing at phase C

The feature vector under single phasing event at phase C and distance of 6.25 km in line L1 from Bus 1 (one cycle) is [E_4 E_5 E_6] = [0.352918 13.68065 69.0077]. If this feature vector feed to FIS, then FIS will detect and classify it as single phasing and lost phase is C.

5.3 SHORT CIRCUIT FAULT EVENT

Different types of short circuit faults are created in transmission line L_1 at different fault inception angle and fault resistance (R_f). Three phase current at sensitive load 3 is recorded and it is analyzed by DWT to extract feature vector. Then this feature vector is fed to FIS for detection. Here FIS is set to detect single phasing event, so FIS must be detect this short circuit event as non-single phasing event.

5.3.1 SINGLE LINE TO GROUND (SLG) FAULT

Three phase current signal at load 3 with single line to ground fault in phase A in line L_1 is shown in Fig. 5.5 (a). In Fig. 5.5 (a) the fault occurs at an inception angle of 0^o at a distance of 6.25 km in line L_1 from Bus 1 and fault resistance of 0.0001 Ω. The figure shows that the current of the faulted phase at load 3 decreases as the voltage at faulted phase decreases in Bus 2 and Bus 4. Fig. 5.5(b) shows the modal signal corresponding to three phase current signal at load 3. Fig. 5.5(c) shows detail coefficients of 4^{th}, 5^{th} and 6^{th} level decomposition of modal signal which is formed using this unbalance current at load 3 due to single line-A to ground fault.

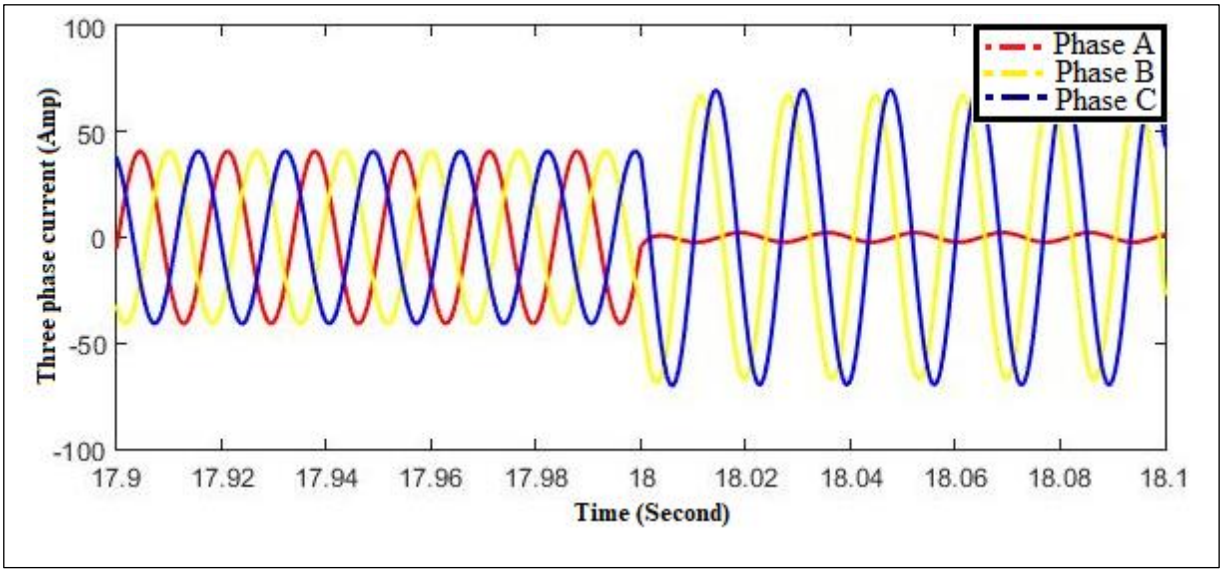

Fig. 5.5(a) Three phase currents observed at load 3 under single line to ground fault at A phase in Line L_1

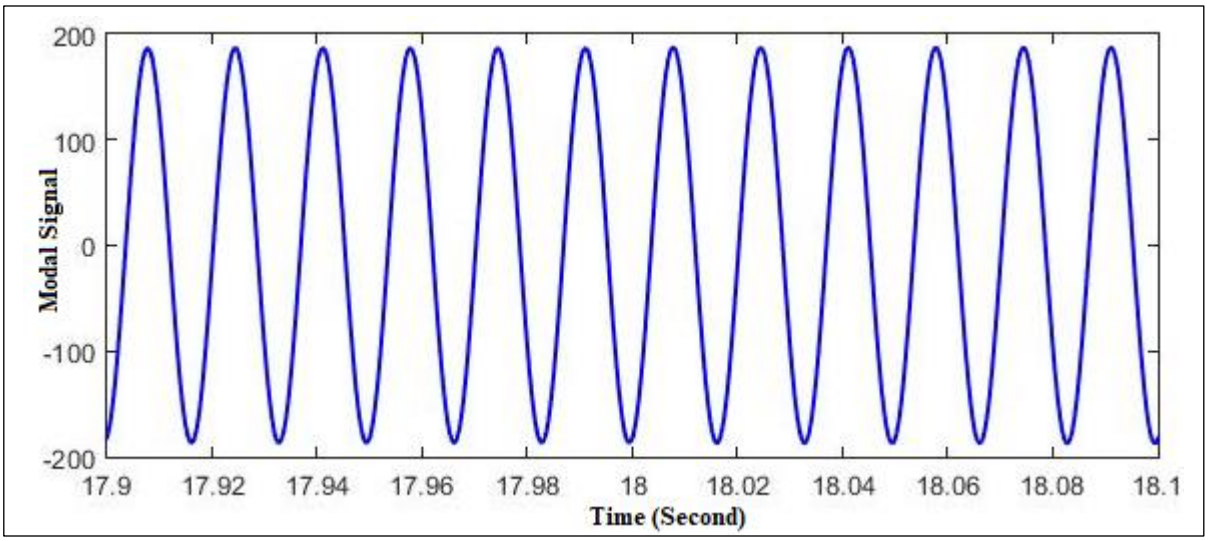

Fig. 5.5(b) Modal current under single line to ground fault at phase A

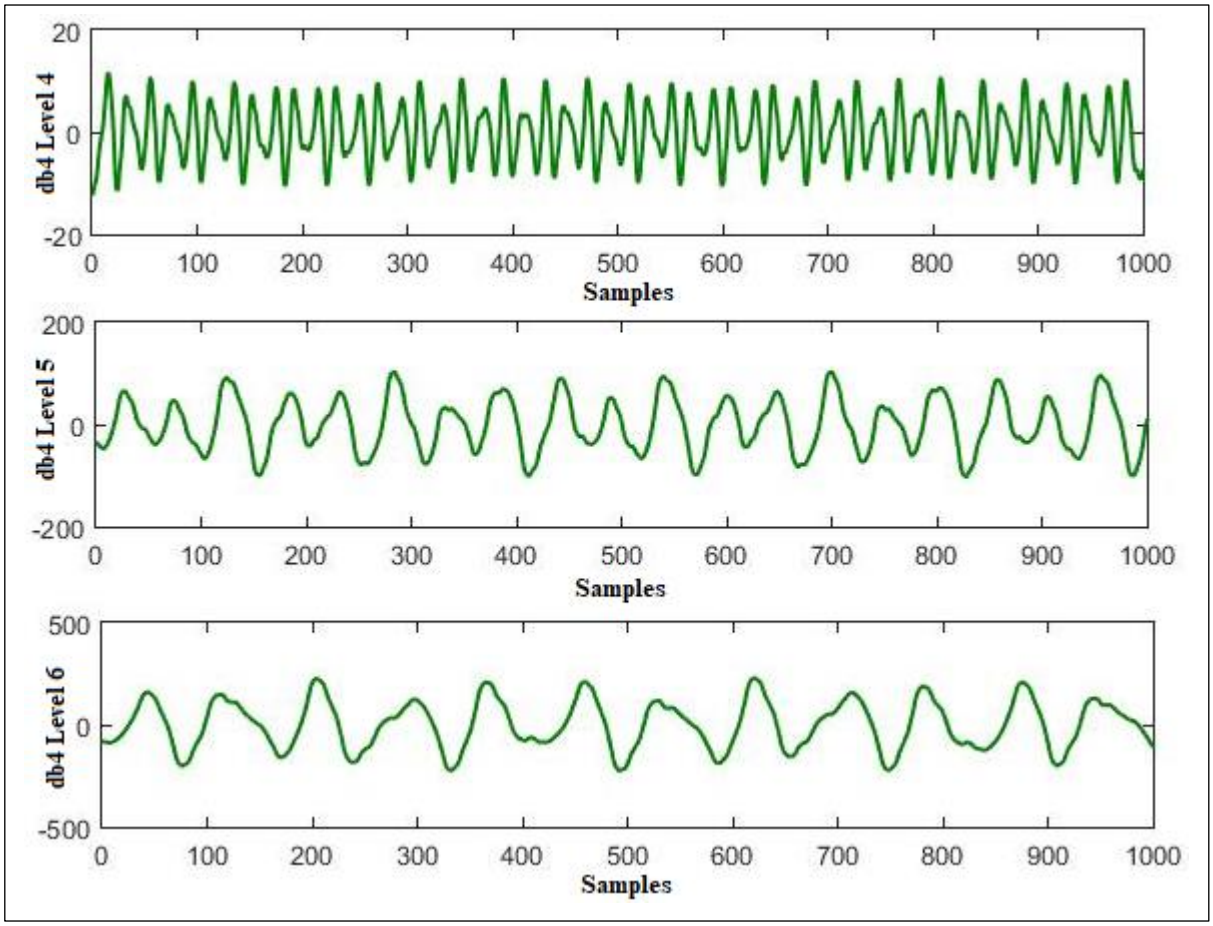

Fig. 5.5 (c) Detail coefficients of modal current of Level 4, Level 5 and Level 6 under single line to ground fault at phase A

The feature vector under single phase to ground fault in phase A at a distance of 6.25 km in line L1 from Bus 1 (one cycle) is [E_4 E_5 E_6] = [0.284673 8.009089 47.26966]. If this feature vector is fed to FIS, then FIS will detect it as non-single phasing event.

Fig. 5.6(a) shows three phase current signal at load 3 with single phase to ground fault in line L_1 in phase B. In Fig. 5.6(a) the fault occurs at an inception angle of 45^o and fault resistance 0.0001 Ω. The modal signal corresponding to three phase current signal at load 3, with single phase to ground fault in phase B in line L_1 is shown in Fig. 5.6(b). Fig. 5.6(c) shows detail coefficients of 4th, 5th and 6th level decomposition of modal signal which is formed using this unbalance current at load 3 due to single phase to ground fault in phase B.

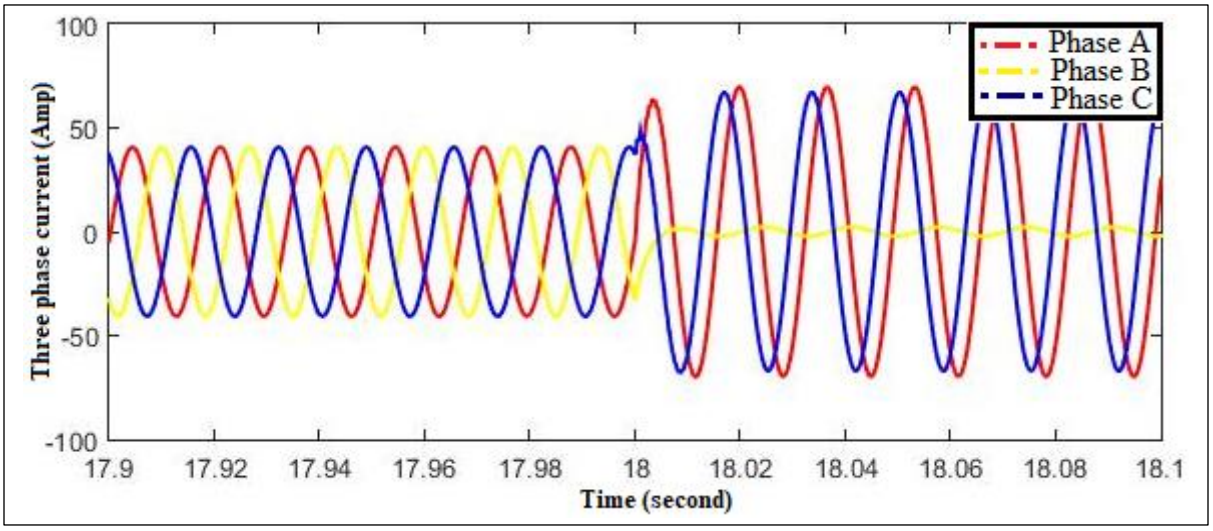

Fig. 5.6(a) Three phase currents observed at load 3 under single line to ground fault at B phase

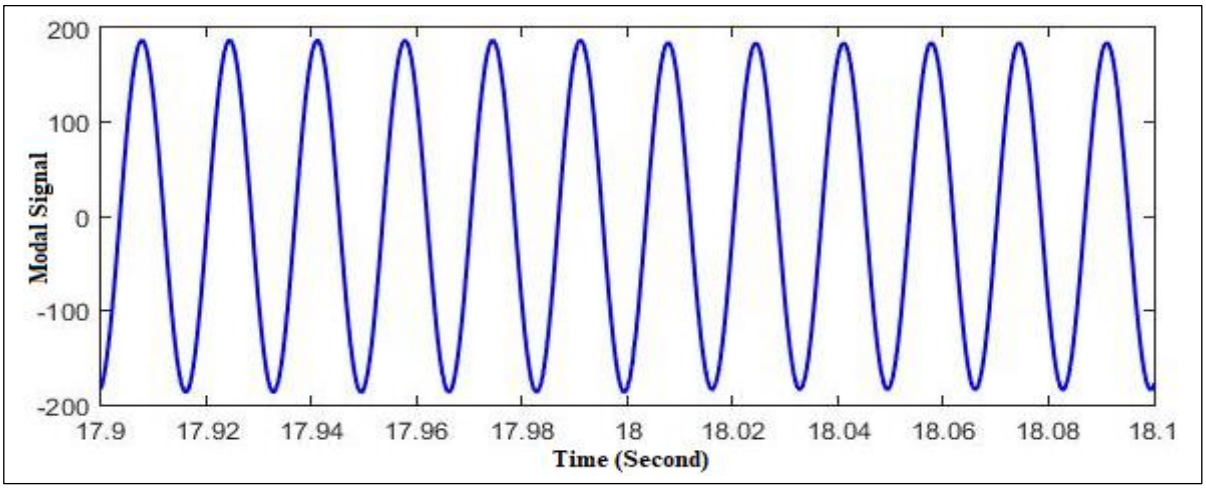

Fig. 5.6(b) Modal current under single line to ground fault at phase B

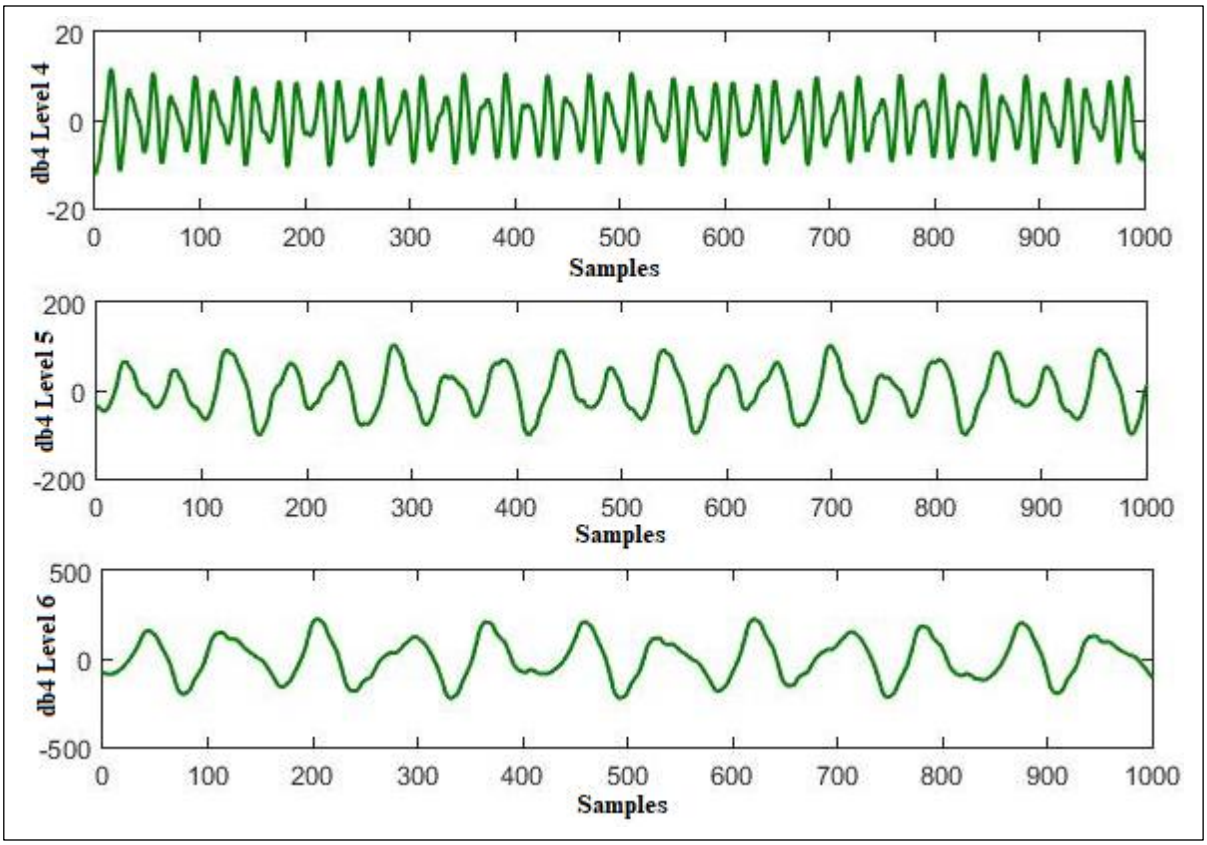

Fig. 5.6 (c) Detail coefficients of modal current of Level 4, Level 5 and Level 6 under single line to ground fault at phase B

The feature vector under single phase to ground fault in phase B, at a distance of 6.25 km in line L1 from Bus 1 (one cycle) is $[E_4\ E_5\ E_6]$ = [0.257 6.870 41.95]. If this feature vector feed to FIS, then FIS will detect it as non-single phasing event.

Three phase current signal at load 3 with single phase to ground fault in line L_1 in phase C is shown in Fig. 5.7(a). In Fig. 5.7(a) the fault occurs at an inception angle of 90^o with fault resistance 0.0001 Ω. The modal signal corresponding to three phase current signal at load 3 with single phase to ground fault in phase C in line L_1 is shown in Fig. 5.7(b). Detail coefficients of 4^{th}, 5^{th} and 6^{th} level decomposition of modal signal which is formed using this unbalance current at load 3 due to single phase to ground fault in phase C is shown in Fig. 5.7(c).

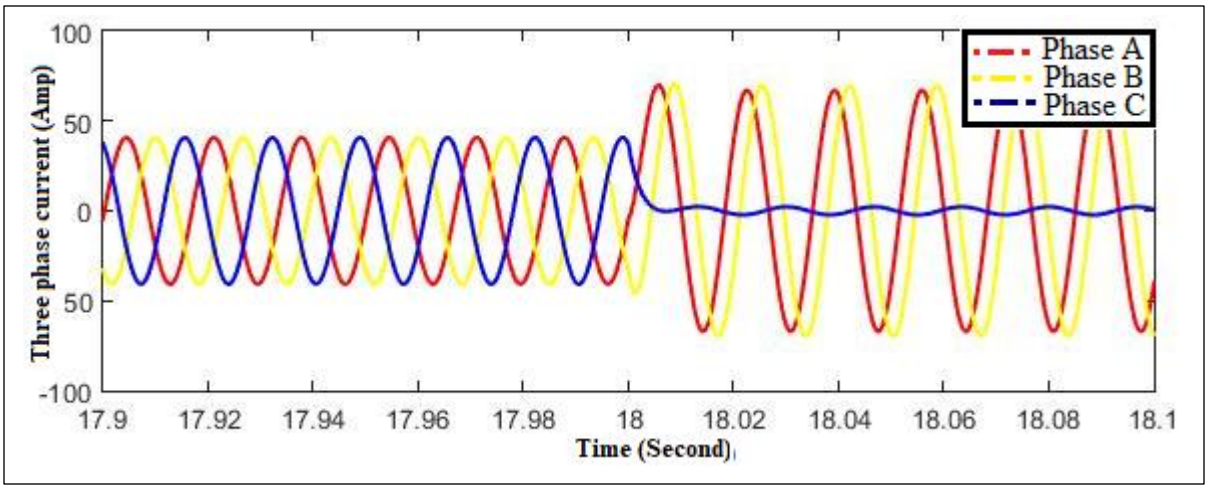

Fig. 5.7(a) Three phase currents observed at load 3 under single line to ground fault at C phase

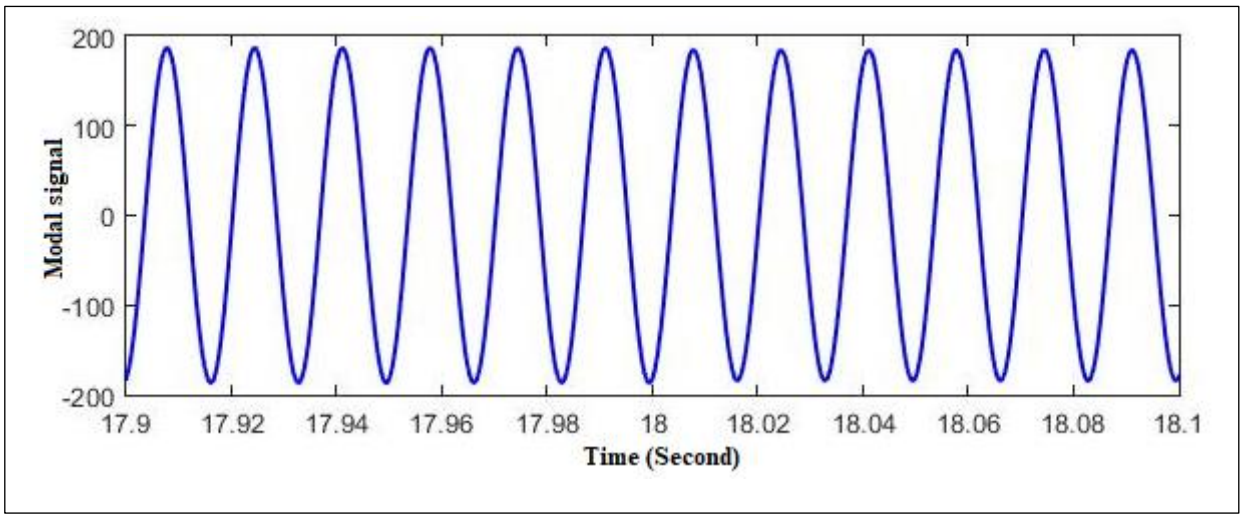

Fig. 5.7(b) Modal current under single line to ground fault at phase C

The feature vector under single phase-C to ground fault at a distance of 6.25 km in line L1 from Bus 1 (one cycle) is [E_4 E_5 E_6] = [0.169 6.724 52.116]. If this feature vector feed to FIS, then FIS will detect it as non-single phasing event.

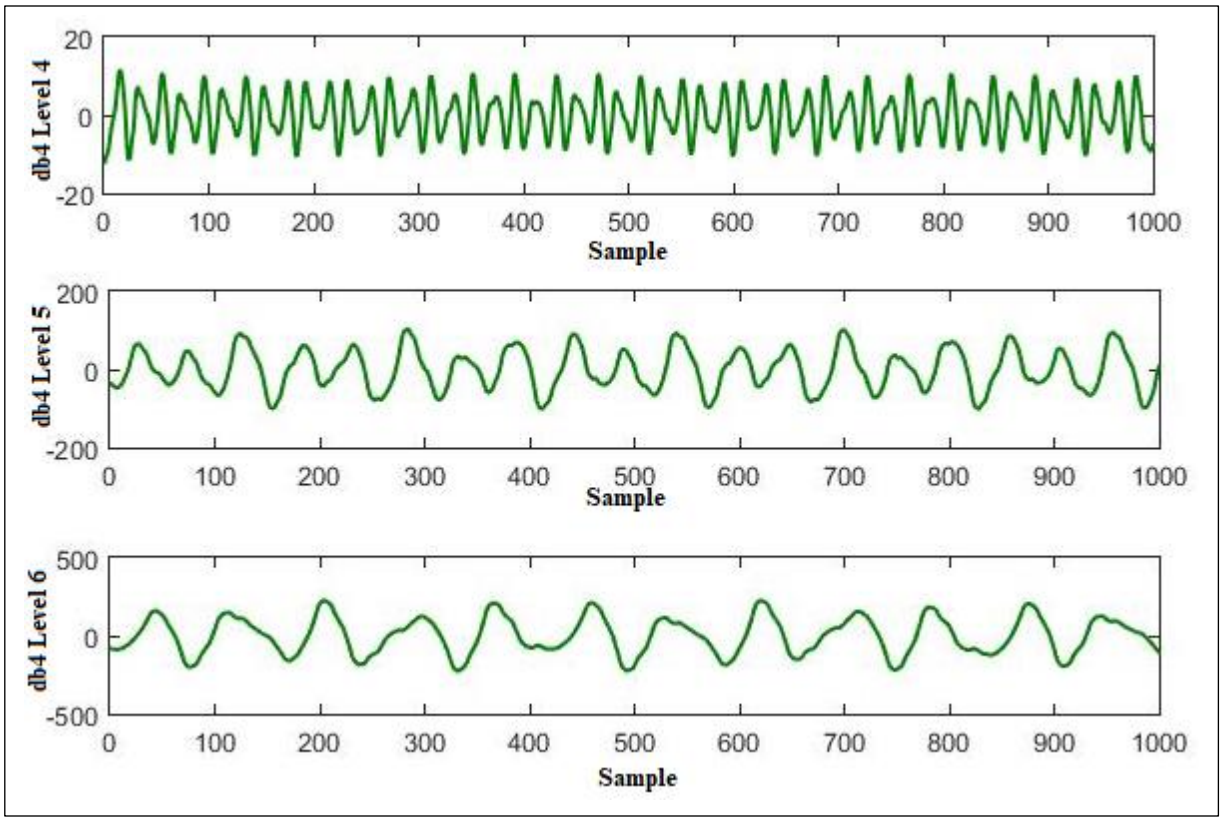

Fig. 5.7 (c) Detail coefficients of modal current of Level 4, Level 5 and Level 6 under single line to ground fault at phase C

5.3.2 DOUBLE LINE TO GROUND (LLG) FAULT

Three phase current signal at load 3 with double line to ground fault in phase A and B in line L_1 is shown in Fig. 5.8 (a). In Fig. 5.8 (a) the fault occurs at an inception angle of 0^o at a distance of 6.25 km in line L_1 from Bus 1 and fault resistance of 0.0001 Ω. The figure shows that currents of the faulted phases at load 3 decrease as the voltage at faulted phase decreases in Bus 2 and Bus 4. Fig. 5.8(b) shows the modal signal corresponding to three phase current signal at load 3. Fig. 5.8(c) shows Db4 detail coefficients of 4^{th}, 5^{th} and 6^{th} level decomposition of modal signal which is form using this unbalance current at load 3 due to double line to ground fault in phase A and B.

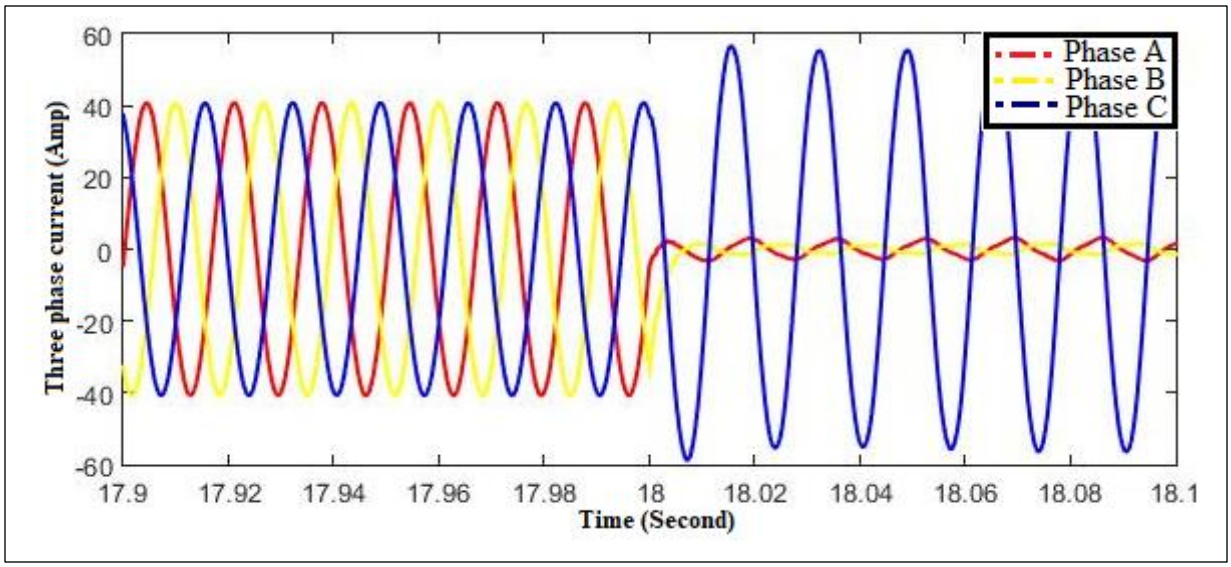

Fig. 5.8(a) Three phase currents observed at load 3 under double line to ground fault in phase A and B

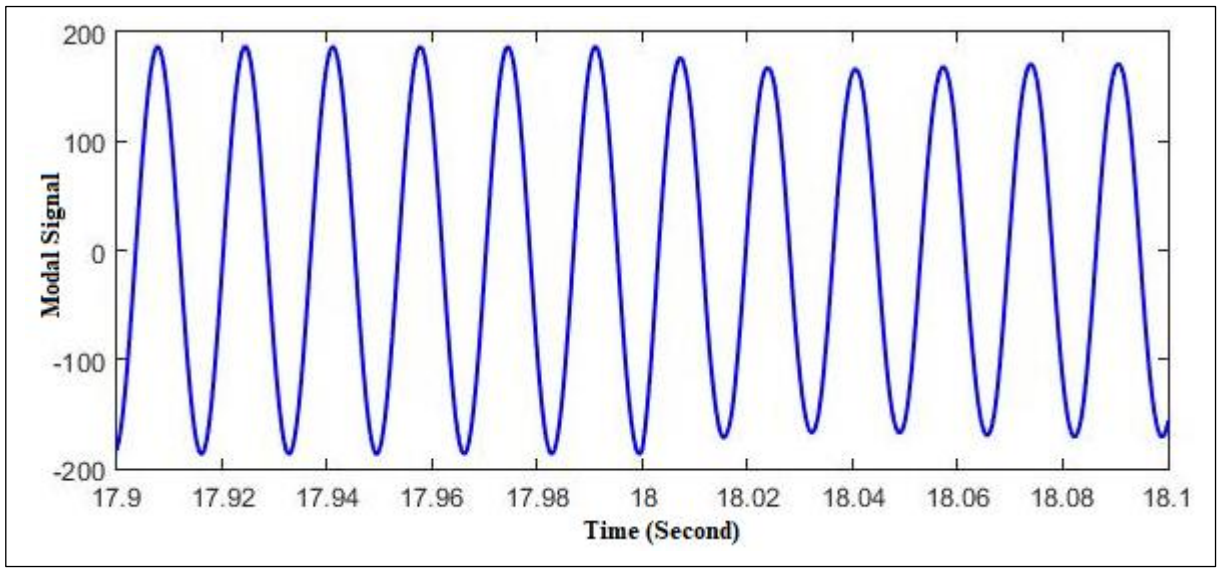

Fig. 5.8(b) Modal current under double line to ground fault in phase A and B

The feature vector under double line to ground fault at a distance of 6.25 km in line L1 from Bus 1 (one cycle) is [E_4 E_5 E_6] = [0.38612 9.980541 53.12059]. If this feature vector is fed to FIS, then FIS will detect it as non-single phasing event.

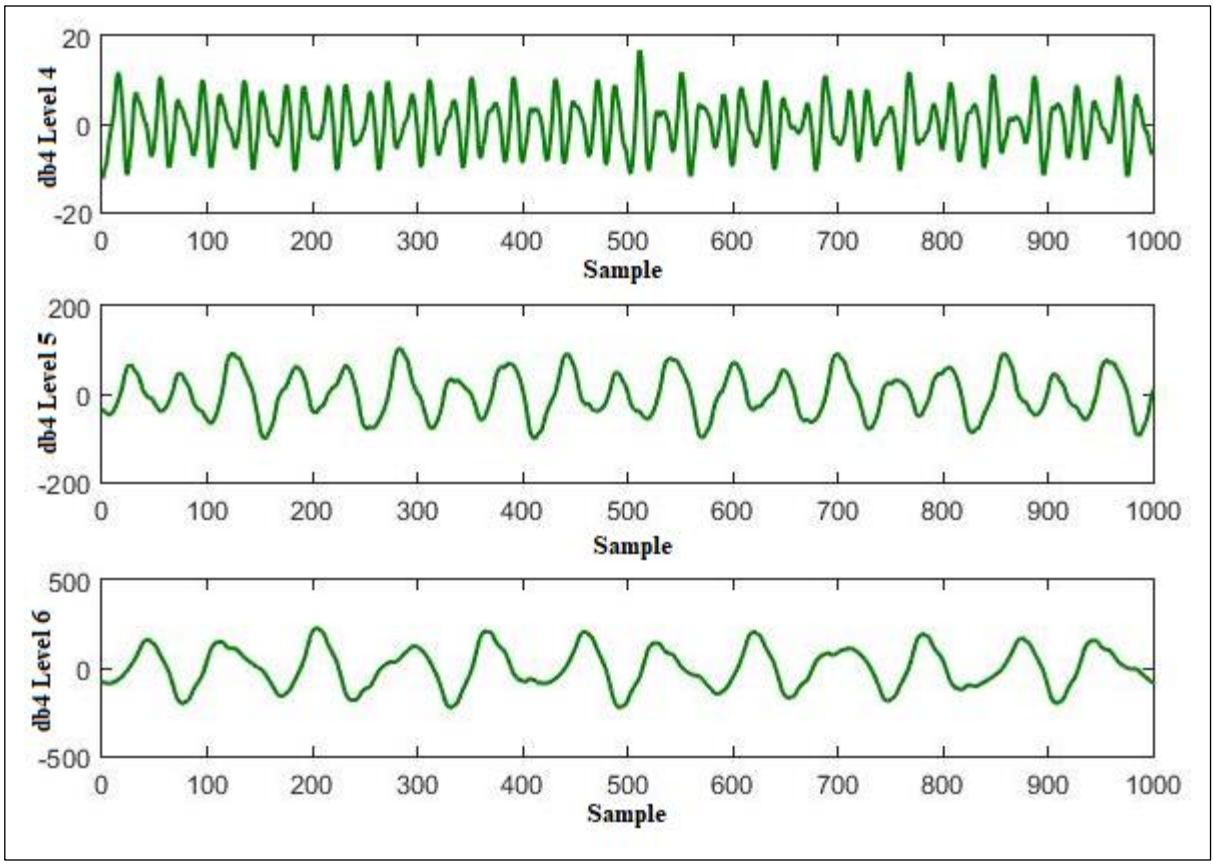

Fig. 5.8 (c) Detail coefficients of modal current of Level 4, Level 5 and Level 6 under double line-AB to ground fault

Fig. 5.9(a) shows three phase current signal at load 3 with double line to ground fault in phase B and C in line L_1. In Fig. 5.9(a) the fault occurs at an inception angle of 45^o and fault resistance 0.0001 Ω. The modal signal corresponding to three phase current signal at load 3 with double line to ground fault in phase B and C in line L_1 is shown in Fig. 5.9(b). Fig. 5.9(c) shows detail coefficients of 4^{th}, 5^{th} and 6^{th} level decomposition of modal signal which is formed using this unbalance current at load 3.

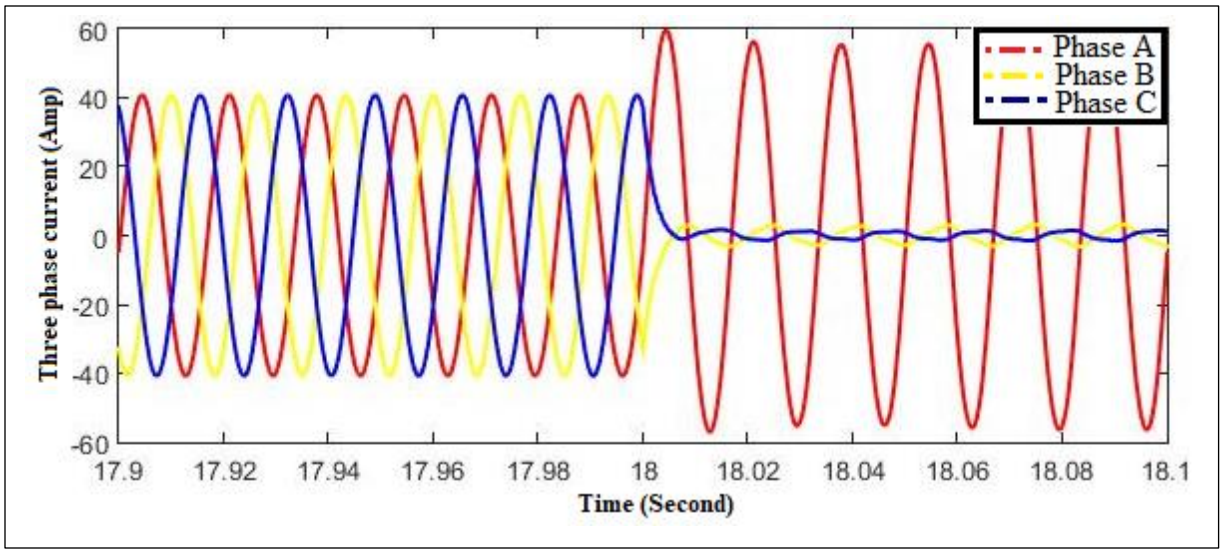

Fig. 5.9(a) Three phase currents observed at load 3 under double line to ground fault in phase B and C

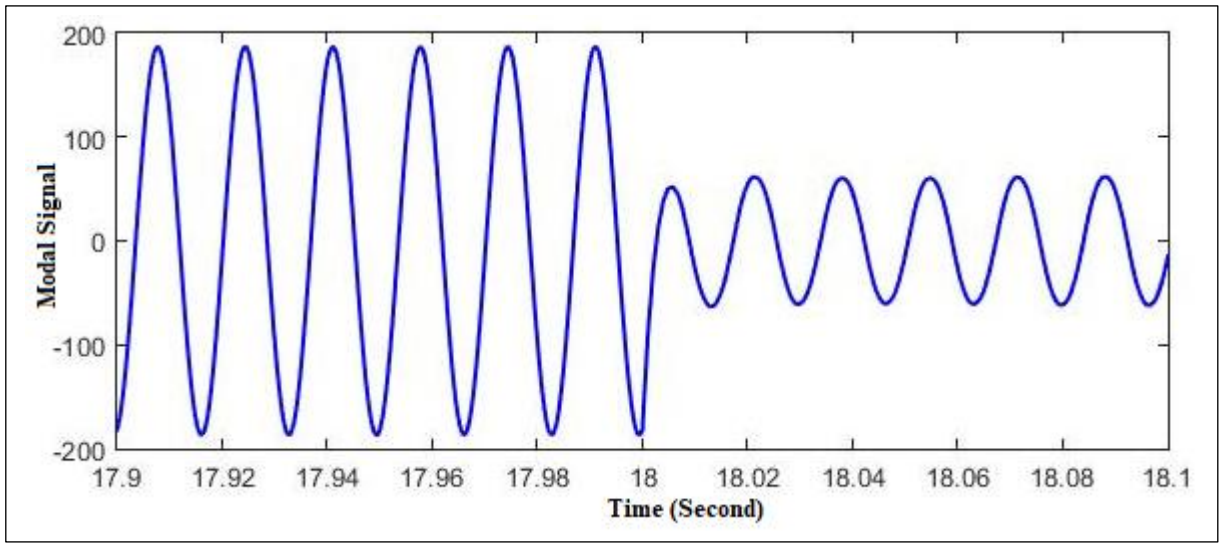

Fig. 5.9(b) Modal current under double line to ground fault in phase B and C

The feature vector under double line to ground fault at a distance of 6.25 km in line L1 from Bus 1 (one cycle) is [E_4 E_5 E_6] = [0.614 9.898 45.865]. If this feature vector is fed to FIS, then FIS will detect it as non-single phasing event.

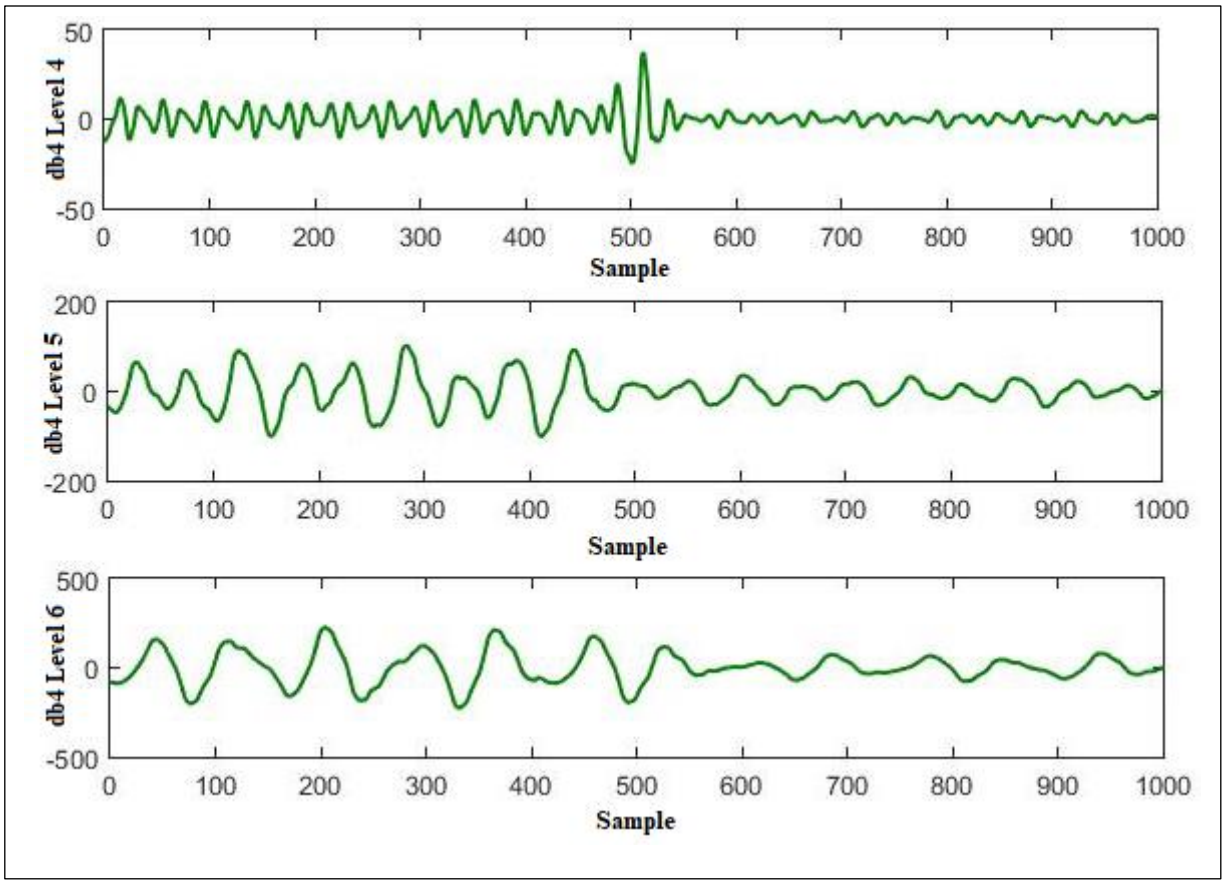

Fig. 5.9 (c) Detail coefficients of modal current of Level 4, Level 5 and Level 6 under double line to ground fault in phase B and C

Three phase current signal at load 3 with double line to ground fault in phase C and A in line L_1 is shown in Fig. 5.10(a). In Fig. 5.10(a) the fault occurs at an inception angle of 90^o and fault resistance 0.0001 Ω. The modal signal corresponding to three phase current signal at load 3 with double line to ground fault in phase C and A in line L_1 is shown in Fig. 5.10(b). Fig. 5.10(c) shows detail coefficients of 4^{th}, 5^{th} and 6^{th} level decomposition of modal signal which is formed using this unbalance current at load 3.

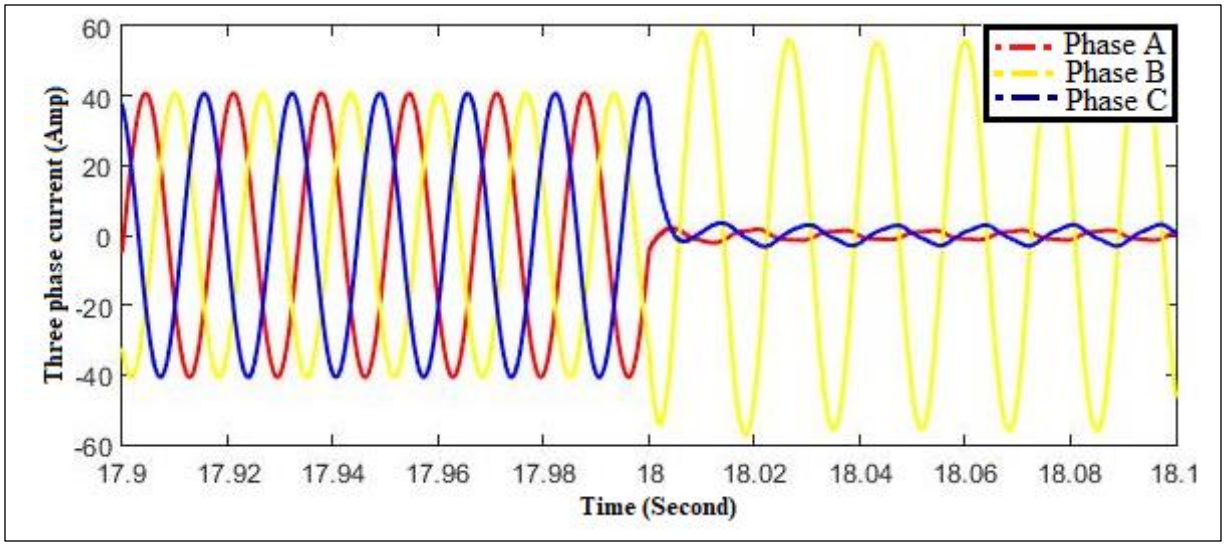

Fig. 5.10(a) Three phase currents observed at load 3 under double line to ground fault in phase C and A

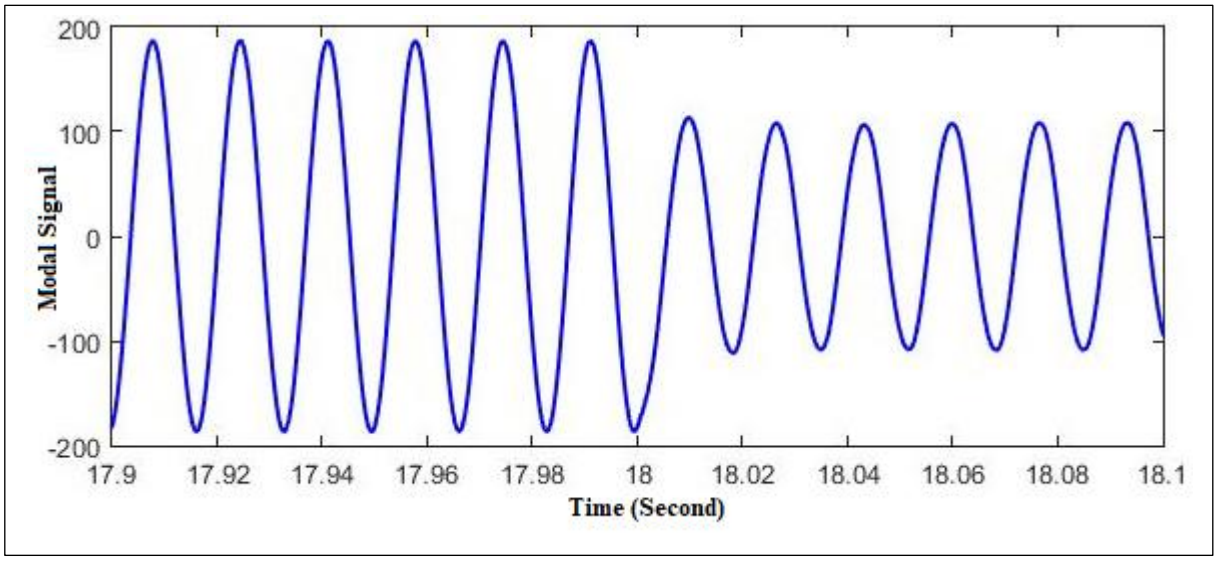

Fig. 5.10(b) Modal current under double line to ground fault in phase C and A

The feature vector under double line to ground fault in phase C and A at a distance of 6.25 km in line L1 from Bus 1 (one cycle) is [E_4 E_5 E_6] = [0.086 1.241 14.497]. If this feature vector is fed to FIS, then FIS will detect it as non-single phasing event.

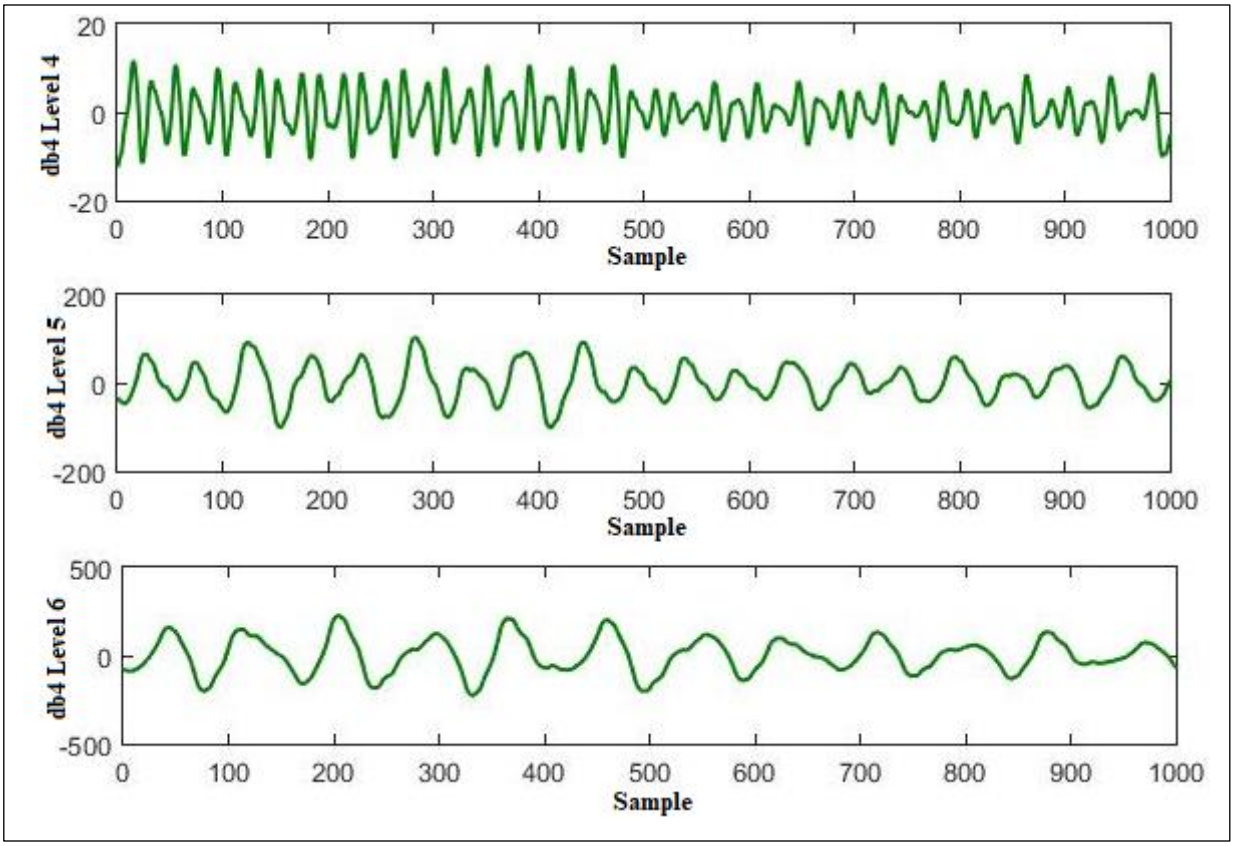

Fig. 5.10 (c) Detail coefficients of modal current of Level 4, Level 5 and Level 6 under double line to ground fault in phase C and A

5.3.3 DOUBLE LINE (LL) FAULT

Three phase current signal at load 3 with double line fault in phase A and B in line L_1 is shown in Fig. 5.11(a). In Fig. 5.11(a) the fault occurs at an inception angle of 0^o at a distance of 6.25 km in line L_1 from Bus 1 and fault resistance of 0.0001 Ω. The figure shows that both currents of the faulted phases at load 3 are decreased as the voltage at faulted phases decrease in Bus 2 and Bus 4. Fig. 5.11(b) shows the modal signal corresponding to three phase current signal at load 3. Fig. 5.11(c) shows detail coefficients of 4^{th}, 5^{th} and 6^{th} level decomposition of modal signal which is formed using this unbalance current at load 3.

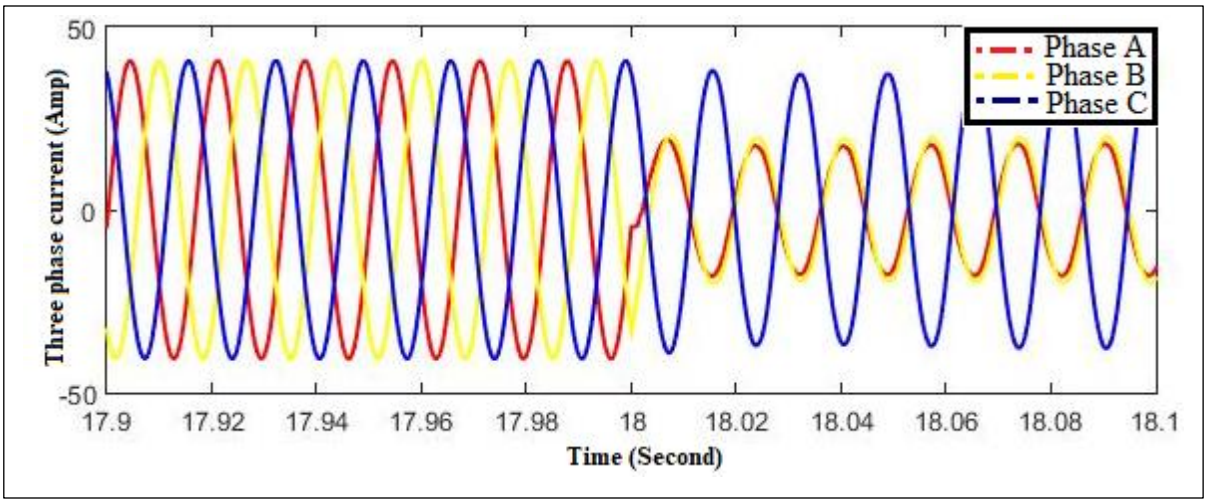

Fig. 5.11(a) Three phase currents observed at load 3 under double line fault in phase A and B

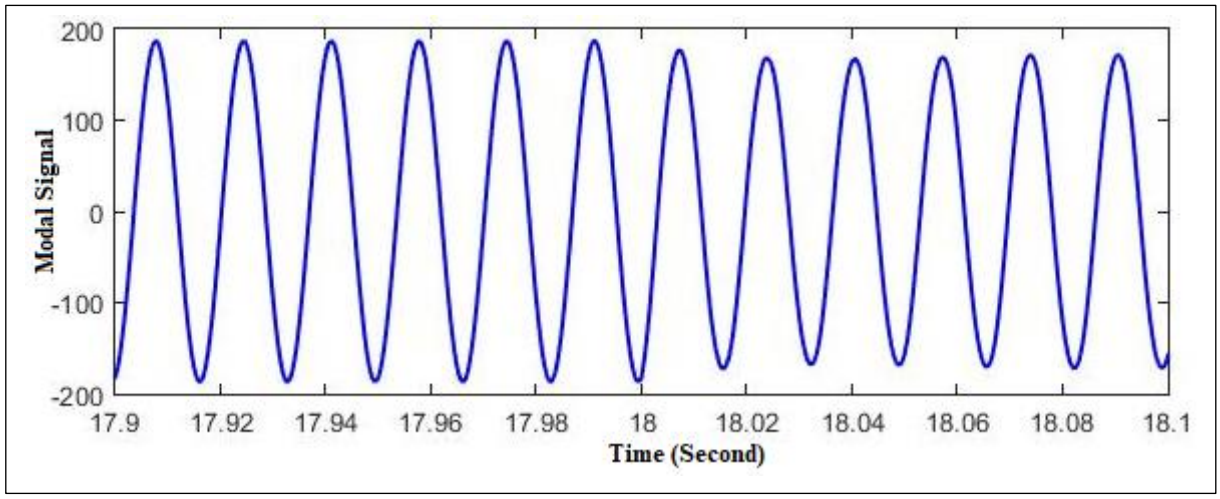

Fig. 5.11(b) Modal current under double line fault in phase A and B

The feature vector under double line fault in phase A and B at a distance of 6.25 km in line L1 from Bus 1 (one cycle) is [E_4 E_5 E_6] = [0.41069 11.54169 60.10621]. If this feature vector is fed to FIS, then FIS will detect it as non-single phasing event.

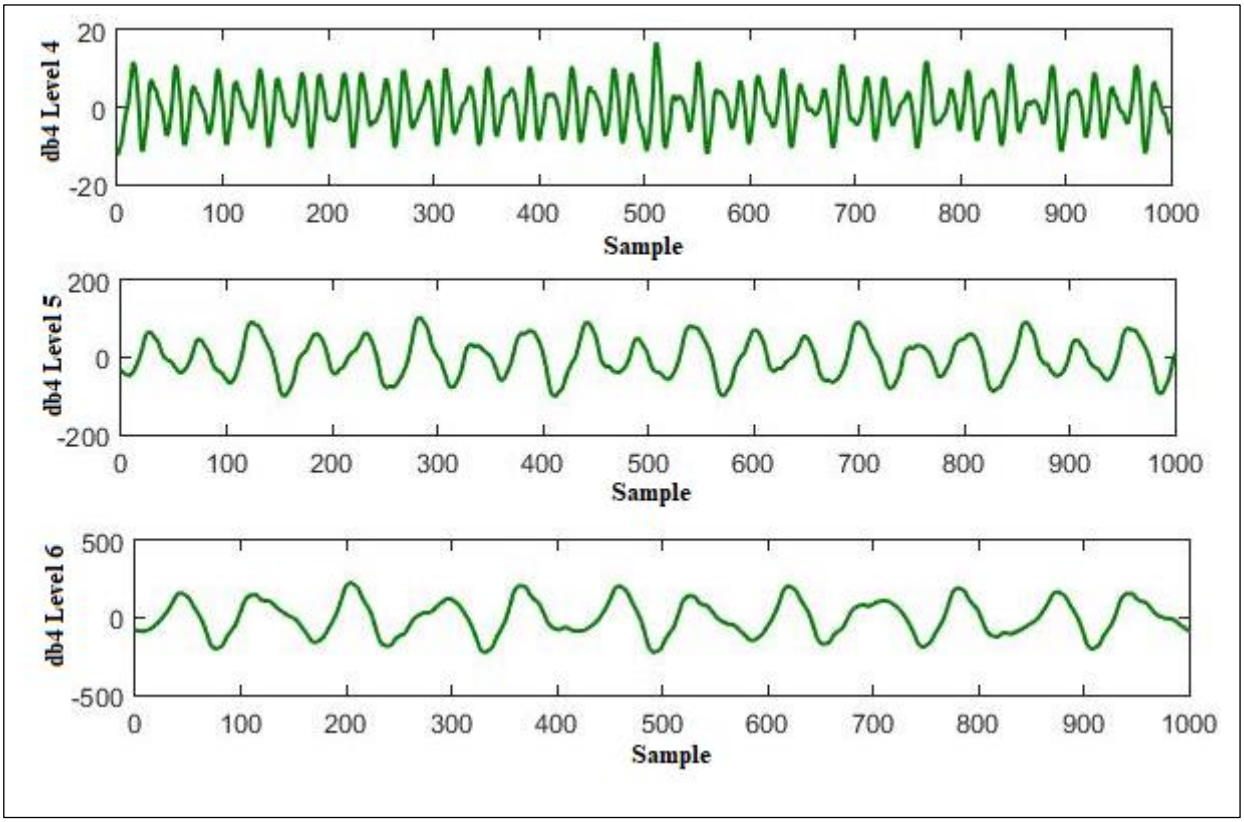

Fig. 5.11 (c) Detail coefficients of modal current of Level 4, Level 5 and Level 6 under double line-AB fault

Fig. 5.12(a) shows three phase current signal at load 3 with double line fault in phase B and C in line L_1. In Fig. 5.12(a) the fault occurs at an inception angle of 45^o and fault resistance 0.0001 Ω. The modal signal corresponding to three phase current signal at load 3 with double line fault in phase B and C in line L_1 is shown in Fig. 5.12(b). Fig. 5.12(c) shows detail coefficients of 4^{th}, 5^{th} and 6^{th} level decomposition of modal signal which is formed using this unbalance current at load 3.

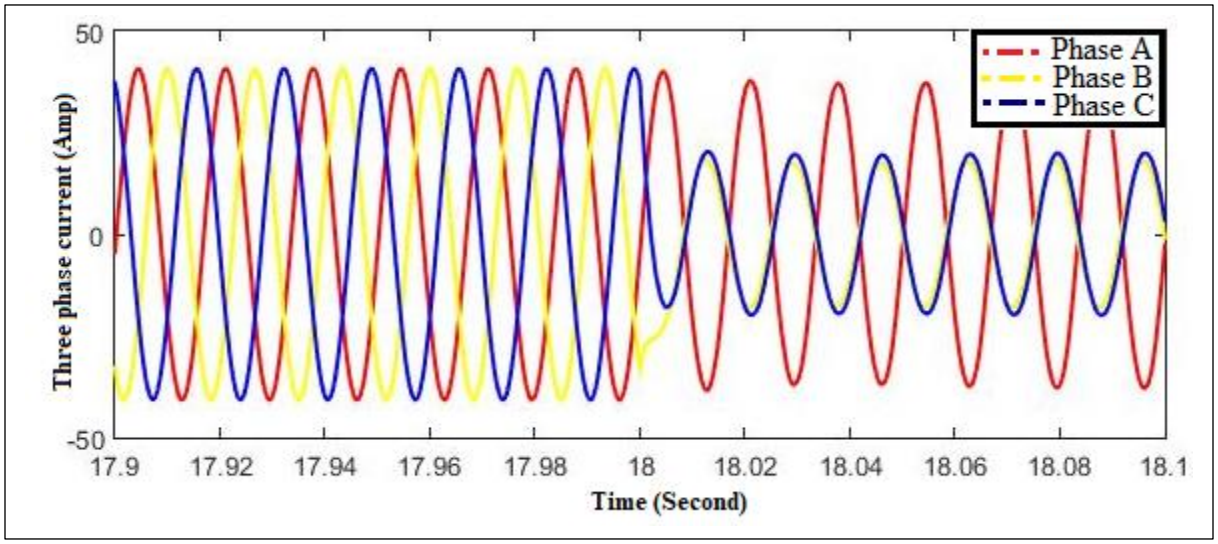

Fig. 5.12(a) Three phase currents observed at load 3 under double line fault in phase B and C

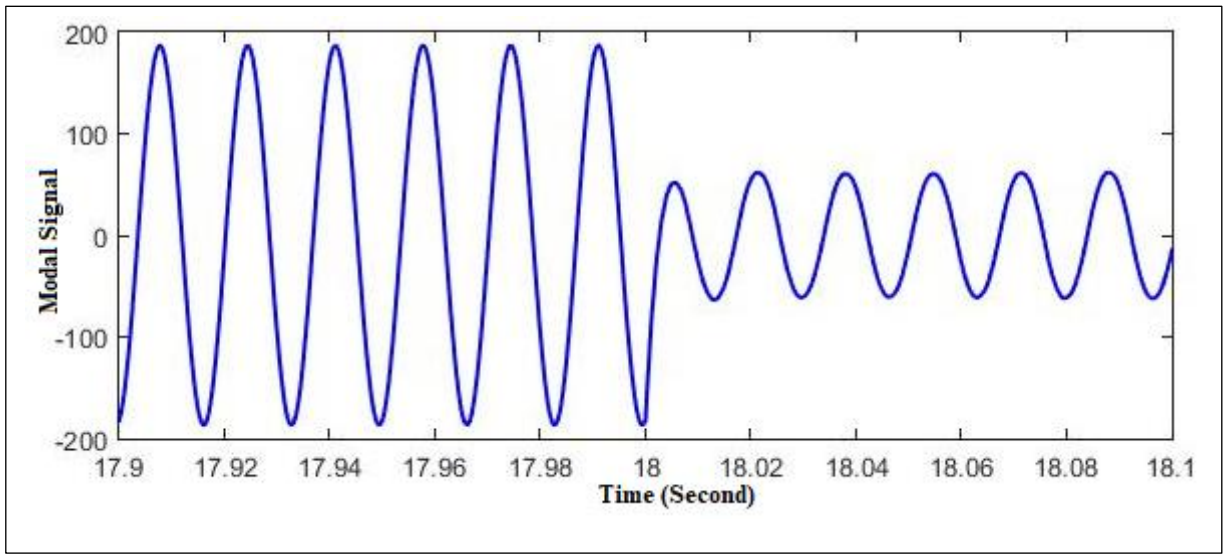

Fig. 5.12(b) Modal current under double line fault in phase B and C

The feature vector under double line fault in phase B and C at a distance of 6.25 km in line L1 from Bus 1 (one cycle) is $[E_4\ E_5\ E_6]$ = [0.7051 11.5001 67.668]. If this feature vector is fed to FIS, then FIS will detect it as non-single phasing event.

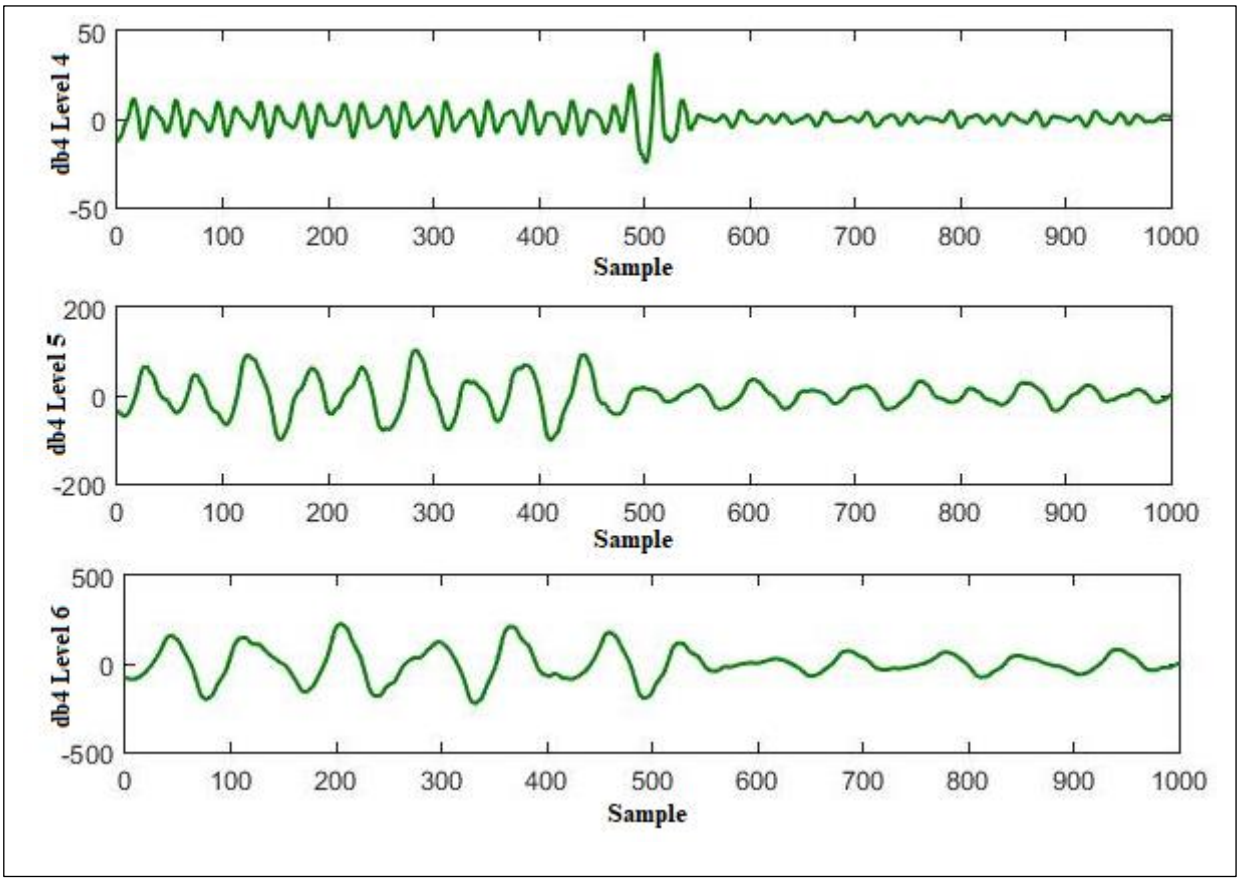

Fig. 5.12 (c) Detail coefficients of modal current of Level 4, Level 5 and Level 6 under double line fault in phase B and C

Three phase current signal at load 3 with double line fault in phase C and A in line L_1 is shown in Fig. 5.13(a). In Fig. 5.13(a) the fault occurs at an inception angle of 90^o and fault resistance 0.0001 Ω. The modal signal corresponding to three phase current signal at load 3 with double line fault in phase C and A in line $L_1$is shown in Fig. 5.13(b). Fig. 5.13(c) shows detail coefficients of 4^{th}, 5^{th} and 6^{th} level decomposition of modal signal which is form using this unbalance current at load 3 due to double line fault in phase C and A.

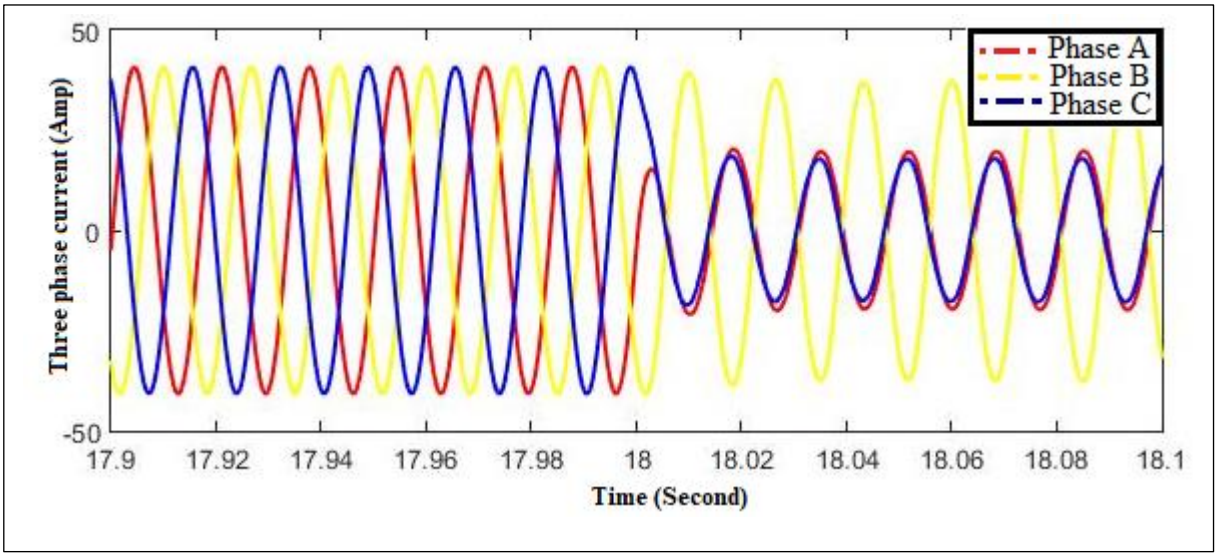

Fig. 5.13(a) Three phase currents observed at load 3 under double line fault in phase C and A

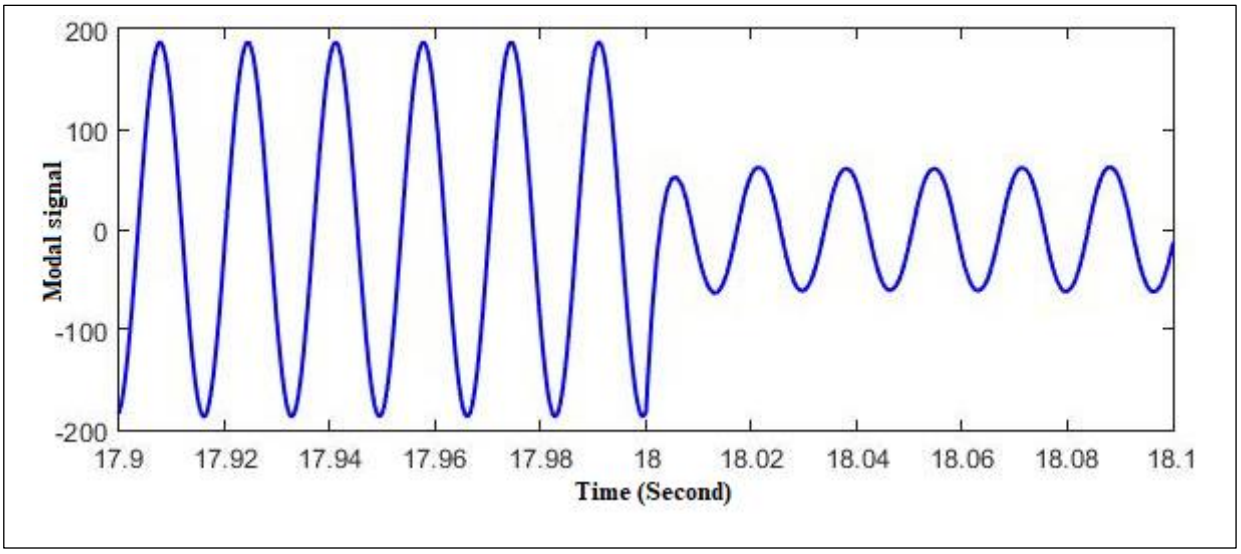

Fig. 5.13(b) Modal current under double line fault in phase C and A

The feature vector under double line fault in phase C and A at a distance of 6.25 km in line L1 from Bus 1 (one cycle) is $[E_4\ E_5\ E_6]$ = [0.235 4.631 28.196]. If this feature vector is fed to FIS, then FIS will detect it as non-single phasing event.

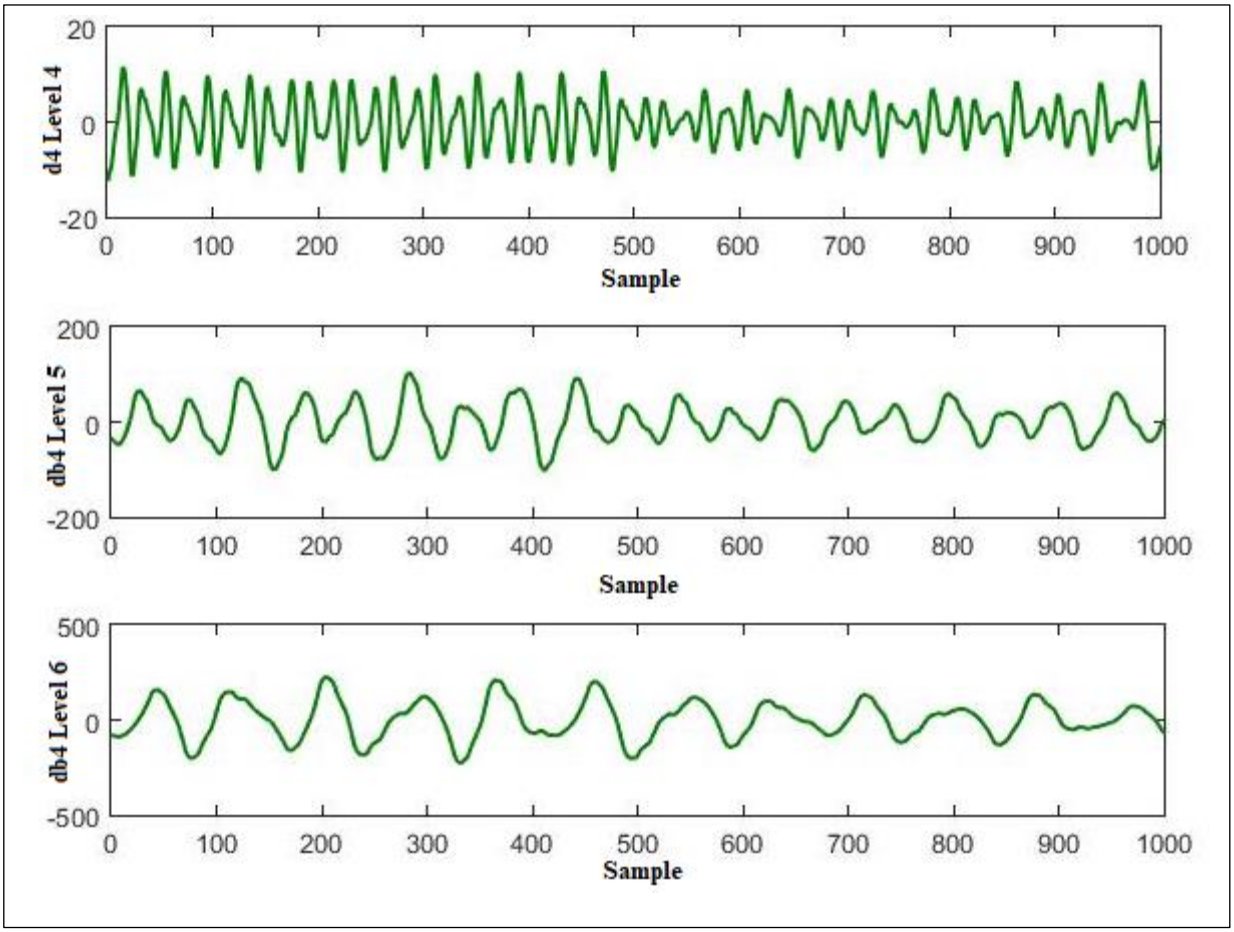

Fig. 5.13 (c) Detail coefficients of modal current of Level 4, Level 5 and Level 6 under double line fault in phase C and A

5.3.4 THREE PHASE TO GROUND (LLLG) FAULT

Three phase current signal at load 3 with three phase to ground fault in line L_1 is shown in Fig. 5.14(a). In Fig. 5.14(a) the fault occurs at an inception angle of 0^o at a distance of 6.25 km in line L_1 from Bus 1 with fault resistance of 0.0001 Ω. The figure shows that all three currents of the faulted phases at load 3 decrease as the voltage at faulted phases decrease in Bus 2 and Bus 4. Fig. 5.14(b) shows the modal signal corresponding to three phase current signal at load 3. Fig. 5.14(c) shows detail coefficients of 4^{th}, 5^{th} and 6^{th} level decomposition of modal signal which is formed using this unbalance current at load 3.

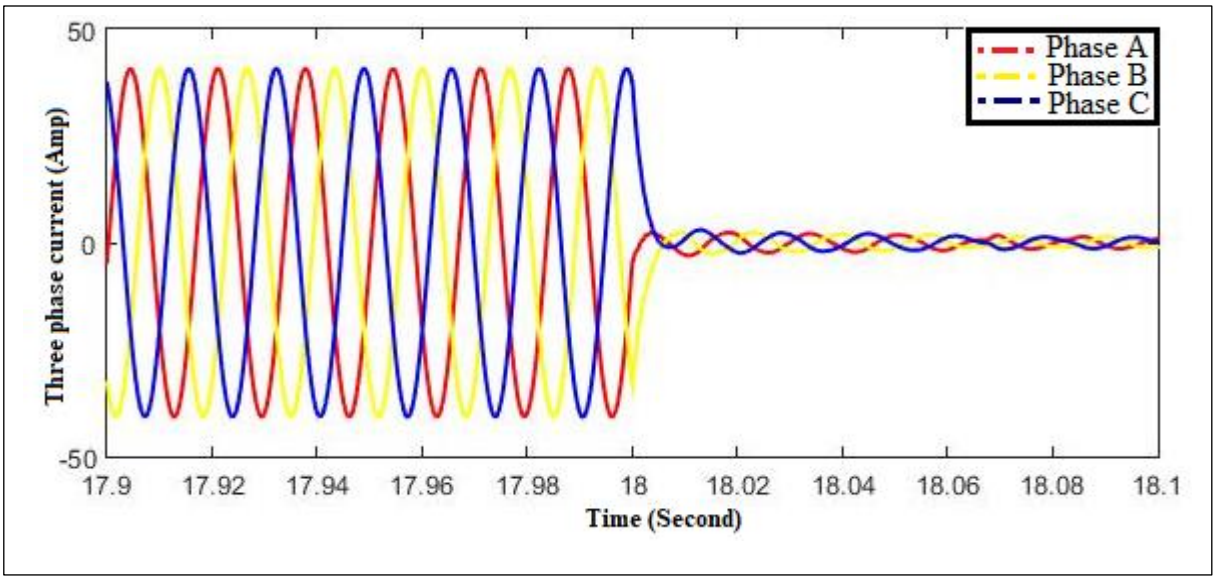

Fig. 5.14(a) Three phase currents observed at load 3 under three phase to ground fault

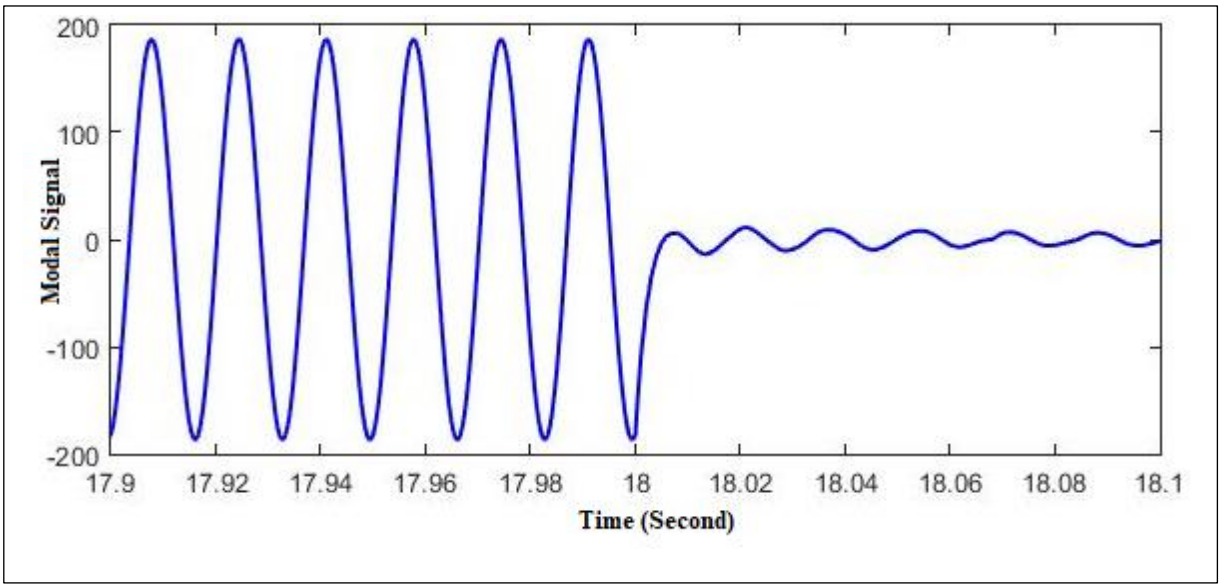

Fig. 5.14(b) Modal current under three phase to ground fault

The feature vector under three phase to ground fault at a distance of 6.25 km in line L1 from Bus 1 (one cycle) is [E_4 E_5 E_6] = [0.14941 0.94368 1.56268]. If this feature vector is fed to FIS, then FIS will detect it as non-single phasing event.

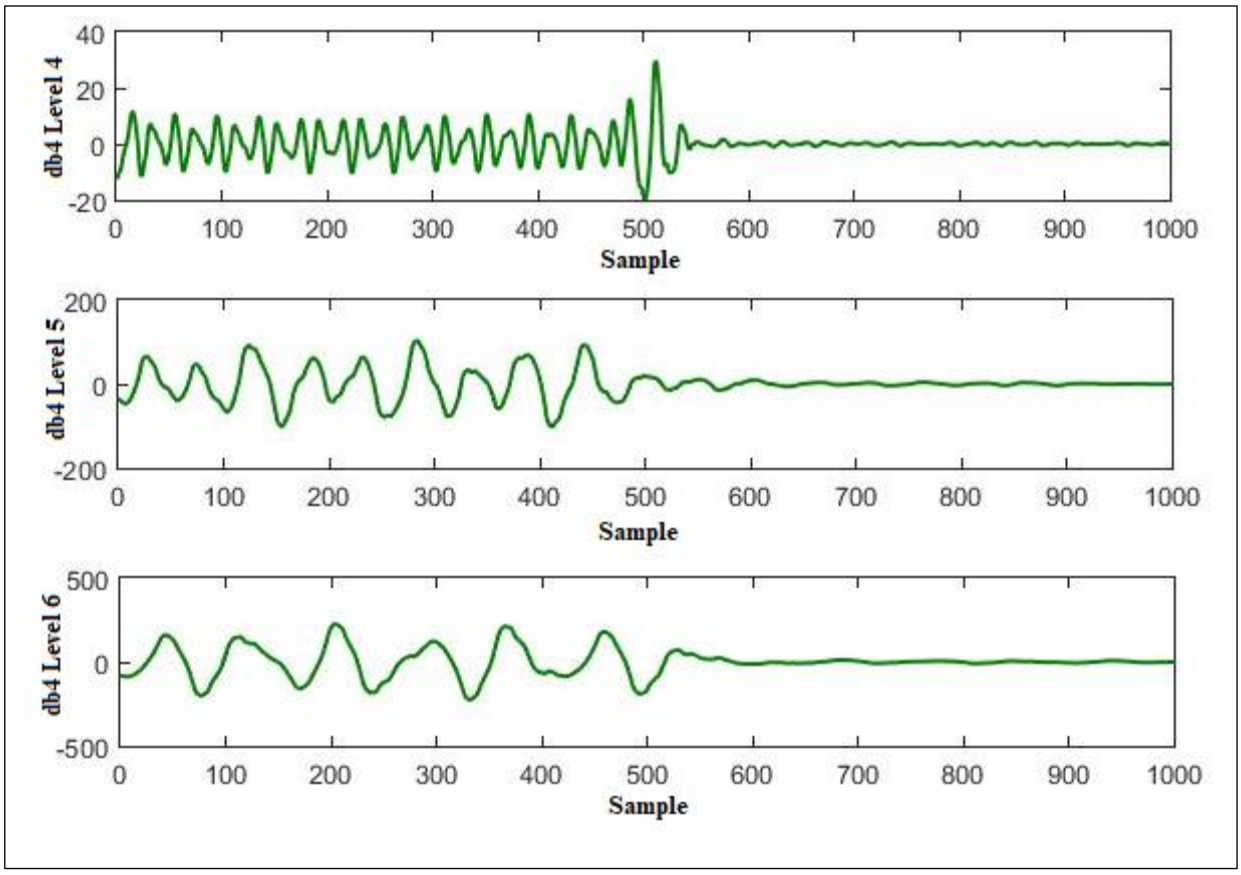

Fig. 5.14 (c) Detail coefficients of modal current of Level 4, Level 5 and Level 6 under three phase to ground fault

5.4 SWITCHING EVENT

Different types of switching events are tested in this research work to test the ability of the proposed method to distinguish single phasing and non-single phasing event. The capacitor at Bus 1 is switched at different inception angles with different capacitor bank rating. Also loads at Bus 3 and Bus 4 are switched at different times to create different switching events.

Fig. 5.16 shows the three phase current at load 3 when capacitor bank of rating 8.5 MVAR is switched off at Bus 1 at 18 second. The figure shows that there is least effect on load 3 for switched off of capacitor bank at Bus 1. Hence, it is not detected as disturbance and classified as non-single phasing event.

Similarly Fig. 5.17 shows three phase current at load 3 when Load 1 is disconnected at Bus 3. The figure shows that there is least effect on load 3 for switched off of Load 1 at Bus 3. Hence, it is not detected as disturbance and classified as non-single phasing event.

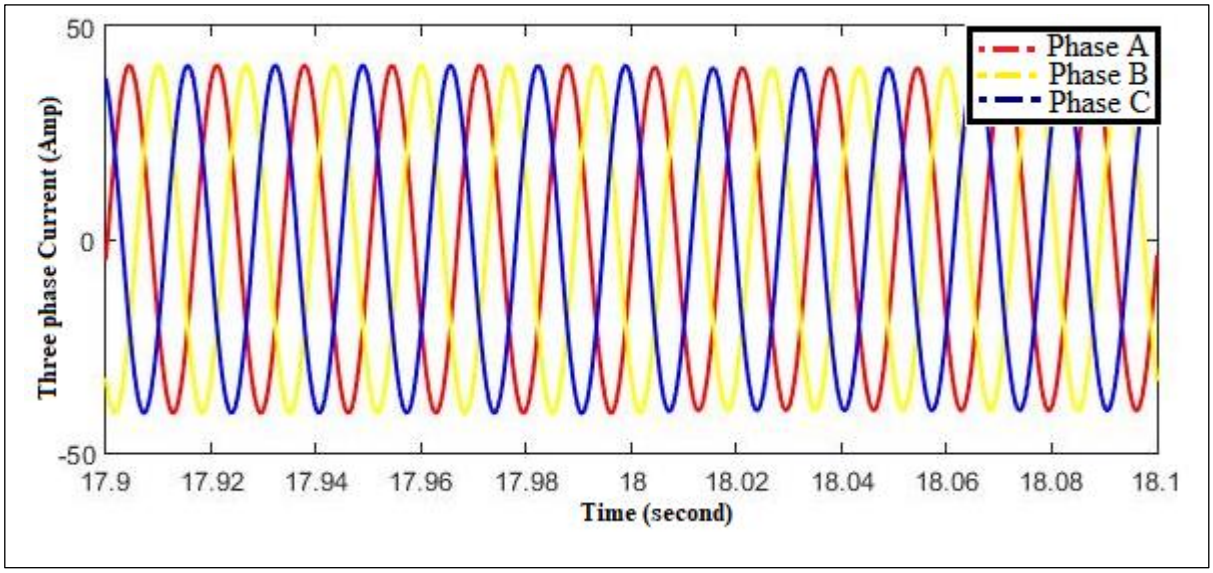

Fig. 5.16 Three phase currents observed at load 3 when capacitor bank at Bus1 is switched off

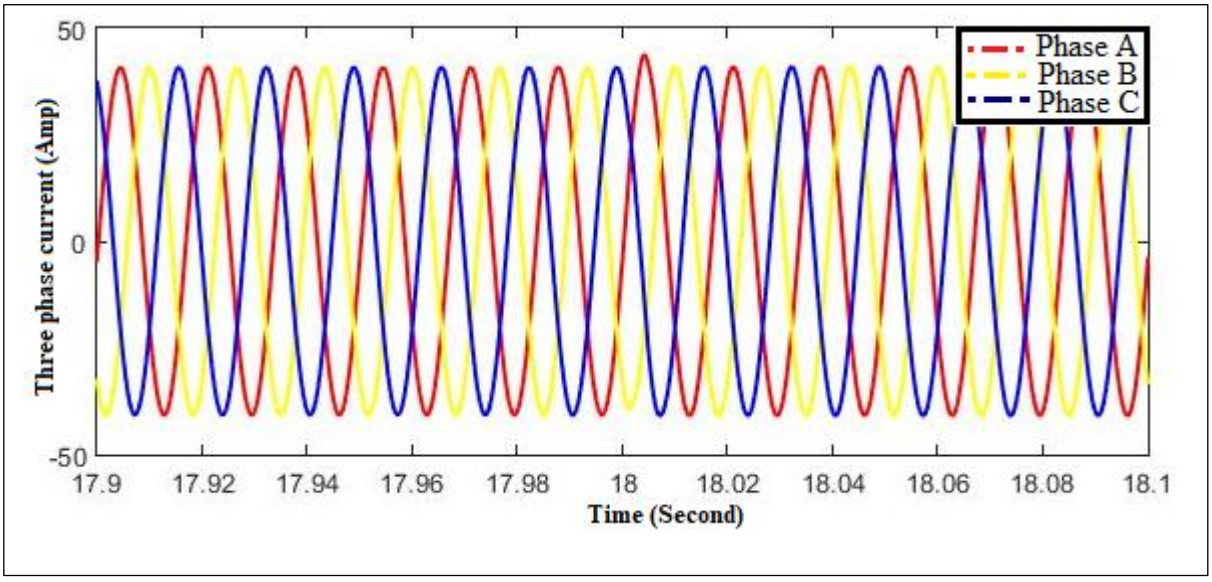

Fig. 5.17 Three phase currents observed at load 3 under Switching off of Load 1 at Bus 3

5.5 DETECTION AND CLASSIFICATION RESULTS

The proposed method is tested for different transient conditions to distinguish between single phasing condition and non-single phasing condition. In each case study, load 3 is monitoring the rms current to detect the transient condition. If the rms current changes by 0.05 p.u. for ten consecutive samples, then transient is detected. If transient condition is detected, the modal signal for 100 samples after the occurrence of transient is decomposed by db_4 mother wavelet upto 6^{th} level and feature vectors are generated which are the spectral energies of the detail coefficients of the modal signal. These feature vectors are applied to the fuzzy inference system which produces the final output viz. whether single phasing has occurred or not and if single phasing is detected, then the lost phase is identified. The total number of case studies can be categorized into three broad sections which are discussed briefly below.

5.5.1 SINGLE PHASING EVENT

In this work single phasing is created by opening one phase of the 600 MVA transformer, connected to the main grid. The single phasing condition has also been created by opening the three phases, one at a time, in line L1 at nine different distances at inception angles of 0°, 45° and 90°.Total 81 numbers of single phasing conditions have been created in line L1. It has also been tested that if any one of the phases supplied from the windfarm connected with line L5 is lost, it is not detected as single phasing event. Total 81 numbers of single phasing events has been created in line L5. Under all conditions the current signals are observed from the sensitive load connected in line L3. The feature vector and corresponding FIS result of single phasing at phase A, single phasing at phase B and single phasing at phasing C are shown in table 5.1, table 5.2 and table 5.3 respectively.

TABLE 5.1 Single phasing at phase A

Distance at Line L_1 from Bus1(km)	Inception Angle (Degree)	E_4	E_5	E_6	FIS Result
0	0º	0.06234	0.51581	17.61454	SPA
	45º	0.06234	0.51581	17.61454	SPA
	90º	0.06234	0.51581	17.61454	SPA
1	0º	0.06139	0.407674	17.64333	SPA
	45º	0.06149	0.515028	17.64832	SPA
	90º	0.06149	0.515028	17.64832	SPA
3	0º	0.061234	0.41055	17.66406	SPA
	45º	0.059325	0.409262	17.65021	SPA
	90º	0.059325	0.409262	17.65021	SPA
5	0º	0.062958	0.51481	17.6007	SPA
	45º	0.059902	0.409823	17.72188	SPA
	90º	0.059902	0.409823	17.72188	SPA
6.25	0º	0.063437	0.514421	17.58263	SPA
	45º	0.062512	0.512965	17.63242	SPA
	90º	0.062512	0.512965	17.63242	SPA
7	0º	0.064345	0.519147	17.65818	SPA
	45º	0.059902	0.409823	17.72188	SPA
	90º	0.059902	0.409823	17.72188	SPA
9	0º	0.059845	0.411333	17.60513	SPA
	45º	0.061479	0.407659	17.67475	SPA
	90º	0.061479	0.407659	17.67475	SPA
11	0º	0.060389	0.411298	17.61343	SPA
	45º	0.060389	0.411298	17.61343	SPA
	90º	0.060389	0.411298	17.61343	SPA

TABLE 5.2 Single phasing at phase B

Distance at Line L_1 from Bus1(km)	Inception Angle (Degree)	E_4	E_5	E_6	FIS Result
1	0º	0.090284	3.289561	35.03123	SPB
	45º	0.090284	3.289561	35.03123	SPB
	90º	0.097497	3.793717	37.4418	SPB
3	0º	0.101984	4.003176	38.39526	SPB
	45º	0.101984	4.003176	38.39526	SPB
	90º	0.095024	3.790286	37.18345	SPB
5	0º	0.10046	4.010164	38.40289	SPB
	45º	0.10046	4.010164	38.40289	SPB
	90º	0.093627	3.740268	37.16582	SPB
	0º	0.100702	4.028296	38.33058	SPB

6.25	45º	0.100702	4.028296	38.33058	SPB
	90º	0.096474	3.763632	37.2789	SPB
7	0º	0.100702	4.028296	38.33058	SPB
	45º	0.100702	4.028296	38.33058	SPB
	90º	0.096474	3.763632	37.2789	SPB
9	0º	0.10408	3.998467	37.45905	SPB
	45º	0.10408	3.998467	37.45905	SPB
	90º	0.09355	3.685505	37.15447	SPB
11	0º	0.090465	3.261367	34.95244	SPB
	45º	0.090465	3.261367	34.95244	SPB
	90º	0.095065	3.746644	37.25552	SPB

TABLE 5.3 Single phasing at phase C

Distance at Line L_1 from Bus1(km)	Inception Angle (Degree)	E_4	E_5	E_6	FIS Results
1	0º	0.338446	14.01368	72.67209	SPC
	45º	0.330978	13.3794	69.32712	SPC
	90º	0.330978	13.3794	69.32712	SPC
3	0º	0.338166	13.34267	67.53165	SPC
	45º	0.34666	14.3797	73.89753	SPC
	90º	0.34666	14.3797	73.89753	SPC
5	0º	0.34524	13.55718	68.95712	SPC
	45º	0.34524	13.55718	68.95712	SPC
	90º	0.34524	13.55718	68.95712	SPC
6.25	0º	0.321693	14.0712	72.72522	SPC
	45º	0.352918	13.68065	69.0077	SPC
	90º	0.352918	13.68065	69.0077	SPC
7	0º	0.342173	13.50836	69.35211	SPC
	45º	0.342173	13.50836	69.35211	SPC
	90º	0.342173	13.50836	69.35211	SPC
9	0º	0.347242	13.51187	68.91626	SPC
	45º	0.347242	13.51187	68.91626	SPC
	90º	0.347242	13.51187	68.91626	SPC
11	0º	0.342215	13.59575	69.06394	SPC
	45º	0.342215	13.59575	69.06394	SPC
	90º	0.342215	13.59575	69.06394	SPC

5.5.2 SHORT CIRCUIT EVENT

The proposed scheme has been tested to distinguish single phasing events from different types of short circuit faults. All types of short circuit faults viz. single line to ground fault, double line to ground fault, line to line fault and three phase symmetrical fault have been created in lines L1, L2, L3, L4 and L5 considering nine fault resistances in the range of 0 ohm to 1500 ohm at three different inception angles. The faults have been created at three different distances in each line. Total 1620 numbers of faults were created. It is observed that when faults occur in lines L2, L3 and L5, disturbance was detected as non- single phasing event from the sensitive load 3. When faults occur in lines L1 and L4, the faults were detected as non-single phasing events. The feature vector and corresponding FIS result of all type of fault with different inception angle and different fault resistance is shown in Table 5.4 and Table 5.5.

Table 5.4 Single line to ground and double line to ground fault

Type of fault	Distance at Line L_1 from Bus1(km)	Fault Resistance (Ω)	Inception Angle (Degree)	E_4	E_5	E_6	FIS Results
Single line to ground fault in phase A	1	0.001	0^o	0.285477	8.046836	47.48486	NSP
			90^o	0.290012	8.080455	47.88540	NSP
		80	0^o	0.317386	9.420024	83.87475	NSP
			90^o	0.320155	9.501289	83.95120	NSP
		200	0^o	0.375096	11.99056	66.94601	NSP
			90^o	0.380015	12.00150	66.99019	NSP
	6.25	0.001	0^o	0.284673	8.009089	47.26966	NSP
			90^o	0.285471	8.012412	47.59076	NSP
		80	0^o	0.316253	9.381784	53.67434	NSP
			90^o	0.325813	9.392192	53.90587	NSP
		200	0^o	0.369485	11.97685	66.76794	NSP
			90^o	0.370158	12.00891	66.89451	NSP
	11	0.001	0^o	0.284023	7.966153	47.02773	NSP
			90^o	0.290256	7.990167	47.19086	NSP
		80	0^o	0.314907	9.349774	53.63967	NSP
			90^o	0.316896	9.376169	53.88510	NSP
		200	0^o	0.346051	10.01985	54.02561	NSP
			90^o	0.350128	10.03089	54.03598	NSP
		0.001	0^o	0.380638	9.970371	53.01858	NSP
			90^o	0.382509	9.990523	53.54890	NSP
		20	0^o	0.124281	4.699037	43.00534	NSP

Double line to ground fault in phase A and B	1		90º	0.129215	4.710569	43.21506	NSP
		200	0º	0.061364	1.664981	27.22358	NSP
			90º	0.0625049	1.700125	27.36509	NSP
	6.25	0.001	0º	0.3861205	9.980541	53.12059	NSP
			90º	0.3957121	9.986079	53.26579	NSP
		20	0º	0.1426780	4.726211	43.601168	NSP
			90º	0.1456002	4.751452	43.682101	NSP
		200	0º	0.0559821	1.612591	17.941001	NSP
			90º	0.0560145	1.624580	17.942014	NSP
	11	0.001	0º	0.3800145	9.9400145	52.98542	NSP
			90º	0.3812547	9.9512501	53.012891	NSP
		20	0º	0.1195981	4.6762452	42.985012	NSP
			90º	0.1201459	4.6905841	42.998711	NSP
		200	0º	0.0550158	1.610078	17.950021	NSP
			90º	0.0560014	1.632569	17.659128	NSP

Table 5.5 Double line and three phase fault

Type of fault	Distance at Line L_1 from Bus1(km)	Fault Resistance (Ω)	Inception Angle (Degree)	E_4	E_5	E_6	FIS Results
Double line fault in phase A and B	1	0.001	0º	0.413361	11.56316	60.29621	NSP
			90º	0.423510	11.60125	60.36159	NSP
		20	0º	0.098475	1.221383	19.41421	NSP
			90º	0.099106	1.240159	19.43510	NSP
	6.25	0.001	0º	0.410691	11.54169	60.10621	NSP
			90º	0.425963	11.58261	60.21059	NSP
		20	0º	0.970985	1.219206	19.40689	NSP
			90º	0.982549	1.235981	19.42699	NSP
	11	0.001	0º	0.414891	11.570469	60.35021	NSP
			90º	0.421069	11.591987	60.40015	NSP
		20	0º	0.9568710	1.2389561	19.42698	NSP
			90º	0.9610981	1.2400691	19.42936	NSP
Three phase fault	1	0.001	0º	0.143574	0.914633	1.536826	NSP
			90º	0.149351	0.9194851	1.549421	NSP
		10	0º	0.293144	8.143481	54.38811	NSP
			90º	0.299281	8.210598	54.40698	NSP
	6.25	0.001	0º	0.149417	0.9436823	1.562682	NSP
			90º	0.149658	0.9496871	1.569121	NSP
		10	0º	0.289114	8.1337181	54.58917	NSP
			90º	0.292211	8.150518	54.60791	NSP
		0.001	0º	0.148464	0.924613	1.546721	NSP

	11		90^o	0.149511	0.9264591	1.550411	NSP
		10	0^o	0.295240	8.163241	54.42815	NSP
			90^o	0.297173	8.180182	54.43668	NSP

5.5.3 SWITCHING EVENT

Different switching events may be falsely detected as single phasing event as current transients are created during switching operations. An 8.5 MVAR capacitor bank connected to the low tension side of the main grid transformer is switched on/ off at three different inception angles of 0^o, 45° and 90^o. Also the rating of the capacitor bank has been changed to 4 MVAR and 17 MVAR and switching operations were carried out. According to the proposed algorithm capacitor switching is not detected as disturbance and hence it is not misclassified as single phasing event.

Switching operations were also carried out by opening and closing the circuit breakers to analyze the effect of load switching on the detection of single phasing event. Again one phase of load 1 and load 2 are disconnected one at a time and also simultaneously at different inception angles to test the effect of load switching on the proposed algorithm. In each case it has been found that though the load switching events were detected as disturbance but all of them were detected as non-single phasing event by the proposed FIS. Total 72 numbers of switching events were created to confirm the dependability of the proposed algorithm.

5.6 EVALUTION OF PROPOSED METHOD

In this section the authors have evaluated the performance of the FIS in presence of non-linear load, non-linear high impedance fault (HIF), change in wind speed and change in source strength.

5.6.1 PRESENCE OF NON-LINEAR LOAD

A dc load of 75 kW, 3.6 kV is connected in parallel with load 2 through a 6 pulse converter. In presence of this load, 54 numbers of single phasing events have been created in line L1 at 6 different locations and different 3 different inception angles. Each event is detected as single phasing event and corresponding phase is identified. Again 27 short circuit faults have been created in line L1 with different fault resistances and each event has been

detected as non-single phasing event. Table 5.6 shows the change in spectral energies when single phasing occurs at 0° inception angle at a distance of 6.25km from CB2 in presence of non-linear load.

Table 5.6 Effect of the presence of non linear load

Single phasing at phase	Without non-linear load			With non-linear load		
	E_4	E_5	E_6	E_4	E_5	E_6
A	0.06343	0.51442	17.5826	0.05963	0.40626	17.6179
B	0.09041	3.24264	34.9714	0.10402	4.02012	38.7798
C	0.32169	14.0712	72.7252	0.32830	13.2284	68.6565

5.6.2 PRESENCE OF NON-LINEAR HIF

The model adopted for HIF has been shown in Fig. 1.4. The model has two dc voltage sources V_p and V_n, connected in anti-parallel by two diodes D_p and D_n and two resistances R_p and R_n. Different values of V_p, V_n, R_p and R_n have been chosen according to [24]. Total 27 numbers of single line to ground HIF have been created in line L1 at different inception angles and in different phases. Each fault has been detected as non-single phasing event.

5.6.3 CHANGE IN WIND SPEED AT WIND FARM

Change in wind speed is a common phenomenon in wind firm, so its effect for single phasing detection needs to be analyzed. It has been observed that the proposed method can detect single phasing for 0.1867 p.u. change in wind speed. Table 5.7 shows spectral energies for two wind speeds when single phasing occurs at 0° inception angle and 6.25km from CB2 in line L_1.

Table 5.7 Effect of change of wind speed

Single phasing at phase	Wind speed 1 p.u.			Wind speed 1.1 p.u.		
	E_4	E_5	E_6	E_4	E_5	E_6
A	0.06343	0.51442	17.5826	0.06401	0.51245	17.5876
B	0.09041	3.24264	34.9714	0.10402	4.02012	35.0967
C	0.32169	14.0712	72.7252	0.32944	13.4493	69.1145

5.6.4 CHANGE IN SOURCE STRENGTH

The proposed method has also been tested for change in source strength. The proposed method can tolerate 0.16p.u. variation in source strength of 120 kV, 500 MVA grid. Table 5.8 shows spectral energies for two different values of source strength when single phasing occurs at 0° inception angle and 6.25km from CB2 in line L_1.

Table 5.8 Effect of change of source strength

Single phasing at phase	Source strength 500 MVA			Source strength 550 MVA		
	E_4	E_5	E_6	E_4	E_5	E_6
A	0.06343	0.51442	17.5826	0.05923	0.40959	17.6915
B	0.09041	3.24264	34.9714	0.10078	4.01666	38.3847
C	0.32169	14.0712	72.7252	0.33471	13.4776	69.3140

CHAPTER 6

CONCLUSIONS AND FUTURE SCOPE OF WORK

In this research work a scheme has been developed for single phasing detection and classification in power system distribution in presence of DG unit based on the wavelet analysis and fuzzy inference system. A simple radial power system network with six buses has been considered and it has been shown that single phasing detection and classification is possible considering only current signal at sensitive load.

6.1 CONCLUSIONS

This paper proposes a technique for single phasing detection in distribution system using spectral energies in the wavelet domain. DWT has been integrated with fuzzy inference system to detect and classify single phasing event. A single modal signal has been synthesized from the combination of three phase current signals at the sensitive load. This reduces the computational burden. The proposed algorithm uses spectral energies of higher level detail coefficients to capture the distinctive features from the modal signal. This algorithm is able to differentiate short circuit faults and switching cases from single phasing events. The algorithm is robust and gives accurate results under different dynamic situations.

Single phasing detection and classification based on DWT and ANN has been presented in [1] whereas the proposed algorithm uses DWT and fuzzy logic. Compared to fuzzy logic, ANN requires large training data involving more time, cost and computational complexity. Moreover as paper [1] uses only first level detail coefficients i.e. higher frequency transients, it cannot detect single phasing events occurring on the high voltage side of the main grid transformer. The proposed method can detect and classify single phasing events occurring on the high voltage side of the main grid transformer also as it uses higher level detail coefficients which captures lower frequency transients. The single phasing detection accuracy and classification accuracy in [1] are 99.3% and 93% respectively, whereas the proposed algorithm detects and classifies single phasing events with 100% accuracy.

6.2 SCOPE FOR FUTURE WORK

This work may encourage further analysis and practical studies in the fields of fault detection and classification on transmission line in presence of DG units. Based on this dissertation, the following area of work is suggested for further exploration:

- A laboratory prototype can be made for the developed model.
- In future, it can be proposed to find the location of single phasing in presence of DG units on power distribution system.
- The proposed algorithm may be modified to detect and classify single phasing in transmission lines using FACTS devices.
- Moreover, for complex distribution system it is important to detect single phasing in presence of DG units. The proposed approach may be used for detection of single phasing in a complex distribution system in presence of DG units.

REFERENCES:

1] M.S. ElNozahy, R.A. EL-Shatshat, M.M.A. Salama, "Single-phasing detection and classification in distribution systems with a high penetration of distributed generation," *Electric Power Systems Research*, 2016, vol. 131, pp. 41-48.

[2] Shail Abdul Gafoor, P. V Ramana Rao, "wavelet based fault detection, classification and location in transmission line", First International power Energy conference, Malaysia, Nov. 2006.

[3] M.F Othman, M. Mahfouf, D. A Linkens, "Transmission line fault detection, classification and location using an intelligent Power system Stabiliser", IEEE International conference on Electric Utility Deregulation, Restructuring and Power technologies (DRPT2004) April 2004 Hong Kong.

[4] S. Zarbita, A. Lachouri, H. Boukadoum, "A new approach of fast fault detection in HV-B transmission lines based on detail spectrum Energy analysis using oscillogrohic data", Electrical Power and Energy systems 73(2015) pp. 568-575.

[5] Yellaji Allipilli, G Narasimha Rao, "Detection and classification of faults in transmission lines based on Wavelets", International conference on Electrical, Electronics, Signals, Communication and Optimization (EESCO) – 2015.

[6] M. Jayabharata Reddy, D.K Mohanta, "A wavelet-fuzzy combined approach for classification and location of transmission line faults", Electric Power and Energy Systems 29(2007) pp. 669-678.

[7] D. Das, N.K. Singh, A.K. Singh, " A Comparison study of Fourier transform and Wavelet transform Methods for Detection and Classification of Faults on Transmission Lines", Proc. 2006 IEEE Power India conf., New Delhi, India, Ab. Sl. No. 237, April 2006.

[8] Ravi Kumar Goli, Abdul Gafoor Shaik, S.S. Tulsi Ram, "A Transient current based double line transmission system protection using fuzzy-wavelet approach in presence of UPFC", Electrical Power and Energy Systems 70(2015) pp. 91-98.

[9] Weilin Li, Antonello Monti, Ferdinanda Ponci, "Fault detection and classification in Medium Voltage DC Shipboard Power Systems with Wavelet and Artificial Neural Networks", IEEE TRANSACTIONS ON INSTRUMENTATION AND MEASUREMENT, VOL.63, NO. 11 NOV. 2014.

[10] K. Gayathri, N. Kumarappan, " Comparative study of Fault Identification and classification on EHV Lines using Discrete Wavelet Transform and Fourier Transform Based ANN", World Academy of Science, Engineering and Technology International Journal of Electrical, computer, Energetic, Electronic and Communication Engineering Vol: 2, No: 5, 2008.

[11] S.A Shaaban, Prof. Takashi Hiyama, "Transmission Line Faults classification using wavelet Transform", Proceeding of the 14th international Middle East Power Systems Conf. (MEPCON'10), Cairo University, Eygpt, Dec. 19-21-2010, Paper ID 225.

[12] Satish Karekar, Varsha Thakur, Manju, "A Novel Scheme of Transmission Line Faults Analysis and Detection by using MATLAB Simulation", International Journal of Engineering Research and General Science Vol. 4, Issue 1, January-February, 2016.

[13] K. Saravanababu, P. Balakrishnan, Dr. K. Sathiyasekar, "Transmission Line Fault Detection, classification and Location using Discrete Wavelet Transform", 2013 International conf. on Power, Energy and Control (ICPEC).

[14] Shahzad Ali Rana, Aziz Ahmad, Mohammad Noorullah Quadri, "Faults detection and classification on Long Transmission Line using wavelet Analysis", IJREAT International Journal of Research in Engineering & Advance Technology, Volume 2, Issue 3, June-July,2014.

[15] Murat Uyar, Selcuk Yildirim, Muhsin Tanay Gencoglu, "An effective wavelet based feature extraction method for classification of power quality disturbance signals", Electric Power Systems Research 78(2008) pp. 1747-1755.

[16] A.M El-Zonkoly and H. Desouki, "Wavelet entropy based algorithm for fault detection and classification in FACTS compensated transmission line". Electrical Power and Energy Systems 33(2011) pp. 1368-1374.

[17] Sami Ekici, Selcuk Yildirim, Mustafa Poyraz, "Energy and entropy based feature extraction for locating fault on transmission lines by using neural network and wavelet packet decomposition", Expert systems with Application 34(2008) pp. 2937-2944.

[18] Hosung Jung, Young Park, Moonseob Han, Changmu Lee. Hyunjune Park, Myongchul Shin, "Novel technique for fault location estimation on parallel transmission lines using wavelet", Electrical Power and Energy Systems 29(2007) pp. 76-82.

[19] S. E. Safty and A. El-Zonkoly, "Applying wavelet entropy principle in fault classification", Electrical Power and Energy Systems 31(2009) pp. 604-607.

[20] Ch. Madhavi, M. Bala Subbareddy, D. Srilatha, "Transmission Line Protection using Wavelet Transform", International Journal of Engineering Research & Technology Vol. 2, Issue 11, Nov, 2013.

[21] Mayuresh Rao and R. P. Hasabe, "Detection and classification of Faults on transmission line using Wavelet transform and Neural Network", International Journal of Advance Electrical and Electronics Engineering (IJAEEE), Vol. 2, Issue 5, Nov, 2013.

[22] K. M. Silva, B. A. Souza, N. S. D Brito, "Fault Detection and Classification in Transmission lines based on Wavelet Transform and ANN", IEEE TRANSACTIONS ON POWER DELIVERY, VOL. 21, NO. 4, OCTOBER 2006.

[23] P.S. Bhowmik, P. Purkait, K. Bhattacharya, "A novel wavelet transform aided neural network based transmission line fault analysis method", Electrical Power and Energy Systems 31(2009) pp. 213-219.

[24] A. H. Etemadi and M. Sanaye-Pasand "High-impedance fault detection using multi-resolution signal decomposition and adaptive neural fuzzy inference system" IET Gener. Transm. Distrib., 2008, 2, (1), pp. 110–118.

[25] Anamika Yadav, A. S. Thoke, "ANN based directional fault detector/classifier for protection of transmission lines", Int. J. Comput. Sci. Inf. Technol., (IJCSIT), International Journal of Computer Science and Information Technologies, Vol. 2 (5) , 2011, 2426-2433.

[26] E. Koley, A. Yadav, A.S Thoke,: 'Six phase to ground fault detection and classification of transmission line using ANN', Int. J. Comput. Appl., 2012, 41, (4), pp. 6–10.

[27] A. Yadav, P. Warlyani, A.S. Thoke,: "Fault classification, distance location and faulty section identification in teed transmission circuits using artificial neural network", Int. J. Comput. Appl., 2012, 47, (15), pp. 14–21.

[28] S.R. Nam, J.K. Park, Y.C. Kang, and T.H. Kim,: "A modeling method of high impedance fault in a distribution system using two series time varying resistances in EMTP". IEEE Power Eng. Soc. Summer Meeting, 15–19 July 2001, vol. 2,pp. 1175–1180.

[29] A.E. Emanuel, D. Cyganski, J.A. Orr, S. Shiller, and E.M. Gulachenski,: "High impedance fault arcing on sandy soil in 15 kV distribution feeders: contribution to the evaluation of the low frequency spectrum", IEEE Trans. Power Deliv., 5, (2), pp. 676–686.

[30] O.A.S. Youssef, "Fault classification based on wavelet transform" Transmission and Distribution Conference and Exposition IEEE/PES, vol. 1, pp. 531-536, 2001.

[31] A. Borghetti, S. Corsi, C.A. Nucci, M. Paolone, L. Peretto, R. Tinarelli, "On the use of continuous wavelet transform for fault location in distribution power systems", Electrical Power and Energy Systems 28(2006) pp. 608-617.

[32] Li Zhihua, "A novel fault Diagnostic Method Based on Node-Voltage Vector Ambiguity Sets", IEEE TRANSACTIONS ON INSTRUMENTATION AND MEASUREMENT, VOL.63, NO. 8 AUG. 2014.

[33] F. Martin and J.A. Aguado, "Wavelet Based ANN Approach for Transmission Line Protection", IEEE TRANSACTIONS ON POWER DELIVERY, VOL. 18, NO. 4, pp. 1572-1574 OCTOBER 2003.

[34] A. I. Megahed, A. Monem Moussa, and A. E. Bayoumy, "Usage of wavelet transform in the protection of series compensated transmission lines" IEEE TRANSACTIONS ON POWER DELIVERY, VOL. 21, NO. 3, pp. 1213-1221, JULY, 2006.

[35] Wavelet Toolbox user's guide, the Math works inc.3 Apple hill drive , Natick, MA 01760-2098 MATLAB 8.3 R2014a

[36] Wen-Hui Chen, Chih-Wen Liu, and Men-Shen Tsai, "On-Line Fault Diagnosis of Distribution Substations Using Hybrid Cause-Effect Network and Fuzzy Rule-Based Method," *IEEE TRANSCATION ON POWER DELIVERY,* VOL. 15, NO. 2, APRIL 2000.